Therapeutic Potential of Pheophorbide A-Mediated Photodynamic Therapy (PA-PDT) and Its Immunomodulation in Human Breast Cancer Treatment

BUI XUAN, Ngoc Ha

A Thesis Submitted in Partial Fulfillment
of the Requirements for the Degree of
Doctor of Philosophy

in

Biochemistry (Medicine)

The Chinese University of Hong Kong
December 2010

UMI®
Dissertation Publishing

ProQuest®

Thesis/Assessment Committee

Professor Chen Zhen Yu (Chair)

Professor Fung Kwok Pui (Thesis Supervisor)

Professor Wong Chun Kwok (Thesis Co-Supervisor)

Professor Leung Kwok Nam (Committee Member)

Professor Chan Pui Kwong (External Examiner)

DECLARATION

I declare that the assignment here submitted is original except for source material explicitly acknowledged. I also acknowledge that I am aware of University policy and regulations on honesty in academic work, and of the disciplinary guidelines and procedures applicable to breaches of such policy and regulations, as contained in the website http://www.cuhk.edu.hk/policy/academichonesty/.

20th December, 2010

_____   _____
Signature   Date

Bui Xuan Ngoc Ha   07067530

_____   _____
Name   Student ID

MEB 635T   Research

_____   _____
Course code   Course title

iii

ABSTRACT

Cancer is one of the most lethal diseases worldwide. Treatments of cancer comprise surgical intervention, radiotherapy or chemotherapy; however, their side effects are still need to be overcome. In order to search for anti-cancer treatments with milder side effects and higher efficiency, traditional Chinese medicine (TCM) has been investigated. Previous study in our laboratory reported that pheophorbide a (Pa), an active compound purified from *Scutellaria barbata*, combined with photodynamic therapy (PDT) approach produces anti-tumour effect in a wide range of human cancers. Because of the lack of protocols for curing late phase breast cancer, my project is to investigate the therapeutic potential of Pa-PDT and its action mechanism on human breast cancer. A human breast cancer cell line MDA-MB-231, which is estrogen receptor nude and resistant to a conventional breast cancer drug tamoxifen, was used as an *in vitro* tumour model in my study to mimic the late stage of breast cancer.

According to the results, Pa-PDT showed inhibitory effect on MDA-MB-231 cells *in vitro* with an IC_{50} value of 0.5 μM at 24 h. Pa-PDT was demonstrated to activate intracellular mitogen activated protein kinases (MAPK) pathways via reactive oxygen species (ROS) production. Pa-PDT is also believed to induce extracellular signal-regulated kinase (ERK)-mediated autophagy and endoplasmic reticulum stress. Pa-PDT in combination with

Tamoxifen is demonstrated to exert a synergetic effect in inhibiting cancer growth. The combination treatment induces both intrinsic and extrinsic apoptosis. Regarding the direct cancer cell killing activity, two dimensional gel electrophoresis screening revealed that Pa-PDT regulates proteins which involve in human leukocyte antigen (HLA) class I-restricted antigen-processing machinery. This activation of antigen presentation was confirmed by Western blot analysis and immunostaining. Furthermore, a cross-presentation of antigen with HLA class I proteins and 70-kDa heat shock protein was found in Pa-PDT-treated cells, as shown by the fluorescent microscopic observation and immunoprecipitation assay. Moreover, the immunogenicity of breast cancer cells was increased by Pa-PDT treatment that triggered phagocytic activity by human macrophages. Our findings provide the first evidence that Pa-PDT can trigger both apoptosis and anti-tumour immunity.

Pheophorbide a (Pa) has been proposed to be a potential photosensitizer for the photodynamic therapy of human cancer. However, the immunomodulatory effect of Pa, in the absence of irradiation, has not yet been investigated. The present study revealed that Pa possessed immunostimulating effect on a murine macrophages cell line RAW 264.7. Pa could stimulate the growth of RAW 264.7 cells with the maximal effect at 0.5 μM after 48 h of treatment, where MAPK family including c-Jun N-terminal kinase (JNK), ERK and p38 MAPK were activated by Pa treatment in a dose-dependent manner. Moreover, the induction

of interleukin-6 and tumour necrosis factor-α secretion, and the enhancement of phagocytic activity were observed in Pa-treated RAW 264.7 cells. The results were similar in Pa-treated human immune competent cells (e.g. CD4+ and CD14+ cells) at higher Pa concentrations (from 1 to 10 μM). The present work is the first report to demonstrate the potential immunomodulatory effects of Pa on immune competent cells, apart from its well-known anti-tumour activity.

ACKNOWLEDGMENTS

I would like to express my sincere acknowledgments to my supervisor Professor Fung Kwok-Pui for his long guidance and support during my PhD study.

I feel also grateful to Professor Wong Chun-Kwok, my co-supervisor. Even being my supervisor for a short time but he spent much effort on my progress in the immunomodulation study of human blood cells. His guidance and advices open to me a new field of research, rewarding my knowledge and technical skills.

A very special thank to Dr Tang Ming Kuen, Patrick for his friendship and joy of life. He is an indispensable labmate for discussion and designing experiments.

Without forgetting Dr. Hu Shuiqing, a very active and compassionated labmate. The progression of the PBMCs study cannot be completed without his technical assistance.

It will be a mistake if I don't mention all my labmates in the Prince of Wales Hospital for their hospitality and my friends in the Main Campus always support me on difficult days.

A special thank for my husband who suffered from my mood swings. My daughter *Quít* who waits for my late coming home patiently during my long days. And my new born daughter *Bòng*, arrived two weeks earlier than expected time, but spends her all day to sleep without long crying, giving me much peaceful time during my thesis writing.

For my Mum and my Dad who follow every step of my life.

For my elder brother that I seldomly see but who supports me mentally (I guess). And my two nieces who I can see their growth only day by day via pictures. For my unique sister-in-law, who swings also between being Mummy and Researcher.

For my in-law family, especially *An*, my preferred one.

For my *Gramp* and my *Tat* who always believe on my ability.

And my grand-mother *Bà Ngoai* and my grand-father *Ông Nôi* that I try to fulfill their expectation.

And at last but not least my unique forever childhood friend-like sister *Trâm* who is always ready for my long complaints.

PUBLICATIONS

1. Tang PM, Zhang DM, **Bui-Xuan NH**, Tsui SK, Waye MM, Kong SK, Fong WP, Fung KP. Photodynamic therapy inhibits P-glycoprotein mediated multidrug resistance via JNK activation in human hepatocellular carcinoma using the photosensitizer pheophorbide a. *Mol Cancer.* 2009, 8:56.

2. Tang PM, **Bui-Xuan NH**, Wong CK, Fung KP. Pheophorbide a mediated photodynamic therapy triggers HLA class I-restricted antigen presentation in human hepatocellular carcinoma. *Transl Oncol.* 2010, 3:144-122.

3. **Bui-Xuan NH**, Tang PM, Wong CK, Fung KP. Photo-activated pheophorbide-a, an active component of Scutellaria barbata, enhances apoptosis via the suppression of ERK-mediated autophagy in the estrogen receptor-negative human breast adenocarcinoma cells MDA-MB-231. *J Ethnopharmacol.* 2010, 131:95-103.

4. **Bui-Xuan NH**, Tang PM, Wong CK, Fung KP. Pheophorbide a: a photosensitizer with immunostimulating activities on mouse macrophage RAW 264.7 cells in the absence of irradiation. *Cell Immunol.* **Revised.**

Remark: Part of the results in this thesis have been published in the above peer-reviewed papers

CONTENTS

CHAPTER 2
Materials and Methods

LIST OF FIGURES

Pa-PDT-treated cells

LIST OF TABLES

ABBREVIATIONS

$^{\circ}C$	Degree Celsius
μg	Microgram
μl	Microliter
μM	Micromolar
$\Delta\psi_m$	Mitochondrial Membrane Potential
%	Percentage
ABCG	ATP-binding cassette sub-family G member 2
ALA	Alpha Lipoic Acid
AO	Acridine Orange
Apaf-1	Apoptotic Protease Activating Factor –1
ATCC	American Type Culture Collection
Bad	Bcl-2-Associated Death Promoter
Bak	Bcl-2 Homologous Antagonist/Killer
Bax	Bcl-2 Associated x Protein
BCA	Bicinchoninic Acid
Bcl-2	B-Cell Leukemia/Lymphoma-2
Bcl-w	Bcl-2-like protein 2
Bid	BH-3 Interacting Domain Death Agonist
Bik	Bcl-2-Interacting Killer
Bim	Bcl-2-interacting mediator of cell death
Blk	B lymphocyte kinase
Bmf	Bcl-2-modifying factor
BNIP3	BCL2/adenovirus E1B 19 kDa protein-interacting protein 3

Bok	Bcl-2-related ovarian killer protein
BZL	Ban Zhi Lian
Caspase	Cysteinyl Aspartic Acid-Protease
CD14	Cluster of differentiation 14
CD16	Cluster of differentiation 16
CD4	Cluster of differentiation 4
CI	Confidence Interval
CLT	Control
cm^2	Square centimeter
CM-H_2DCFDA	5-(and-6)-chloromethyl-2',7'-dichlorodihydrofluorescein diacetate, acetyl ester
CO_2	Carbon Dioxide
CRT	Calreticulin
CT scan	Computerised Tomography Scan
DC	Denritic Cell
DCIS	Ductal Carcinoma In Situ
DES	Diesthylstilbestrol
DMEM	Dulbecco's Modified Eagles's Medium
DMSO	Dehydrated Dimethyl Sulfoxide
DNA	Deoxyribonucleic Acid
DR	Death Receptor
ECL	Enhanced Chemiluminescence
E. coli	*Escherichia coli*
EDTA	Ethylene-Diamine-Tetra-Acetic Acid
e.g.	Exempli Gratia
ELISA	Enzyme-Linked Immunosorbent Assay

ER-α	Estrogen Receptor alpha
ERp57	Protein Disulfide Isomerase Family A, Member 3
ERK	Extracellular Signal-Regulated Kinase
Fas or Fas/CD95	Tumour Necrosis Factor Receptor Superfamily, Member 6
FBS	Fetal Bovine Serum
FITC	Fluorescein Isothiocyanate
g	Relative Centrifuge Force
GM-CSF	Granulocyte-Macrophage Colony-Stimulating Factor
GRP78/BiP	78 kDa Glucose-Regulated Protein/ Binding Immunoglobulin Protein
h	Hour
HER2	Human Epidermal Growth Factor Receptor 2
HLA	Human Leukocyte Antigen
Hrk	Activator of Apoptosis Harakiri
HRP	Horseradish Peroxidase
HSP70	Heat Shock Protein 70
IC$_{50}$	50% Inhibitory Concentration
ICAM-1	Intercellular Adhesion Molecule 1
i.e.	Id Est
IEF	Isoelectric Focusing
IFN-γ	Interferon gamma
IgG	Immunoglobulin G
IL	Interleukin
IPG	Immobilized pH Gradient
J	Joule

JC-1	5,5',6,6'-tetrachloro-1,1',3,3'-tetraethylbenzimidazolyl-carbocyanine iodide
JNK	c-Jun N-terminal Kinase
kDa	Kilo Dalton
LCIS	Lobular Carcinoma In Situ
LH-RH	Luteinizing Hormone-Releasing Hormone
LPS	Lipopolyssacharide
MALDI-TOF MS	Matrix assisted laser desorption-ionization time-of-flight mass spectrometry
MAPK	Mitogen-Activated Protein Kinase
Mcl-1	Induced Myeloid Leukemia Cell Differentiation protein Mcl-1
MDR	Multi-Drug Resistance
mg	Miligram
min	Minute
mm	Milimeter
mM	Milimolar
MTT	Methyl-thiazoldiphenyl Tetrazolium
mW	Mili Watt
NaCl	Sodium Chloride
NaOH	Sodium Hydroxide
NCBI	National Center for Biotechnology Information
NLR	NOD-like Receptor
Noxa	Phorbol-12-Myristate-13-Acetate-Induced Protein 1
nm	Nano meter
p	Probability

p53	Tumour Suppressor Protein 53
Pa	Pheophorbide a
Pa-PDT	Pheophorbide a based Photodynamic Therapy
Pa-PDT-Tam	Pa-PDT combined with Tamoxifen
PARP	Poly(ADP-ribose) Polymerase
PBMC	Peripheral Blood Mononuclear Cell
PBS	Phosphate Buffered Saline
PBS-T	Phosphate Buffered Saline-Tween 20
PDI	Disulfide Isomerase
PDT	Photodynamic Therapy
PKC	Protein Kinase C
pERK	Phosphorylated ERK
PI	Propidium Iodide
pJNK	Phosphorylated JNK
p38	P38 Mitogen-Activated Protein Kinase
pp38	Phosphorylated p38
Puma	p53 Upregulated Modulator of Apoptosis
RLR	RIG-I-like Receptor
RNase A	Ribonuclease A
RNP	Ribonucleoproteins
RNS	Reactive Nitrogen Species
RPMI	Roswell Park Memorial Institute
ROS	Reactive Oxygen Species
SERM	Selective Estrogen Receptor Modulator
SD	Standard Deviation
SDS	Sodium Dodecyl Sulfate

SDS-PAGE	Sodium Dodecyl Sufate Polyacrylamide Gel Electrophoresis
siRNA	Small Interfering Ribonucleic Acid
TAP	Transporter of Antigen Processing
tBid	Truncated Bid
TCM	Traditional Chinese Medicine
TGFβ	Transforming Growth Factor beta
TNF-α	Tumour Necrosis Factor alpha
TNFR	TNF Receptor
TRAIL	TNF-Related Apoptosis-Inducing Ligand
Tris-HCl	Tris(hydroxymethyl)aminomethane-Hydrogen Chloride
UPR	Unfolded Protein Response
V	Volt
v/v	Volume by Volume
VEGF-A	Vascular Endothelial Growth Factor A
VitB2	Vitamin B2
VitB2-PDT	Vitamin B2 based Photodynamic Therapy
W	Watt
WHO	World Health Organization

Chapter 1 – General Introduction

1.1 Breast Cancer

1.1.1 Definition of Breast Cancer

Cancer accounted for 7.4 million deaths worldwide in 2004 and it is estimated to reach 12 million deaths in 2030. Breast Cancer is the fifth most lethal cancer and the most frequent type of cancer among women (WHO, 2009). Breast cancer can be defined as an uncontrolled growth of breast cells. Breast comprises lobes, lobules, glands, ducts and fibrous tissue and breast cells are alimented by lymph vessels and linked to lymph nodes (Figure 1.1).

Lobules   Lobe

Ducts

Nipole

Areola

Fat

Lymph nodes Lymph vessels
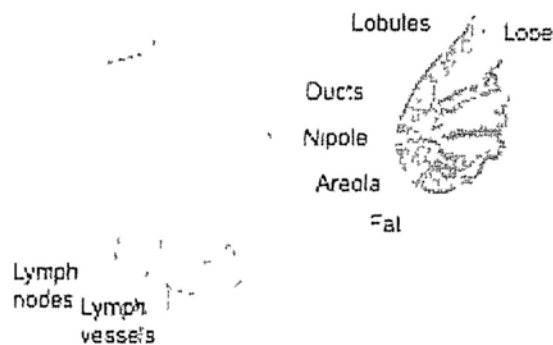
Figure 1.1 – **Structure of the breast** (from U S Department of Heath and Human Services, 2009)

Tumours are cells that overgrow and continuously proliferate. However, tumour can be benign or malignant. Benign tumours can be removed and are not invasive, whereas malignant tumours are difficult to be definitively removed and can become metastatic, being a threat to life. Breast cancer refers to malignant tumour that

has developed from the breast cells. It can begin from the lobules or ducts, rarely from fat and fibrous tissues (U.S Department of heath and human services, 2009).

1.1.2 Causes of breast cancer

5 to 10 % of human cancers are inherited and 90 % are due to genetic changes throughout life due to aging process and life style. Breast cancer is generally due to the mutation of BRCA1 and BRCA2 genes (Duncan *et al.*, 1998). Mutation of those genes in women has 80 % risk of breast cancer before age 50, whereas in men 1 to 6 % risk by age 70, with BRCA1 mutation and BRCA2 mutation respectively. We can distinguish two types of risk factors: risks due to life style and risks due to nature. Breastcancer.org lists out different risks that commonly occur. Most of the risk factors for the development of breast cancer are under control and can be avoided (www.breastcancer.org):

- **Weight:** After menopause, fat tissue becomes the main source of estrogen. Monitoring weight controls estrogen level and thereby lowers breast cancer risk.

- **Diet:** It is still be a controversial issue, however, a low-fat diet rich in fruits and vegetables is generally recommended.

- **Exercise:** Exercise can reduce breast cancer risk. A 45-60 minute of physical exercise on 5 or more days a week is recommended by the American Cancer Society.

- **Alcohol consumption:** Alcohol limits the control of blood levels of estrogen to increase breast cancer risk.

- **Smoking:** Smoking slightly increases risk of breast cancer.

- **Exposure to estrogen:** Long exposure to estrogen increases tumour formation by stimulating breast cells growth.

- **Recent oral contraceptive use:** Slightly increase risk for a limited period of time.

- **Stress and anxiety:** Control stress and anxiety (e.g. by meditation, yoga, visualization exercises, and prayer) may strengthen the immune system.

However there are risk factors that are uncontrollable:

- **Gender:** Women produce more estrogen and progesterone than men and therefore have higher risk of breast cancer.

- **Age:** The risk is 0.43% from age 30 to 39 and increases 4% at age 60.

- **Family history of breast cancer:** Higher risk if a family member experienced breast cancer or ovarian cancer.

- **Personal history of breast cancer:** Higher risk if have breast cancer in one breast or have abnormal breast cells such as atypical hyperplasia, lobular carcinoma in situ (LCIS) or ductal carcinoma in situ (DCIS).

- **Race:** White women are more likely to develop breast cancer than African American women.

- **Radiation therapy to the chest:** The risk is higher if the radiation was given during the young age, while the breasts were still developing.

- **Breast cellular changes:** Hyperplasia and atypical appearance, occur when a breast biopsy is performed.

- **Exposure to estrogen:** Natural exposure such as menstruation, menopause and estrogens in the environment.

- **Pregnancy and breastfeeding:** Reduce the estrogen level by decreasing the overall number of menstrual cycles and therefore lower breast cancer risk.

- **Diesthylstilbestrol (DES) exposure:** DES prevents miscarriage but increase risk of breast cancer.

- **Genome changes:** Mutation in genes such as BRCA1 or BRCA2 increases the risk of breast cancer.

- **Breast density:** Women with larger area of dense tissue from mammograms show higher risk.

1.1.3 Staging

Breast cancer is classified by different stages. Those information describe the nature of the cancer based on the tumour size, invasion nature, the involvement of lymph nodes and the spread of cancer site. To determine the staging of breast cancer, blood tests and other tests such as bone scan, CT scan and lymph node biopsy are performed. We can classify breast cancer into 4 stages (Table 1.1).

(A)   **(B)**
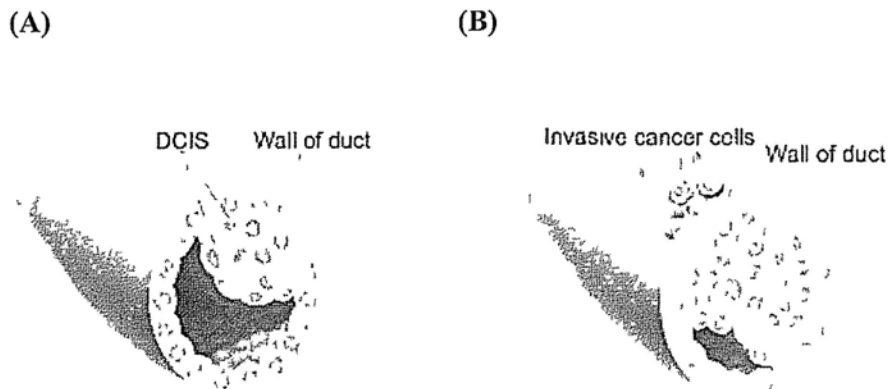
Figure 1.2 – Ductal carcinoma in situ (A) and invasive breast cells (B) (from U S Department of Heath and Human Services, 2009)

Stage	Invasive	At breast site	Tumour size	Spread to lymph nodes	Spread to other structures	
0	No	DCIS or LCIS				
I	Yes	Yes	<2cm	No		
IIA	Yes	No		Axillary lymph nodes		OR
	Yes	Yes	<2cm	Axillary lymph nodes		OR
	Yes	Yes	2cm < size <5cm	No		
IIB	Yes	Yes	2cm < size <5cm	Axillary lymph nodes		OR
	Yes	Yes	> 5cm	No		
IIIA	Yes	No		• Axillary lymph nodes and clumped together or sticking to other structures • Lymph nodes near the breastbone		OR
	Yes	Yes	< 5cm	Axillary lymph nodes and clumped together or sticking to other structures		OR
	Yes	Yes	> 5cm	Axillary lymph nodes and clumped together or sticking to other structures		
IIIB	Yes	Yes	Any size		Chest wall and/or skin of the breast	AND
				• Axillary lymph nodes and clumped together or sticking to other structures • OR lymph nodes near the breastbone		

5

	Yes/No				AND
IIIC	Yes	Any size	Lymph nodes above or below the collarbone	Chest wall and/or skin of the breast	AND
			• Axillary lymph nodes and clumped together or sticking to other structures • OR lymph nodes near the breastbone		
IV	Yes			Other organs such as lugs, liver, bone or brain	

Table 1.1 – Stages of Breast Cancer (modified from breastcancer.org)

1.2. Treatment methods

1.2.1 Surgery

Surgery is the most common treatment for breast cancer. We distinguish two types of surgery: breast-sparing surgery and mastectomy (Veronesi *et al.*, 2002).

- **Breast-sparing surgery:** Also called breast-conserving surgery. It comprises a lumpectomy or a segmental mastectomy. It consists of removing only the cancer but not the breast.

- **Mastectomy:** It is the removal of the entire breast.

After a surgery, other options may happen.

- **Lymph node removal:** removal of one or more lymph nodes

- **Breast reconstruction:** a plastic surgery to rebuilt the breast

- **Prophylactic mastectomy:** a preventive removal of the breast in high-risk people.

- **Prophylactic ovary removal:** preventive surgery to lower estrogen level

- **Cryotherapy:** Also called cryosurgery. An experimental treatment by applying extreme cold system to kill tumour.

1.2.2 Chemotherapy

Chemotherapy uses chemicals to weaken and induce cancer cells death (McKnight, 2003). A combination of drugs is often used to increase the efficiency. Chemotherapy is applied both in early-stage breast cancer after surgery to reduce the risk of new cancer and in advanced-stage breast cancer to reduce cancer cells about 30

to 60 %. Chemotherapy can also be applied before surgery to shrink the tumour size. We distinguish two groups of chemotherapy medicines:

- **Anthracyclines:** which damage the gene of cancer cells. They are adriamycin, Ellence and daunorubicin (Minotti *et al.*, 2004).

- **Taxanes:** interfere with the cell cycle (Takimoto and Calvo, 2008). They are Taxol, Taxotere and Abraxane.

1.2.3 Radiation Therapy

Radiation therapy – also called radiotherapy – is a post surgery treatment. It can reduce the breast cancer recurrence by about 70% by high-energy rays (Camphausen and Cola, 2008). There are two types of radiation:

- **External radiation therapy:** the radiation is applied from outside the body.

- **Internal radiation therapy:** also called implant radiation therapy or brachytherapy. Radioactive substance is loaded inside the tube that is connected into the breast.

1.2.4 Hormonal Therapy

Hormonal therapy is effective only for hormone-receptor positive breast cancers, which comprise about 80% of breast cancer. It acts on estrogen level to inhibit tumour growth. It depends on the age of the patient and that different types of drugs are used.

1.2.4.1 Before menopause

- **Tamoxifen:** an antagonist of the estrogen receptor competes with estradiol to bind to estrogen receptor and therefore decrease the efficiency of estrogen to induce breast cell growth (Brauch *et al.*, 2009).

- **LH-RH** (luteinizing hormone-releasing hormone) **agonist:** a compound that is similar to LH-RH acts on the brain to stop estrogen production (Goel *et al.*, 2009)

- **Oophorectomy:** the surgical removal of an ovary or ovaries to prevent estrogen release from the ovary (Rebbeck *et al.*, 2002).

1.2.4.2 After menopause

- **Aromatase inhibitors:** a class of drugs to block aromatase which converts androgen into estrogen (Gibson *et al.*, 2009)

- **Tamoxifen:** competes with estradiol to bind to estrogen receptor and therefore decreases the efficiency of estrogen to induce breast cell growth (Brauch *et al.*, 2009).

1.2.5 Targeted Therapies

Targeted therapies use drugs that act on a specific target of cancer cells to block cancer growth (Widakowich *et al.*, 2007). Nowadays, three drugs are commonly used:

- **Herceptin** (trastuzumab): acts against HER2-positive breast cancers by binding to HER2 receptor resulting in cancer growth inhibition.

- **Tykerb** (Lapatinib): interferes HER2-related kinases resulting in cancer growth inhibition.

- **Avastin** (Bevacizumab): It is a humanized monoclonal antibody that recognizes and blocks vascular endothelial growth factor A (VEGF-A). VEGF-A is a chemical signal that stimulates the growth of new blood vessels (angiogenesis). Therefore it is a drug against metastatic HER2-negative breast cancer.

1.2.6 Side effects

Each treatment for breast cancer is associated with different side effects. The severity is more or less important depending on the treatment type, the stage of cancer and the physiology of the patient. Table 1.2 below shows different side effects and the concerned treatment type.

Side effects	Surgery	Chemotherapy	Radiation Therapy	Hormonal Therapy	Targeted Therapies	Others
Abdominal Pain						
Addiction		x		Faslodex	Tykerb	Pain medications (e.g. morphine, Demerol, OxyContin
Allergic Reactions	Antibiotics	x		Arimidex, Aromasin, Femara, tamoxifen, Evista, Fareston, Faslodex	Herceptin, Tykerb, Avastin	Pain medications
Anemia		x			Herceptin	
Anxiety		x		Arimidex, Aromasin, Femara, tamoxifen, Evista, Fareston, Faslodex		Pain medications
Appetite Change	x	x	x	Arimidex, Aromasin, Femara, tamoxifen, Evista, Fareston, Faslodex	Herceptin, Tykerb, Avastin	Pain medications
Armpit Discomfort	lumpectomy, mastectomy, lymph node removal					
Back Pain				Faslodex, Femara		Pain medications (e.g. ibuprofen, naproxen)
Bleeding and Bruising Problems		x		Fareston	Tykerb	Pain medications (e.g. aspirin)
Blood Clots and Phlebitis	lymph node removal	x		tamoxifen, Evista, Fareston	Avastin	
Bone and Joint Pain		x		Arimidex, Aromasin, Femara, tamoxifen, Evista, Fareston, Faslodex		Pain medications (e.g. Feldene), osteoporosis medications (e.g. bis-

						phosphonates)
Breathing Problems		x	x	Femara, tamoxifen, Evista, Fareston, Faslodex	Herceptin, Tykerb	Pain medications (e.g. acetaminophen, aspirin, ibuprofen, opiates)
Chest Pain	x		x			Implant
Cold and Flu Symptoms		x		Evista, Faslodex	Herceptin	Pain medications (e.g. ibuprofen, morphine)
Constipation		x		Faslodex, Fareston		Pain medications (e.g. ibuprofen, morphine, codeines, opiates)
Coughing		x	x	Faslodex, Femara		
Dehydration		x				Vomitting, diarrhea
Delay Wound Healing					Avastin	
Depression		x		Arimidex, Aromasin, Femara, tamoxifen, Evista, Fareston, Faslodex		Ovarian removal, pain medications (e.g. opiates)
Diarrhea		x		Faslodex	Avastin, Tykerb	Osteoporosis medications (e.g. bis-phosphonates), pain medications (e.g. ibuprofen, morphine)
Dizziness		x		Faslodex	Herceptin	Antihistamines, antiseizure, antidepressants, tranquilizers, pain medications
Dry Mouth		x				Pain medications, antihistamines, antidepressants
Dry Skin		x	x	x		
Electrolyte		x				Vomiting, diarrhea

Symptom					
Imbalance					
Endometriosis			tamoxifen		
Fainting	x				Pain medications (e.g. morphine, codeine), dehydration, heart problems
Fatigue	x	x	Aridimex, Aromasin, Femara, tamoxifen, Evista, Fareston, Faslodex	Tykerb	Pain medications (e.g. morphine, codeine)
Fertility Issues	x		tamoxifem, Evista, Fareston		Ovarin shutdown
Fever	x	x		Herceptin	Pain medications (e.g. morphine, ibuprofen)
Flatulence	x				Constipation, diarrhea, antibiotics, laxatives, pain medications (e.g. naproxen, ibuprofen)
Hair Changes	x	x	tamoxifem, Aridimex		
Palmar-Plantar Erythrodysesthesia (PPE)	Xeloda, Adrucil, Adriamycin			Tykerb	
Headache	x		Arimidex, Aromasin, Femara, tamoxifen, Evista, Fareston, Faslodex	Herceptin	Pain medications, osteoporosis medications (e.g. bis-phosphonates)
Hearing Problems	x				Pain, antibiotic, anti-nausea medications
Heart Problems	x, Adriamycin	x	Aridimex, Aromasin, Femara, tamoxifen, Faslodex	Herceptin	
Gastro-Esophageal Reflux Disease	x			Tykerb	osteoporosis medications (e.g. bis-

						phosphonates), pain medications (e.g. aspirin, ibuprofen)
(GERD)						
Hematoma	Lymph node removal, lumpectomy, mastectomy					
Hypertension				Arimidex, Aromasin, Femara, tamofixen, Evista, Fareston, Faslodex	Avastin, Herceptin	Pain medicines
High Cholesterol		Halotestin		Femara, Arimidex		
Hot Flashes		x		Aridimex, Aromasin, Femara, tamoxifen, Evista, Fareston, Faslodex		Ovarian shutdown
Infection		x	x	Aridimex, Aromasin, Femara, tamoxifen, Evista, Fareston, Faslodex	Herceptin, Tykerb, Avastin	Pain medicines
Injection Site Reaction		x				
Insomnia		x		Faslodex, Arimidex, Aromasin	Tykerb	Pain medications
Itching		x	x	Aridimex, Aromasin, Femara, tamoxifen, Evista, Fareston, Faslodex		Allergic reaction to pain medications
Kidney Problems		x			Avastin	Pain medications (e.g. aspirin, ibuprofen, naproxen, naproxen sodium, Orudis, Indocin, Feldene, Relafen
Leg Cramps				tamoxifen, Evista		
Hepatotoxity		x		tamoxifen		Pain and anti-inflammatory

						medications (e.g. acetaminophen, aspirin, naproxen, Relafen, steroids
Lost of Libido						Breast cancer treatment side effects (e.g. anxiety, depression, etc.), pain medications
Hypotension		x			Herceptin	Anemia, dehydration, heart problems, infection, gastrointestinal issues
Low White Blood Cell Count		x	x		Herceptin, Tykerb, Avastin	
Lung Problems		x	x	tamoxifen	Herceptin	
Lymphedema	lymph node removal	steroids	lymph node			
Memory Loss		x	x	Aridimex, Aromasin, Femara, tamoxifen, Evista, Fareston, Faslodex		Ovarian removal, insomnia, fatigue, steroids, anti-depressants, sleeping pills, pain medications
Menopause and Menopausal Symptoms		x	x	Aridimex, Aromasin, Femara, tamoxifen, Evista, Fareston, Faslodex		Ovarian shutdown
Mood Swings				Aridimex, Aromasin, Femara, tamoxifen, Evista, Fareston, Faslodex		Ovarian removal, morphine, Duragesic, Dolophine, codeine, hydrocodone, Demerol, steroids
Mucositis		x	x		Herceptin, Tykerb, Avastin	
Myalgia		x	x	Aridimex, Aromasin, Femara,	Herceptin	Osteoporosis medications (e.g.

					bis-phosphonates)
			tamoxifen, Evista, Fareston, Faslodex		
Nail Changes		x	tamoxifen		
Nausea	x	x	Aridimex, Aromasin, Femara, tamoxifen, Evista, Fareston, Faslodex	Herceptin, Tykerb, Avastin	Pain medications (e.g. naproxen sodium, Orudis, Indocin, Relafen, oxycodone, Duragesic, morphine, Dolophine, codeine, hydrocodone, Dilaudid, Demerol), constipation, dehydration
Neuropathy	x	x	Faslodex, Arimidex	Avastin	
Nosebleeds	x	x		Avastin	Pain medications (e.g. aspirin)
Numbness	x	x	Faslodex	Avastin, Tykerb	Pain medicines (e.g. Duragesic)
Osteonecrosis of the Jaw					Osteoporosis medications (e.g. Fosamax, Actonel, Boniva, Aredia, Zometa, Bonefos)
Osteoporosis	x	x	Arimidex, Aromasin, Femara		Ovarian shutdown
Pain	x	x	Aridimex, Aromasin, Femara, tamoxifen, Evista, Fareston, Faslodex	Avastin, Herceptin, Tykerb	Numbness, itching, neuropathy, swelling, depression, fatigue, pain medications
Phantom Breast Pain	Mastectomy				
Post-Traumatic Stress Disorder					Breast cancer diagnosis, cancer recurrence
Rash	x	x	Aridimex, Aromasin, Femara, tamoxifen, Evista, Fareston,	Avastin, Herceptin, Tykerb	Pain medications

			Faslodex	Herceptin	
Runny Nose					
Scar Tissue Formation	x	x			
Seroma	x				
Skin Discoloration	x	x			Pain medications, rash, injection reaction
Skin Sensitivity	x	x			
Sore Throat		x	Faslodex, Arimidex	Tykerb	Pain medications
Swallowing Problems		x			Pain medications, osteoporosis medications (e.g. Zometa, Aredia, Bonefos)
Sweating		x	Aridimex, Aromasin, Femara, tamoxifen, Evista, Fareston, Faslodex		Ovarian shutdown, pain medications
Swelling	x	x	Aridimex, Aromasin, Femara, tamoxifen, Evista, Fareston, Faslodex		Pain and osteoporosis medications, steroids
Taste and Smell Changes		x		Avastin	Pain medications
Urinary Tract Infection (UTI)		x			
Urine Discoloration	x				Multivitamins, dehydration
Vaginal Discharge		x	tamofixen, Fareston		Osteoporosis medications
Vaginal Dryness		x	Aridimex, Aromasin, Femara, tamoxifen, Evista, Fareston, Faslodex		Ovarian shutdown
Vision and Eye		x	Tamoxifen, Fareston, Aromasin	Avastin	Osteoporosis medications (e.g.

Problems				Zometa, Reclast), pain medications
Vomitting	x	Femara, Arimidex, Faslodex	Herceptin, Tykerb	Ovarian shutdown with Lupron, pain medications, anticonvulsants, osteoporosis medications
Weakness	x	Aridimex, Aromasin, Femara, tamoxifen, Evista, Fareston, Faslodex	Avastin, Herceptin, Tykerb	Ovarian shutdown with Lupron, pain medications, anticonvulsants, antidepressants
Weight Changes	x	Aridimex, Aromasin, Femara, tamoxifen, Evista, Fareston, Faslodex	Avastin	Pain medications, anticonvulsants, osteoporosis medications, steroids

Table 1.2 – Side effects of breast cancer treatments (modified from breastcancer.org)

1.3 New alternatives

From the table above, each method for breast cancer treatment engenders several side effects that can weaken the patient health. Special cares are needed to support patients with cancer. Nevertheless, some patients suffer more from side effects than cancer itself. Researchers and doctors are continuously looking for new alternatives to treat cancer with milder and controlled side effects, e.g. minimizing the damage of the immune function.

1.3.1 Traditional Medicine

One of the new alternative is looking inside archaic medicine such as herbal, Ayurveda, Siddha medicine, Unani, ancient Iranian medicine, Islamic medicine, traditional Chinese medicine, acupuncture, Muti, Ifá, traditional African medicine etc. Those methods are called traditional medicine which is defined by the World Health Organization (WHO) as: "the health practices, approaches, knowledge and beliefs incorporating plant, animal and mineral-based medicines, spiritual therapies, manual techniques and exercises, applied singularly or in combination to treat, diagnose and prevent illnesses or maintain well-being." (WHO, 2008). In our study, we focused on traditional Chinese medicine (TCM) as an alternative to treat cancer.

TCM is explored about 2000 to 3000 years ago, originated from China. The diagnosis is based on the yin-yang and five element theories. TCM comprises acupuncture, herbal medicine and gigong exercises. TCM is a complex system to understand and practice. In the present study, we focused in the herbal remedies. Herbs are derived from plant, animal, and mineral substances. Each herb is qualified

19

according to four properties according to the theory of TCM: nature, taste, affinity and primary action.

- **Nature:** It is described as cooling or heating, but it can also be defined as moistening, relaxing and energizing.

- **Taste:** There are five tastes: sour, bitter, sweet, spicy and salty. Herbs with different tastes are used to treat different conditions.

- **Affinity:** It is the affinity of a herb for a particular organ network.

- **Primary action:** It refers to the primary effect of the herb: dispel, astringe, purge or tonify.

1.3.2 Scutellaria barbata

Scutellaria barbata, Ban Zhi Lian (半枝蓮) in Chinese, is belonged to the Labiatae family. The plant is a small-leaved mint, producing purple flowers (Figure 1.3). It is grown in the southeast of the Yellow River and collected in early June while it blooms. Only the top of the plant is called Scutellaria which is different from the root part called as *Scutellaria baicalensis*(黃芩) (Dharmananda, 2004).
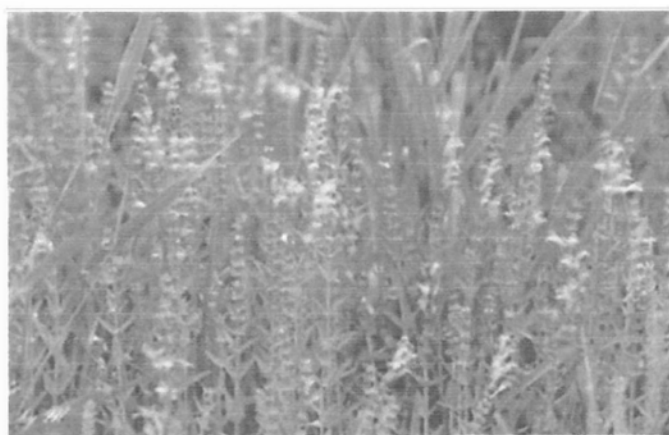
Figure 1.3 – Scutellaria barbata (from Dharmananda, 2004)

1.3.2.1 Scutellaria barbata use in TCM

Together with Oldenlandia, Scutellaria are used in modern Chinese Medicine for treatment of viral infections and cancers and also acne, boils and other skin ailments (Dharmananda, 2004). *Scutellaria barbata* is seldomly used in TCM but becomes intensively prescribed and studied in the 20th century due to its potential in cancer treatment. The herb is composed essentially of alkaloids and flavones (Jiangsu New Medical College, 1977). The main components of its essential oil are hexahydrofarnesylacetone, 3,7,11,15-tetramethyl-2-hexadecen-1-ol, menthol and 1-octen-3-ol, and showed antimicrobial activity (Yu *et al.*, 2004).

1.3.2.2 Clinical trial of BZL-101 for breast cancer

Recently, anti-cancer property of Scutellaria barbata has been reported and the clinical trial of its water extract, called BZL-101, for advanced breast cancer treatment is ongoing in US (Rugo *et al.*, 2007; Fong *et al.*, 2008; Perez *et al.*, 2010). In the phase 1 clinical trial, BZL-101 inhibits breast cancer cell line by inducing apoptosis. It was safe and demonstrated adequate toxicity (Rugo *et al.*, 2007). In the phase 1B clinical trial, oral administration of BZL-101 was safe, tolerated, and showed potential antitumour activity for metastatic breast cancer women (Perez *et al.*, 2010).

1.3.3 Pheophorbide a and photodynamic therapy

Scutellaria barbata is used to treat cancer in TCM, especially used as formula to treat liver disease. Previous studies have shown that the water and organic solvent extracts of *Scutellaria barbata* can significantly inhibit the growth of human tumours (Wong *et al.*, 2009; Dai *et al.*, 2008; Kim *et al.*, 2008; Kim *et al.*, 2007; Suh *et al.*,

2007; Goh *et al.*, 2005; Cha *et al.*, 2004; Yin *et al.*, 2004). However, limited works have been attempted to elucidate its active components (Wu and Chen, 2009; Yu *et al.*, 2007). Our previous study revealed that Pheophorbide a (Pa), is one of the active components purified from *Scutellaria barbata* by using a bioassay-guided method, possessing anti-tumour activity (Chan *et al.*, 2006), that is consistent with other reports about Pa (Nakamura *et al.*, 1996; Hibasami *et al.*, 2000). Pa has been commercial available as it can be purified from a number of traditional medicine sources such as *Scutellaria barbata*, *Psychotria acuminata*, as well as silkworm excreta (Chan *et al.*, 2006; Glinski *et al.*, 1995; Lim *et al.*, 2002).

1.3.3.1 Pheophorbide a

Pheophorbide a is a derivative product of chlorophyll a degradation during leaf senescence. The chlorophyll breakdown pathway is fully understood only in the beginning of 2000s. It starts with the removal of phytol and magnesium (Pruzinská *et al.*, 2007) leading to the formation of pheophorbide a (Figure 1.4). Thus, pheophorbide a is formed during the early stage of the chlorophyll degradation while the tetrapyrrol macrocyclic ring is not yet cleaved. Therefore, the photodynamic action of pheophorbide a is still kept and the Pa is greenish in color.
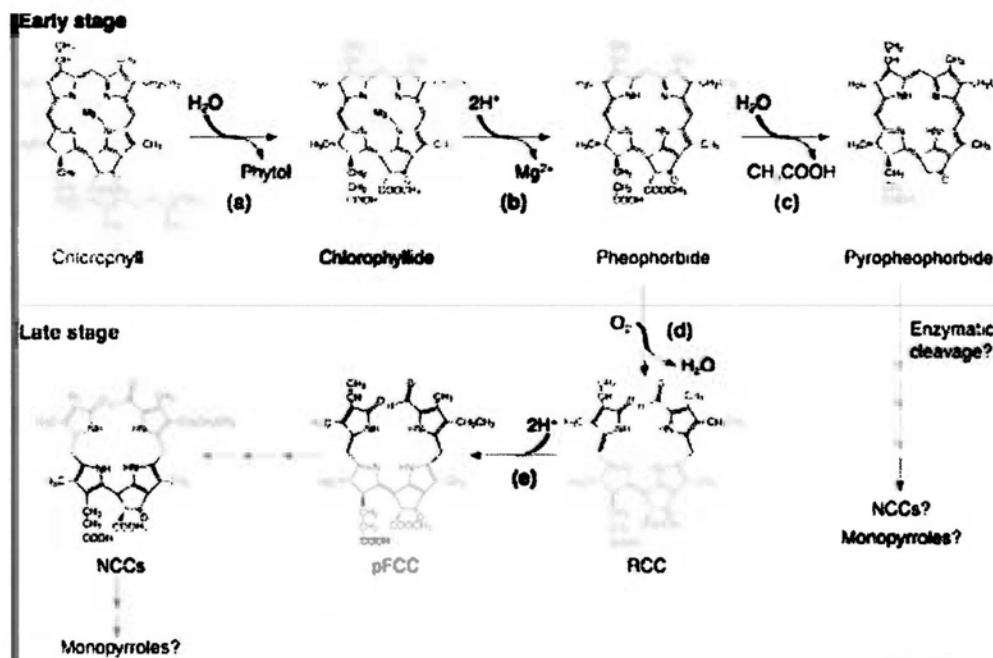
Figure 1.4 – Chlorophyll a degradation pathway (from Takamiya *et al.*, 2000)

Belonging to porphyrin family, the fluorescent spectrum of Pa shows an excitation wavelength at 680 nm. This property confers to Pa as a potential photosensitizer suitable for photodynamic therapy (PDT). Common photosensitizers actually are commercially available, either in trials or in development processes in clinics. However, their shorter wavelength limits their penetration (Table 1.3). Pheophorbide a based photodynamic therapy (Pa-PDT) promises a good new therapy in treating cancer.

1.3.3.2 The Principle of photodynamic therapy

Therapy based on light energy has been utilized for treating various human diseases in the ancient civilizations such as Egyptian, Indian and Chinese three thousand years ago (Dougherty *et al.*, 1992). However, PDT has been scientifically named since the end of the nineteenth century (Daniell and Hill, 1991; Ackroyd *et al.*, 2001), and the therapeutic potential of PDT was firstly investigated by Raab in 1900 and nominated by Tappeiner and Jesoniek in 1903 (Rabb, 1900; Tappeiner and

23

Jesoniek, 1903). PDT is achieved by the synergistic effect of two non-toxic elements: photosensitizer and light energy, where photosensitizer is a kind of molecule that can be accumulated more or less specifically in the malignant tissue and the introduction of light illumination with suitable wavelength will excite the photosensitizer to produce reactive oxygen species (ROS) that are toxic to the treated cancer cells (Buytaert et al., 2007).
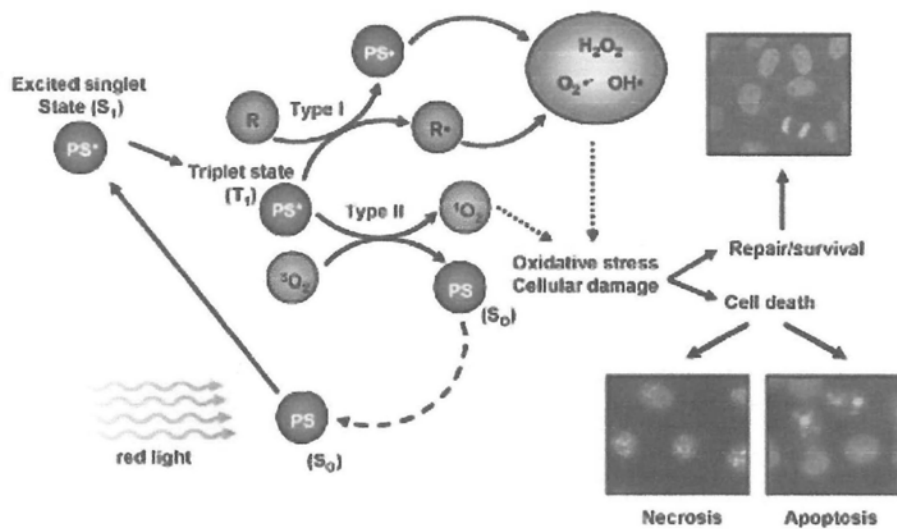
Figure 1.5 – Photodynamic Therapy mechanism (modified from Juarranz et al., 2008)

Recently, PDT has been approved in developed countries for treating actinic keratosis, macular degeneration, Barrett's esophagus, obstructing esophageal carcinoma, early and obstructing tracheobronchial carcinoma, palliative treatment of head and neck cancer, and basal and squamous cell skin cancers (Klein et al., 2008; Biel, 2006).

Allison et al. (2004) proposed a guideline for good photosentitizers comprising 19 criteria: toxicity, mutagenicity/carcinogenicity, elimination,

selectivity/targetability, activation, sunlight precautions, administration, indications, reliability, pain-free therapy, outpatient therapy, availability, cost, safety, biochemistry, wavelength, integrative ability, forgiving, and transparency. Porfimer sodium (Photofrin®) is the first photosensitizer approved for clinical use that is developed by Macdonald and Dougherty (2001). New photosensitizers are still being developed, and the second-generation photosensitizers can be classified into different groups: phthalocyanine, porphyrin, chlorin, chloromethyl-X-Rosamine, phenantroperylenequinone, chlorophyll-a derivative and porphycene (McCaughan, 1999). We herein compare the quantitative criteria such as wavelength and cost.

Platform	Drug	Substance	Wavelength (nm)	Cost
Porphyrin	Photofrin	HpD	630	15mg, 257 euros
Porphyrin	Levulan	ALA	400-450/635	100 USD / tube (Zane et al., 2007)
Porphyrin	Metvix	M-ALA	635	168mg, 306 euros
Porphyrin	Visudyne	Vertiporfin	689	15mg/10ml, 1256 euros
Texaphyrin	Antrin	Lutexaphyrin	730	n/a
Chlorin	Foscan	Temoporfin	650	4mg/5ml, 5848 euros
Chlorin	LS11	Talaporfin	660	n/a
Chlorin	Photochlor	HPPH	665	n/a
Dye	Photosens	Phthalocyanine	675	n/a
Porphyrin		**Pheophorbide a**	680	50 mg, 58 USD (Frontier Scientific Inc.)

Table 1.3 – Comparison between Pheophorbide a and other photosensitizers (modified from Allison et al., 2004; Potelle et al., 2008)

Photosensitizers tend to localize in tumour site and the light is illuminated specifically on the tumour. However, PDT can cause burns, swelling, pain, and scarring in nearby healthy tissue (Vrouenraets et al., 2003). Other side effects of PDT are related to the area that is treated and are only temporary, including coughing, trouble swallowing, stomach pain, painful breathing or shortness of breath.

25

1.3.3.3 Research of Pa-PDT

Many studies have been conducted to clarify the capacity of photosensitizers in cancer eradication during PDT (Marchal *et al.*, 2005; Kinzler *et al.*, 2007; Rodriguez *et al.*, 2009; O'Connor *et al.*, 2009). At a very high dose, Pa exerts anti-tumour activity by disrupting the integrity of tumour DNA (Nakamura *et al.*, 1996; Hibasami *et al.*, 2000; Chan *et al.*, 2006). Previous study on anti-tumour activity of Pa revealed that the photo-activity of Pa (Pa-PDT) enhances cancer suppression and reduces the effective Pa dosages (Hajri *et al.*, 2002; Lee *et al.*, 2004; Lim *et al.*, 2004; Li *et al.*, 2007; Rapozzi *et al.*, 2009). Our group demonstrated that pheophorbide-a is a natural efficient photosensitizer for cancer treatment (Tang *et al.*, 2006; Tang *et al.*, 2009a; Tang *et al.*, 2009b; Tang *et al.*, 2010; Bui-Xuan *et al.*, 2010). Pa is also attributed to many different functions. Pa has been shown to be a specific probe for ATP-binding cassette sub-family G member 2 (ABCG) protein, a protein involving in multidrug resistance (Robey *et al.*, 2004). On the other hand, Pa can be modified to enhance its photodynamic activity (Iriuchishima *et al.*, 2008; Galindev *et al.*, 2008; Knop *et al.*, 2009). Pa attributes many diverse properties including chlorophyll degradation, anti-tumour proliferation and serves as a special probe for P-glycoprotein function and inhibition.

1.4 Aim of the study

Breast is an outgrowing organ which facilitates the use of photodynamic therapy comparing to other internal organs such as liver or lung. No studies of the effect of Pa-PDT on breast cancer have been reported. We propose for the first time to

investigate the therapeutic potential of Pa-PDT on human advanced breast cancer using MB-MDA-231 cell line as the model. MB-MDA-231 cells are nude of estrogen-receptor alpha and therefore mimic the advanced stage of breast cancer. We investigate the effects of Pa-PDT on different aspects including the mechanistic study of Pa-PDT inducing cell death and the immunomodulation of Pa-PDT. In pratical PDT, Pa is injected into the blood stream. Therefore, the effects of Pa without PDT on the immune competent cells are also investigated to find whether Pa influence the immune system of the body. A macrophage murine cell line RAW 267.3 and human peripheral blood mononuclear cells (PBMCs) are used to investigate the immuno-stimulating effects of Pa on the immune competent cells. My study is divided in two main parts: the direct cytotoxicity of Pa-PDT towards the cancer cells and the immunomodulation of Pa-PDT or Pa alone.

Chapter 2

Materials and Methods

2.1 Materials

All chemicals were purchased from Sigma Chemical Co (St Louis, MO, USA). Pheophorbide-a was purchased from Frontier Scientific Inc (Logan, UT, USA). A 4mM stock solution of pheophorbide-a was prepared by dissolving Pa powder in dehydrated dimethyl sulfoxide (DMSO) and ethanol in the v/v ratio 1:9. Riboflavin was dissolved in NaOH solution to obtain stock solution at 1mM. Further dilutions were performed using culture media.

2.2 MDA-MB-231 and MCF-7 cell cultures

The human breast adenocarcinoma cell line MDA-MB-231 (e.g. estrogen receptor negative) and MCF-7 (e.g. estrogen receptor positive) was purchased from the American Type Culture Collection (Manassas, VA, USA). The cell line was maintained in RPMI-1640 medium supplemented with 10 % fetal bovine serum and 1% v/v antibiotics (penicillin and streptomycin) (Invitrogen Co, Carlsbad, CA, USA). The cells in the growth media were incubated at 37°C under 5% CO_2 in a humidified incubator.

2.3 Murine macrophage culture

Murine RAW 264.7 macrophages were purchased from the American Type Culture Collection (Rockville, MD, USA). The cells were maintained in Dulbecco's Modified Eagles's Medium (DMEM) supplemented with 10 % of heat-inactivated fetal bovine serum and 1 % v/v of antibiotics (penicillin and streptomycin) (Invitrogen, Carlsbad, CA, USA) at 37°C with 5 % CO_2.

2.4 Primary human monocyte and lymphocyte culture

Fresh human buffy coat obtained from healthy volunteers of Hong Kong Red Cross Blood Transfusion Service was diluted two-fold with PBS at 4°C and centrifuged using an isotonic Percoll solution (density 1.082 g/ml; Amersham and Pharmacia Biotech, Uppsala, Sweden) for 30 min at 1000g without deceleration. After centrifugation, four layers of fluids appeared in the column. The thin white interface between the top and third layers containing the viable peripheral blood mononuclear cells including lymphocytes and monocytes was collected. The collected peripheral blood mononuclear cells were cultured with RPMI for 2 h, and the adherent cells in the culture flask were used as human monocytes and suspended cells were considerate as human lymphocytes.

2.5 Illumination of photosensitizer

Cells were pre-loaded with photosensitizer (Pa or riboflavin). Following incubation, the cells were irradiated for 20 min using a 600 W quartz-halogen lamp with infrared irradiation attenuated by a 10 cm layer of water and a coloured filter cut-on 610 nm as described in our previous studies. The light intensity was 70 mW/cm^2 (i.e., 20 min of irradiation = 84 J/cm^2).

2.6 Measurement of cell viability

2.6.1 Measurement of cytotoxicity induced by Pa-PDT

The survival rate of tested cells was measured by methyl-thiazoldiphenyl tetrazolium (MTT) assay. MDA-MB-231 cells (1 x 10^4/well) were seeded on each well of a 96-

well culture plate and incubated for 24 h to allow attachment. After treatment with photosensitizer or vehicle control and tamoxifen for 2 h and the subsequent photo-activation, the cells were incubated at 37°C for another 24 h. For tamoxifen treatment without combined to PDT, tamoxifen with various concentrations were added to the cells and kept in dark for 24 h before the assay. For assay with MAPK inhibitors, after treatment with appropriate concentrations of Pa with or without MAPK inhibitors (Merck Biosciences, San Diego, CA, USA) and the subsequent photo-activation, the cells were incubated at 37°C for another 24 h. For Pa treatment without PDT, appropriate concentrations of Pa were added to the cells and kept in dark for 24 h before the assay. Culture medium was removed and 30 µl MTT solution (5 mg/ml in PBS) was added to each well and incubated for 4 h at 37°C. After the removal of MTT solution, 100 µl DMSO was added to each well to dissolve the formazan dye. The absorbance at 540 nm was measured and the data obtained were presented as the percentage of control.

2.6.2 Measurement of cell growth stimulated by Pa

RAW 264.7 cells (5 x 10^3) were seeded in 96-well plate and incubated at 37°C to allow attachment. The cells were then treated with vehicle control or Pa with various concentrations or 5 µM of MEK1/2 inhibitor (U0126) (Promega Corporation, Madinson, WI, USA) for 24, 48 or 72 h in dark. Culture medium was removed and 30 µl methyl-thiazoldiphenyl tetrazolium (MTT) solution (5 mg/ml in sterilized PBS) was added to each well and incubated for 2 h at 37°C. DMSO was added (100 µl) to each well to dissolve the formazan dye after removing MTT solution. The absorbance at 540 nm was read and the data obtained were presented as the percentage of control.

2.7 Intracellular localization of Pa

MDA-MB-231 cells or RAW 264.7 cells (5×10^4/well) grown on the coverslip were incubated with 4 µM Pa at 37°C for 2 h without PDT treatment. After washing with PBS, the cells were then incubated with 800 nM MitoTracker Green (Molecular Probe, CA, USA) for further 45 min at 37°C in dark. The fluorescence of Pa or MitoTracker was observed by using a Nikon TE2000 fluorescence microscope (Nikon Corp., Japan) with an excitation wavelength at 578 nm or 490 nm; and an emission wavelength at 610 nm or 516 nm, respectively. The images of Pa were assigned as red, and MitoTracker Green were shown in green. Images were merged together by using the MetaMorph software (MDS Inc, CA, USA).

2.8 Detection of the change in mitochondrial membrane potential ($\Delta\Psi m$)

MDA-MB-231 cells (3×10^5/well) or RAW 264.7 cells (3×10^5/well) or human immune competent cells (10^6/well) were seeded on each well of a 6-well culture plate and incubated 24 h to allow attachment. The Pa-PDT treated cells were harvested and washed twice with cold PBS at 1 h. Membrane potentials of MDA-MB-231 cells were analyzed by flow cytometry after staining for 15 min at 37°C with 10 µg/ml JC-1 (5,5',6,6'-tetrachloro-1,1',3,3'-tetraethylbenzimidazolyl-carbocyanine iodide) (Invitrogen, Carlsbad, CA, USA), a fluorescent cationic dye that binds to polarized mitochondrial membrane and accumulates as aggregates in the mitochondria of normal cells. The mitochondrial membrane potential was analyzed by FACSCanto flow cytometer (Becton, Dickinson & Company, CA, USA) using argon excitation at 488 nm.

2.9 Measurement of ROS concentration

The ROS concentration was detected using 5-(and-6)-chloromethyl-2',7'-dichlorodihydrofluorescein diacetate, acetyl ester (CM-H$_2$DCFDA) dye (Invitrogen, Carlsbad, CA, USA) (Limoli et al., 2003). MDA-MB-231 cells (10^4/well) or RAW 264.7 cells (5 x 10^3/well) or human immune competent cells (10^4/well) were seeded in 96-well plate and incubated overnight at 37°C to allow attachment. The MDA-MB-231 cells were then treated with the vehicle control or with various drug concentrations for 2 h following by photo-activation. For RAW 264.7 cells, cells were treated with the vehicle control or with Pa in dark. At 4 h or 24 h later (e.g. for MDA-MB-231 cells or RAW 264.7 cells, respectively), culture medium was removed and cells were gently rinsed with PBS and incubated with 10 μM of dye at 37°C for 10 minutes in dark. Fluorescence signals were acquired by a FLUOstar Galaxy plate reader (BMG Labtech, Offenburg, Germany) with the excitation and the emission wavelengths at 485 nm and 520 nm, respectively.

2.10 Cell cycle analysis

Cells (4x10^5/well) were seeded in a 6-well plate and incubated with vehicle control or Pa at 0.5, 1.0 and 2.0 μM in dark for 24h. Cells were then resuspended in cold 70% ethanol for 24h at 4°C. The fixed cells were washed twice with PBS and stained with propidium iodide (PI) (10 μg/ml) and RNase A (50 μg/ml) in PBS buffer. Then cells were subjected to flow cytometric analysis using BD FACSCanto flow cytometer.

2.11 Detection of DNA fragmentation

MDA-MB-231 cells (2×10^6) were seeded on each 100-mm culture dish and incubated for 24 h to allow attachment before photodynamic treatment. After 24 h incubation at 37°C, the cells were harvested and washed twice with PBS. Then the cells were resuspended in 400 µl of DNA lysis buffer (200 mM Tris-HCl, 100 mM EDTA, 1% SDS, pH 8.3). Twenty µl protease K (10 mg/ml) solution was added and incubated for 2 h at 37°C. Saturated sodium chloride solution (150 µl) was added and mixed thoroughly. The samples were centrifuged at 6500 x g for 15 min at 4°C. Supernatant was collected and mixed with 1 ml cold ethanol before centrifuged at 15000 x g for 20 min. The pellets were washed with 1 ml cold 75 % ethanol and dried briefly. Twenty µl ribonuclease A (RNase A) (0.2 mg/ml) was added and incubated at 37°C for 90 min. The extracted DNA ladder fragmentation was visualized by electrophoresis in 1.2 % agarose gel containing ethidium bromide and analysed under ultraviolet light.

2.12 Western blot analysis

MDA-MB-231 or MCF-7 cells (3×10^6 cells) or RAW 264.7 cells (1.5×10^6 cells) were seeded on 90-mm culture dish and incubated for 24 h to allow attachment. The cells were harvested and washed twice with PBS at the appropriate treatment. After centrifugation, the cell pellets were lysed by the whole cell extraction buffer [2 % sodium dodecyl sufate (SDS), 10 % glycerol, 625 mM Tris-HCl (pH 6.8), β-mercaptoethanol (5 % v/v)] for 1 h at 4°C. The samples were boiled in water for 10 min, and the protein content in each sample was determined by bicinchoninic acid (BCA) assay. Protein samples (30 µg) was resolved by 12.5 % sodium dodecyl sufate

polyacrylamide gel electrophoresis (SDS-PAGE), and then transferred to 0.45 μm polyvinylidene fluoride membrane (Immobilon, Millipore) by electro-blotting. The membrane was blocked with 5 % non-fat milk in PBS-T (PBS supplemented with 0.1% Tween-20) and incubated with primary antibodies at 4°C overnight. Then the membrane was washed with PBS-T and probed with horseradish peroxidase-conjugated secondary antibodies for 2 h at room temperature. Finally the target proteins were visualized by the enhanced chemiluminescence (ECL) detection kit (Amersham Life Science, Pittsburgh, PA, USA) and the signal was detected using autoradiography film.

2.13. Immunofluorescent staining of intracellular molecules for flow cytometric analysis

2.13.1 For ER-α detection

MDA-MB-231 cells (3×10^5) were seeded on each well of a 6-well culture plate and grown for 24 h to allow attachment, then incubated with vehicle control or desired Pa concentration for 2 h followed by 20 min of photoactivation and incubated for further 24 h. Then, cells were collected and fixed with 4% of chloroform at 37°C for 10 min and were permeabilized with 90% of methanol on ice for an other 30 min. Cells were then washed twice with cold PBS supplemented with 1% saponin and incubated with ER-α antibody (1:50) (Santa Cruz Biotechnology Inc., Santa Cruz, CA, USA) at 4°C for 50 min. After incubation, cells were washed with 1% saponin cold PBS and probed with FITC conjugated goat anti-rabbit IgG (1:250) (Zymed

Laboratories Inc., South San Francisco, CA, USA) at 4°C for 25 min. Cells were then washed and subjected to flow cytometric analysis using BD FACSort. flow cytometer.

2.13.2 For MAPKs detection

Human immune competent cells (10^6) were seeded on each well of a 6-well culture plate and incubated with vehicle control or desired Pa concentration for 2 h. Then, cells were collected and fixed with 4% of BD Cytofix (Becton Dickinson Biosciences, San Jose, CA, USA) at 37°C for 10 min and were permeabilized with Perm Buffer II (Becton Dickinson Biosciences, San Jose, CA, USA) on ice for an other 30 min. Cells were then washed twice with cold PBS supplemented with 1% saponin and incubated with primary antibodies (e.g. pERK, pJNK and pp38) (1:80) (Becton Dickinson Biosciences, San Jose, CA, USA) at 4°C for 50 min. After incubation, cells were washed with 1% saponin cold PBS and probed with FITC conjugated goat anti-mouse IgG (1:250) (Zymed Laboratories Inc., South San Francisco, CA, USA) at 4°C for further 25 min. Cells were then washed and subjected to FACSCanto flow cytometric analysis (Becton Dickinson Biosciences, San Jose, CA, USA).

2.14 Autophagy detection with acridine orange staining

MDA-MB-231 cells (5×10^4/well) grown on the coverslips overnight were treated with Pa-PDT treatment as described previously. The treated cells were stained with 10 μg/ml acridine orange (AO) for 15 min at room temperature in dark and washed 3 times with PBS and observed by using a Nikon TE2000 fluorescence microscope with an excitation wavelength at 578 nm and an emission wavelength at 610 nm (Kanzawa *et al.*, 2003).

2.15 Immunohistochemistry

MDA-MB-231 cells (5×10^4/well) grown on the coverslips were preloaded with Pa and incubated for 2 h at 37°C followed by 20 min PDT treatment. After further 1 h incubation, the cells were fixed with iced cold fixation buffer (70 % methanol and 30 % water) for 20 min at -20°C, and then blocked with PBS-T containing 10 % FBS for 30 min at 4°C. The fixed samples were incubated overnight at 4°C with primary antibody, and then incubated with FITC conjugated IgG for further 2 h. Finally, the samples were stained with 10 μM Hoechst 33342 for 15 min at room temperature in dark and washed 3 times with PBS and observed using a Nikon TE2000 fluorescence microscope (Nikon Instruments Inc., Japan).

2.16 Confocal microscopic examination

Cells (3×10^5/well) grown on the coverslips were treated with Pa-PDT. The cells were immediately incubated with 800 nM MitoTracker Green (Molecular Probe) for 45 min at 37°C, and further stained with 10 μg/ml AO for 10 min at room temperature. After washing 3 times with PBS, the cells were viewed under a Leica SP5 confocal microscope. MitoTracker Green and AO fluorescence was detected by using the excitation (490 nm and 578 nm) and emission (516 nm and 610 nm) wavelengths; AO was assigned as red, and MitoTracker Green was shown in green. Images were merged together by using the MetaMorph software (Universal Imaging Corp).

2.17 Two-dimensional Gel Electrophoretic Analysis

The previous method was adopted (Tang *et al.*, 2010). Cells (1×10^6) were seeded to 90mm-culture dish and incubated for 24 h to allow attachment. Six hours after photodynamic treatment with 0.5 μM Pa or vehicle control, the cells were collected and washed five times with cell washing buffer (10 mM Tris-base, 250 mM sucrose, pH 7.4). The cells were then lysed in a lysis buffer (8 M urea, 4% CHAPS, 2% pharmalyte 3-10) following by 10 min of sonification. The supernatant is collected and subjected to first-dimension isoelectric focusing (IEF) with a 13-cm immobilized pH gradient (pH) strip (pH3-10 Immobiline DryStrip; Amersham Bioscience, Pittsburgh, PA, USA). The IEF was processed by using the Ettan IPGphor™ Isoelectric Focusing Unit (Amersham Biosciences, Pittsburgh, PA, USA) with the following profile: 30 V for 10 h (gradient), 200 V for 1 h (step-and-hold), 500 V for 1 h (step-and-hold), 8,000 V for 30 min (gradient), 8,000 V for 6.5 h (step-and-hold) until a total of 60,000 voltage-hours had been achieved. The IPG strips were then subjected to the second-dimension electrophoretic analysis with a 10 % SDS polyacrylamide gel. The cassette was running in the SE 600 Ruby Electrophoresis Unit (Amersham Biosciences, Pittsburgh, PA, USA) at a constant 150 V, and the collected gel was finally visualized by using of PlusOne™ Silver Staining Kit (Amersham Biosciences, Pittsburgh, PA, USA). The gel result was scanned and analyzed by software Image Master 2D version 2.0 (Amersham Biosciences, Pittsburgh, PA, USA). The mediated protein spots were excised and extracted from the gel using in-trypsin digestion. The extracted protein was purified with ZipTipC18 (Millipore Corporate, Billerica, MA, USA) and identified by Matrix assisted laser desorption-ionization time-of-flight mass spectrometry (MALDI-TOF MS) (Voyager-DE STR Biospectrometry workstation, Applied Biosystems, Foster City, CA, USA).

The list of peptide mass was submitted for search against the NCBI database using the MASCOT search engine (Matrix Science Ltd, London, UK).

2.18 Immunoprecipitation

The PDT-treated cells (3×10^6/dish) collected at 4 h after PDT were lysed by incubating in 1 ml of non-denaturing lysis buffer (20 mM Tris-HCl, pH 8.0, 137 mM NaCl, 10% glycerol, 1% Triton X-100, 2 mM EDTA, and 20 µg/ml aprotinin) for 30 min at 4°C. The supernatant was collected after centrifugation for 20 min at 12,000g. The collected cell lysate (200 µg) was incubated with anti-HLA class I antibody (Abcam, Cambridge, UK) at 4°C overnight, and then 70 µl of pre-swollen protein-A-conjugated beads was added into the sample and incubated for 4 h. After removing the supernatant and washing with lysis buffer three times. Twenty five µl of whole-cell extraction buffer was added to denature the protein and separate it from the protein-A beads. The samples were analyzed by Western blot with anti-HSP70 antibody to study the interaction between HSP70 and HLA class I proteins.

2.19 Assay of phagocytic activity

2.19.1 Human macrophages separation

Previous method was adopted (Tang *et al.*, 2010). Fresh human buffy coat obtained from healthy volunteers of Hong Kong Red Cross Blood Transfusion Service was diluted two-fold with PBS at 4°C and centrifuged using an isotonic Percoll solution (Amersham and Pharmacia Biotech, Uppsala, Sweden) for 30 min at 1000g without deceleration. The thin white interface between the top and third layers

containing the viable peripheral blood mononuclear cells including lymphocytes and monocytes was collected. The collected peripheral blood mononuclear cells were cultured with RPMI 1640 medium for 2 h, and the adherent cells in the culture flask were used as human macrophages.

2.19.2 Phagocytic activity assay

The experiment was performed using Vybrant phagocytosis Kit (Invitrogen, CA, USA). PBMCs (10^5) or RAW 264.7 cells (5×10^4) were seeded into 96-well plates, treated with solvent vehicle or different types of MDA-MB-231 cell lysate in dark for 2 h. Culture medium was removed and replaced with fluorescein-labeled *Escherichia coli* for 2 h. After the excessive fluorescein-labeled *E. coli* were removed, trypan blue (100 μl) was added and was extracted immediately after 1 minute. The fluorescence was read at 450 nm and corrected at 570 nm.

2.20 Isolation of human CD4+ and CD14+ cells

Fresh human buffy coat obtained from healthy volunteers of Hong Kong Red Cross Blood Transfusion Service was diluted 1:2 with PBS and centrifuged using an isotonic Percoll solution. Peripheral blood mononuclear cells (PBMC) fraction was obtained from the thin middle layer. CD4+ T helper cells were isolated by depletion of non CD4+ cells (Miltenyi Biotec, Bergisch Gladbach, Germany). CD14+ monocytes were isolated by positive immunomagnetic selection using anti-CD14 microbeads (Miltenyi Biotec, Bergisch Gladbach, Germany).

2.21 Isolation of human neutrophils

All standard protocols were performed as previously described (Hu *et al.* 2010). Briefly, fresh human buffy coat obtained from healthy adult volunteers was diluted 1:2 with PBS at 4°C and centrifuged using an isotonic Percoll solution (density 1.082 g/ml) for 30 min at 1,000 g. The peripheral blood mononuclear cells (PBMC) at the interface were collected firstly. The granulocyte fraction was incubated with anti-CD16 magnetic beads at 4°C for 45 min. CD16-positive cells were depleted by passing through a LS+ column within a magnetic field (Miltenyi Biotec, Bergisch Gladbach, Germany). CD16+ neutrophils were immediately collected by pipetting the wash buffer and applying the plunger onto the column. Neutrophils (5×10^4) were centrifuged at 300 rpm for 3 min on microscopic slide by the Shandon Cytospin Centrifuge (Cometa Scientific, Nottingham, UK). The cells were air-dried, stained with Harleco hemacolor staining solutions, and examined using Nikon Eclipse E800 microscope (Nikon Corp., Tokyo, Japan). Only neutrophils with the purity more than 95% were used for functional study.

2.22 Measurement of cytokine concentration by ELISA

The concentrations of cytokines were measured using enzyme-linked immunosorbent assay (ELISA). RAW 264.7 cells were seeded (0.5×10^5/well) into 96-well plates and grown for overnight at 37°C. The cells were treated with vehicle, lipopolysacharide (LPS) or Pa (0.5 and 1.0 μM) with or without specific p38 inhibitor (SB20219) (Merck Biosciences, San Diego, CA, USA) for 24 h. The cytokine concentration in culture supernatant was measured using ELISA kit (BD Biosciences, CA, USA).

2.23 Quantification of human IL-6, IL-12, IL-17, IFN-γ, TNF-α and GM-CSF

Concentrations of cytokine IL-6, IL-12, IL-17, IFN-γ, TNF-α and GM-CSF in culture supernatant were measured by Bio-Plex cytokine assay kit (Bio-Rad Laboratories, CA, USA).

2.24 Statistical analysis

Data were presented by mean ± SD. Statistical analysis was performed using GraphPad Prism 5.0 (GraphPad Software, Inc, CA, USA). Student's t-test was used to compare the variance between different set of data. Any difference with probability (p) value less than 0.05 was considered to be significant.

Chapter 3

Photo-activated pheophorbide-a, an active component of *Scutellaria barbarta*, enhances apoptosis via the suppression of ERK-mediated autophagy in the estrogen receptor-negative human breast adenocarcinoma cells MDA-MB-231

3.1 Introduction

Scutellaria barbata D.Don (Ban Zhi Lian, BZL), is a traditional Chinese medicine for clearing heats, relieving toxicity, reducing swelling, sores and abscesses (Dharmananda, 2004). Its anti-cancer property has recently been reported and the clinical trial of its water extract for advanced breast cancer treatment is ongoing in US (Fong *et al.*, 2008).

Previous studies have shown that the water and organic solvent extracts of BZL can significantly inhibit the growth of human tumors (Wong *et al.*, 2009; Dai *et al.*, 2008; Kim *et al.*, 2008; Kim *et al.*, 2007; Suh *et al.*, 2007; Goh *et al.*, 2005; Cha *et al.*, 2004; Yin *et al.*, 2004). However, limited works have been attempted to elucidate its active components (Wu and Chen, 2009; Yu *et al.*, 2007). Our previous study revealed that Pheophorbide a (Pa), is one of the active components purified from *Scutellaria barbata* by using a bioassay-guided method, possessing anti-tumour activity (Chan *et al.*, 2006), that is consistent with other reports about Pa (Nakamura *et al.*, 1996; Hibasami *et al.*, 2000). Pa has been commercial available as it can be purified from a number of traditional medicine sources such as *Scutellaria barbata*, *Psychotria acuminata*, as well as silkworm excreta (Chan *et al.*, 2006; Glinski *et al.*, 1995; Lim *et al.*, 2002). Previous studies have suggested that the therapeutic potential of Pa-mediated photodynamic therapy (Pa-PDT) on leukaemia, pigmented melanoma, colonic cancer, hepatoma and uterine carcinosarcoma (Lee *et al.*, 2004; Lim *et al.*, 2004; Hajri *et al.*, 2002; Tang *et al.*, 2006, 2009b; Li *et al.*, 2007; Tang *et al.*, 2009a).

In this present study, the therapeutic potential of Pa-PDT is demonstrated on a human breast cancer cell line MDA-MB-231 which is lack of estrogen-receptor expression, as an *in vitro* model of late phase human breast cancer (Stein *et al.*, 2008).

3.2 Results

3.2.1 Anti-proliferative effect of Pa-PDT on MDA-MB-231 cells

The dose-response curve of Pa-PDT-treated cells was shown in Figure 3.1. The cell viability decreased with an increase of Pa concentration, where IC_{50} value was found to be 0.5 μM Pa-PDT at 24 h but the viability of Pa-treated cells without illumination was more than 90% at this dosage. In contrast, the IC_{50} value of tamoxifen was found to be 20.0 μM at 24 h (data not shown).

3.2.2 Subcellular localization of Pa and collapse of mitochondria in MDA-MB-231 cells after Pa-PDT

The intracellular localization of photosensitizer is important for its activities; therefore localization of Pa in MDA-MB-231 cells was examined. The co-staining images of Pa and MitoTracker Green showed a good overlapping of both fluorescent signals at 2 h (Figure 3.2A) and 24 h (data not shown), suggested that Pa localized specifically at the mitochondria in MDA-MB-231 cells. Pa-PDT is able to trigger the collapse of mitochondria by a rapid generation of ROS (e.g. peroxidants) in the intracellular environment. The mitochondrial membrane potential was changed in a dose-dependent manner in Pa-PDT treated MDA-MB-231 cells at 1 h by JC-1 staining assay, as shown in Figure 3.2B. The change in population was counted as 17.4 % in control and gradually increased to 55.1 %, 96.9 % and 99.8 % by 0.25 μM, 0.5 μM and 0.75 μM Pa-PDT treatments, respectively.

3.2.3 Activation of MAPK pathway in Pa-PDT treated MDA-MB-231 cells

PDT can trigger the generation of ROS by exciting the photosensitizer, and the produced high-energy molecules can collapse the subcellular organelles where the photosensitizer is located and initiate the cell death process. As shown in Figure 3.3A, intracellular ROS (e.g. peroxidants) level was increased in a dose-dependent manner during Pa-PDT treatment. High level of intracellular ROS concentration can activate the MAPKs, so activation of MAPKs, including extracellular signal-regulated kinase (ERK), c-Jun N-terminal kinase (JNK) and p38, in the Pa-PDT treated cells were monitored by Western blotting. Significant phosphorylation of JNK and mild activation of p38 were found, whereas the phosphorylation of ERK was strongly suppressed in the Pa-PDT treated cells (Figure 3.3B). Similarly, the phosphorylation of JNK was increased in a dose-dependent manner whereas the phosphorylation of ERK was slightly increased at 0.5 μM and strongly suppressed at higher concentration of Pa-PDT in the treated cells (Figure 3.3C).

3.2.4 Effect of MAPK inhibitors on Pa-PDT induced cell death in MDA-MB-231 cells

The activation of JNK is supposed to facilitate programmed cell death, however, pharmacological inhibition of JNK and/or p38 could not prevent Pa-PDT-treated MDA-MB-231 cells from death (Figure 3.4). This result suggested that Pa-PDT may induce cell death by other pathways besides apoptosis.

3.2.5 Pa-PDT mediated apoptosis induction in MDA-MB-231 cells

Genomic DNA fragmentation was detected on Pa-PDT treated MDA-MB-231 cells even at low Pa concentration (0.25 μM, 0.5 μM and 0.75 μM), and no DNA ladder pattern can be detected on the control sample which was illuminated without Pa (Figure 3.5).

3.2.6 Pa-PDT activated JNK induced endoplasmic reticulum stress

Analysis of protein expression profile of MDA-MB-231 cells revealed the involvement of endoplasmic reticulum stress during Pa-PDT treatment by two-dimensional PAGE gel method. Modulation of two endoplasmic reticulum chaperone calcium binding proteins, calreticulin and GRP78/BiP, was founded (data not shown). Perturbation of endoplasmic reticulum homeostasis upregulated GRP78/BiP, calreticulin and ERp57, and resulted in unfolded protein response (UPR). GRP78/BiP is belonged to heat shock protein 70 family which played an important role in pro-survival mechanism of the cells under the endoplasmic reticulum stress. In addition, ERp57, a lumenal protein of the endoplasmic reticulum which belonged to disulfide isomerase (PDI) family, works together with lectine endoplasmic reticulum chaperones calnexin and calreticulin in many protein folding processes. In this study, calreticulin was found to be up-regulated at the first 2 hours and degraded at 4 hour in Pa-PDT treated cells (Figure 3.6A). Nevertheless, the expression of GRP78/BiP was regressed after Pa-PDT treatment, whereas ERp57 was upregulated after Pa-PDT only at 4 h. Furthermore, the increase of calreticulin and ERp57 and the decrease of GRP78/BiP were observed at the early time in a dose dependent manner (Figure 3.6B).

3.2.7 Induction of autophagy in Pa-PDT treated MDA-MB-231 cells

Autophagy is recently proposed as a programmed cell death mechanism as apoptosis, it can lead to cell suicide with or without the induction of apoptosis and can be induced by endoplasmic reticulum stress. Activation of ERK and down-regulation of Bcl-2 are suggested to enhance the induction of autophagy in cancer cells (Kondo and Kondo, 2006; Motyl *et al.*, 2006). In our study, the activation of ERK (Figure 3.3C) and the downregulation of Bcl-2 (Figure 3.7A) were both found in Pa-PDT treated cells, therefore further experiments were conducted to investigate whether Pa-PDT could induce autophagy in the breast cancer cells. LC3 is a major constituent of autophagosome, a double membrane to sequester target organelles.

During autophagy, cytosolic LC3 is recruited to autophagosome formation. LC3-I is converted to LC3-II and associated to the autophagic vesicles (Kondo and Kondo, 2006). As shown in Figure 3.7B, expressions of LC-3B was significantly increased, the results were confirmed by Western blot in the cells treated with 0.25, 0.5 and 0.75 μM Pa-PDT (Figure 3.7C). Furthermore, the formation of acidic vesicle organelle, another hallmark of autophagy which can be visualized by acridine orange (AO) staining, was found in the cells treated with 0.5 μM Pa-PDT. The inhibition of ERK activity with a pharmacological co-treatment with an ERK inhibitor PD98059 (Merck Biosciences, San Diego, CA, USA), could reduce vesicle formation in the Pa-PDT treated cells (Figure 3.7D). Nevertheless, the formation of autophagosomes may aim at removing the damaged organelles such as mitochondria in order to rescue the Pa-PDT treated cells. According to the confocal microscopic observation (Figure 3.7E), the images of mitochondria (left upper panel) and cellular acidic compartment (right upper panel) in the 0.5 μM Pa-PDT treated MDA-MB-231 cells could not be completely merged (left lower panel); and inhibition of ERK reduced the cytotoxicity

of Pa-PDT treatment on the MDA-MB-231 cells (Figure 3.7F). Our results therefore implied that ERK could mediate autophagy, and the induced autophagy enhanced the anti-tumour effect of Pa-PDT on MDA-MB-231 cells.

3.3 Discussion

In this study, we evaluated the therapeutic potential of Pa-PDT on human breast cancer, as breast is an out-growing organ that is suitable for the application of PDT protocol which has been used to treat head and neck cancers in clinics. PDT was reported to inhibit cancers through different cell death pathways and its effectiveness is dependent on the types of cancer cell lines and photosensitizers (Buytaert *et al.*, 2007; Zuluaga and Lange, 2008). Previous studies on the potential of Pa as a photosensitizer have suggested that Pa is effective to inhibit cancer growth by the induction of apoptosis (Inanami *et al.*, 1999; Hajri *et al.*, 1999; Hajri *et al.*, 2002; Lee *et al.*, 2004; Lim *et al.*, 2004; Tang *et al.*, 2006; Tang *et al.*, 2007; Tang *et al.*, 2009a; Tang *et al.*, 2009b; Li *et al.*, 2007; Radestock *et al.*, 2007; Kishino *et al.*, 2008; Rapozzi *et al.*, 2009). We speculated that apoptosis is a general anti-tumour mechanism of Pa-PDT on human cancers. Our present study is the first report to demonstrate the therapeutic potential of Pa-PDT on human estrogen-negative breast carcinoma treatment by using MDA-MB-231 cells as a late phase of human breast carcinoma model; and most important is that our finding revealed autophagy is also contributed to the Pa-PDT mediated cancer cell death.

Our findings showed that Pa-PDT can significantly inhibit the growth of MDA-MB-231 cells with an IC_{50} value of 0.5 μM for 24 h incubation (Figure 3.1), light has shown no effect on cell growth inhibition (data not shown). This value is

consistent with that of our previous reports on human hepatoma cells Hep3B, multidrug-resistant human hepatocellular carcinoma cells RHepG2 and uterine carcinosarcoma cells MES-SA with IC_{50} values of 0.8 μM, 0.6 μM and 0.5 μM, respectively (Tang *et al.*, 2006; Tang *et al.*, 2007; Tang *et al.*, 2009a). The potency of Pa-PDT is much higher than the anti-breast cancer agent tamoxifen, whose IC_{50} value is 19 μM for 24h incubation (data not shown) as tamoxifen establishes its anti-tumour effects via estrogen receptor-mediated pathway whereas MDA-MB-231 cells are estrogen receptor null. In the case of Pa-PDT, cell death is triggered independently of estrogen receptor, according to the similar IC_{50} values on MCF-7 and MDA-MB-231 cells (data not shown), which are estrogen-receptor-positive and negative cells respectively. In addition, Pa showed no significant cellular toxicity without light illumination at low concentrations (Figure 3.1). In higher concentration (e.g. 40 μM), Pa exhibits anti-tumour effect (Chan *et al.*, 2006). that is an advantage of Pa-PDT in clinical applications since adjustment of light illumination area can avoid the damage to normal tissue in the breast cancer bearing patients.

The cellular localization is important to the action mechanism of photosensitizers (Dolmans *et al.*, 2003; Buytaert *et al.*, 2007). Pa was found to be localized in the mitochondria of MDA-MB-231 cells (Figure 3.2A), similar to its subcellular location in the Hep3B and MES-SA cells (Tang *et al.*, 2006; Tang *et al.*, 2009a). The rapid generation of ROS (e.g. peroxidants) found in Pa-PDT-treated cells (Figure 3.3A) would induce damage to mitochondria and lead to the changes in mitochondrial membrane potential (Figure 3.2B), thereby triggering the activation of the intrinsic apoptotic caspase cascade (Tang *et al.*, 2006; Tang *et al.*, 2007; Tang *et al.*, 2009a; Tang *et al.*, 2009b; Tang *et al.*, 2010; Lim *et al.*, 2004; Hajri *et al.*, 2002;

Li *et al.*, 2007). Pa-PDT treated-MDA-MB-231 cells resulted in a typical laddering of genomic DNA which is a hallmark of apoptotic cell death (Figure 3.5). Similar results were also observed in MCF-7 cells, an estrogen-receptor positive cell line (data not shown). Therefore, Pa-PDT is a promising apoptosis inducer on the breast cancer cells and other types of human cancer cells (Lim *et al.*, 2004; Hajri *et al.*, 2007; Li *et al.*, 2007, Tang *et al.*, 2006; Tang *et al.*, 2007; Tang *et al.*, 2009a; Tang *et al.*, 2009b; Tang *et al.*, 2010).

No previous literatures have reported other possible anti-tumour mechanisms of Pa-PDT for the inhibition of human breast cancer cell growth. According to Figure 3.3A, a dose-dependent induction of ROS was detected in the Pa-PDT-treated MDA-MB-231 cells. Recent study has suggested that ROS sustains the activation of MAPK signal cascade in cancer cells (Wu *et al.*, 2008). In our study, modulation of JNK and ERK, which are regulators for mitochondrial membrane metastasis, endoplasmic reticulum stress and autophagy (Hoye *et al.*, 2008; Urano *et al.*, 2000; Corcelle *et al.*, 2007), were found in Pa-PDT-treated cells (Figure 3.3B). Our observation therefore suggested that Pa-PDT could activate MAPK pathway by the rapid induction of intracellular ROS stress in the treated tumour cells. The results are consistent with our findings on multidrug resistant human hepatoma cells RHepG2 (Tang *et al.*, 2009b). However, neither JNK nor p38 inhibitors could prevent Pa-PDT induced cell death (Figure 3.4). Therefore, the Pa-PDT induced MAPK activation may trigger different intracellular pathways in a cell type specific manner. Results from Figure 3.4 suggested that Pa-PDT could induce different cell death pathways whereas the stress related one is an additional pathway for Pa-PDT induced cancer cell death in MDA-MB-231 cells.

Further investigation of the MAPK activation revealed two non-apoptotic mechanisms that were also triggered in MDA-MB-231 cells during Pa-PDT treatment. Mitochondrial plasma membrane collapse increases intracellular ROS concentration, leading to endoplasmic reticulum stress. Endoplasmic reticulum is an organelle involving in protein synthesis, folding, post-translational modification, as well as calcium homeostasis. The phosphorylation of JNK (Figure 3.3C) after Pa-PDT indicated that JNK is induced by endoplasmic reticulum stress (Srivastava et al., 1999). It is supported by the upregulation of calreticulin (Figure 3.6B) which is a calcium dependent molecular chaperone protein involved in many biological functions such as immunity, apoptosis and endoplasmic reticulum stress (Michalak et al., 2009; Ni and Lee, 2007). In order to recover the endoplasmic reticulum homoeostasis and maintain cell survival, the unfold protein response (UPR) involving different endoplasmic reticulum chaperone proteins mediated by a HSP70 family protein GRP78/BiP for the inhibition of apoptosis, is initiated (Lee, 2007; Kim et al., 2006). In addition, down-regulation of GRP78/BiP is accompanied by the up-regulation of another ER chaperon protein ERp57 (Xu et al., 2009). We found that GRP78/Bip and ERp57 were down- and up-regulated, respectively, during Pa-PDT treatment (Figure 3.6A and 3.6B). Together, endoplasmic reticulum chaperones such as calreticulin require the interactive partner GRP78/BiP for UPR. However, GRP78/BiP is suppressed by the up-regulation of ERp57. As a result, calreticulin cannot decrease protein misfolding due to the lack of GRP78/BiP, and therefore enhanced the Pa-PDT mediated cancer cell death in MDA-MB-231 cells.

Autophagy is responsible for protein degradation and recycling in order to maintain cell survival, tissue remodeling as well as tumour suppression. It is a newly suggested programmed cell death pathway for tumour cells (Yorimitsu and Klionsky, 2007, Motyl *et al.*, 2006; Hippert *et al.*, 2006; Kondo and Kondo, 2006). Activation of ERK was occurred in Pa-PDT treated MDA-MB-231 cells at 20 min where no p38 was stimulated (Figure 3.3B). Specific activation of ERK has been suggested for the induction of autophagy (Corcelle *et al.*, 2007). Autophagic vacuolation was observed in the Pa-PDT treated MDA-MB-231 cells and its formation was significantly suppressed by ERK inhibitor (Figure 3.7D). In addition, increase in the expression of lipidated LC3B (LC3-II form), another hallmark of autophagy, was found in the Pa-PDT treated cells (Figure 3.7B and 3.7C). The findings supported the induction of autophagy in the MDA-MB-231 cells during Pa-PDT treatment. Nevertheless, the acidic vesicles were not located at mitochondria (Figure 3.7E), thereby implying that the induced autophagosomes were not for eliminating of the photo-damaged mitochondria in the Pa-PDT treated cells. Our suggestion is supported by the co-treatment of Pa-PDT with ERK inhibitor,where the cytotoxicity of Pa-PDT on MDA-MB-231 cells could not be inhibited when the autophagy was suppressed by ERK inhibitor (Figure 3.7F). Autophagy occurred only at low concentration (up to 0.5 μM) of Pa-PDT; whereas, the rapid cell death process can abolish the contribution of autophagy when higher dosage was applied, as ERK was totally inactivated at 0.75 μM Pa-PDT (Figure 3.3C). Therefore, no significant effect of ERK inhibitor could be observed on the cell survival rate at the high Pa dosage (Figure 3.7F). These findings suggested that the induction of autophagy occurred in parallel with apoptosis for the multiple anti-tumour activities of low dose Pa-PDT on MDA-MB-231 cells.

The antitumour mechanism of doxorubicin, a well known antitumour drug, is multiple depending on treatment concentrations (Gewirtz, 1999). From low to high concentrations, doxorubicin induced cancer growth arrest via the induction of cell differentiation and interference with the DNA-topoisomerase II interaction. Free radicals mediated toxicity is observed only at high concentration of doxorubicin (Gewirtz, 1999). Doxorubicin could induce apoptosis in MDA-MB-231 cells at high concentration via mitochondrial machinery (Aroui et al., 2009). Other group also reported that when apoptosis is partially blocked, doxorubicin induced MDA-MB-231 cell death by autophagy (Di et al., 2009). Therefore, Pa-PDT exerts multiple cancer cell death pathways in the treated MDA-MB-231 cells depending on the drug concentration as the case of doxorubicin.

3.4 Conclusion

Our present work revealed the therapeutic potential of Pa-PDT on estrogen receptor negative human breast carcinoma MDA-MB-231 cells. The potent antitumour effect of Pa-PDT on MDA-MB-231 cells was established via additive death pathways. The induction of mitochondria dependent apoptosis is amplifying by endoplasmic reticulum stress linked to autophagy that was served as an additive anti-cancer effect. Pa-PDT is therefore a potential protocol to treat human breast tumour cells at late phase via multiple death pathways. It suggests that Scutellaria barbata extract, from which Pa is purified, may be considered as a new TCM related photosensitizer in breast cancer treatment.
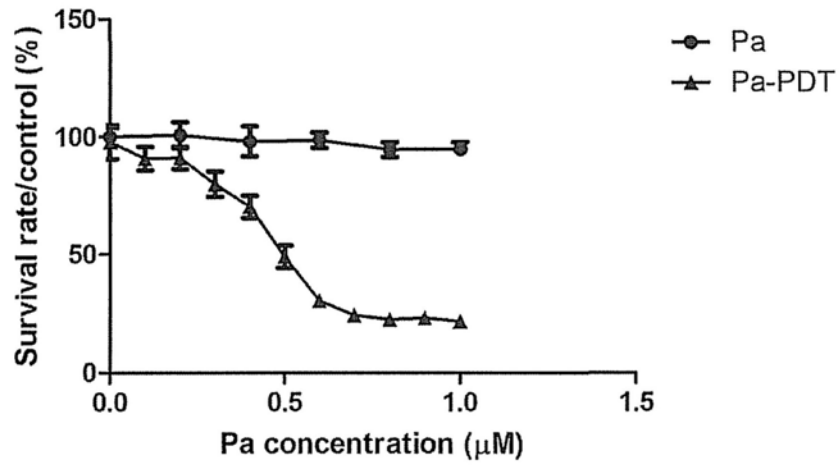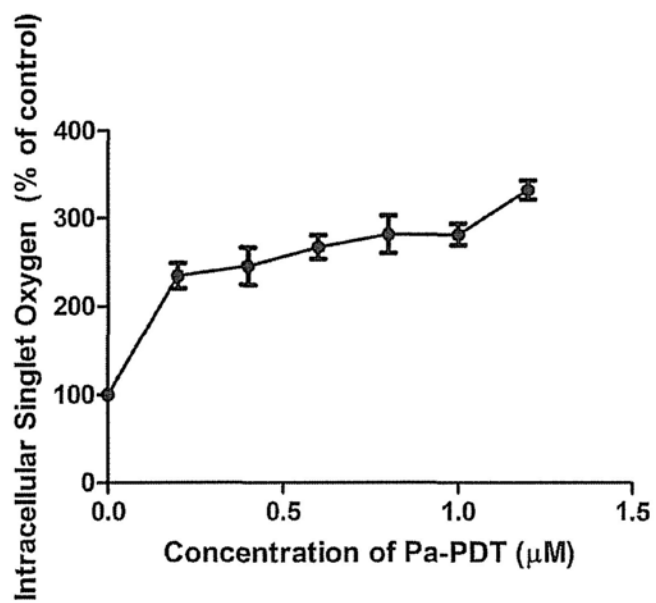
Figure 3.1 – The inhibitory effect of Pa-PDT on MDA-MB-231 cells *in vitro*. Cells were pre-incubated with Pa for 2 h, and then illuminated. No illumination was applied on the dark control. Cell activity was measured by MTT assay at 24 h after each treatment. The results are reported as mean ± S.D. with 3 independent experiments.
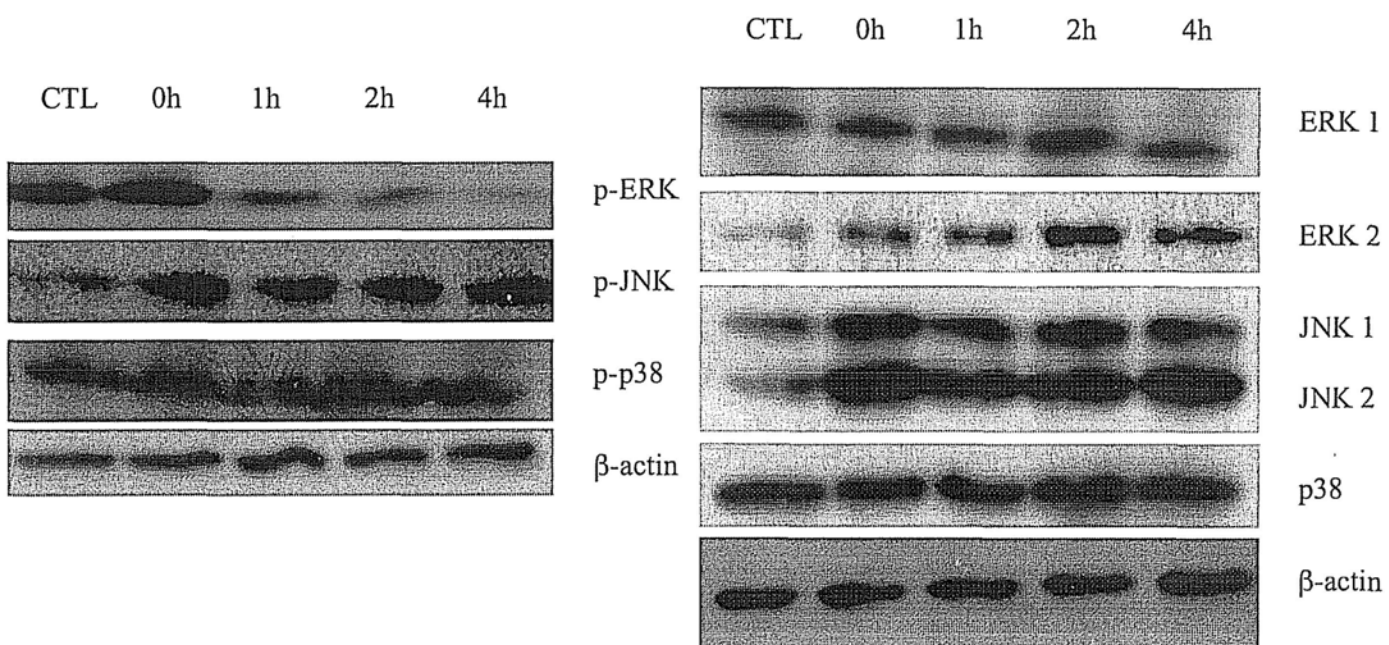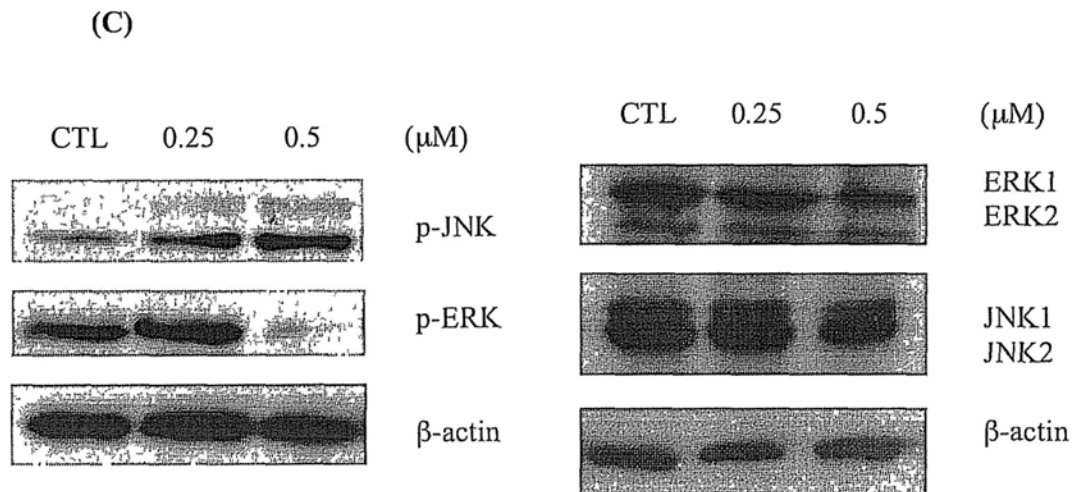
(A)

Pheophorbide a   Mito-Tracker Green   Merged Image

(B)
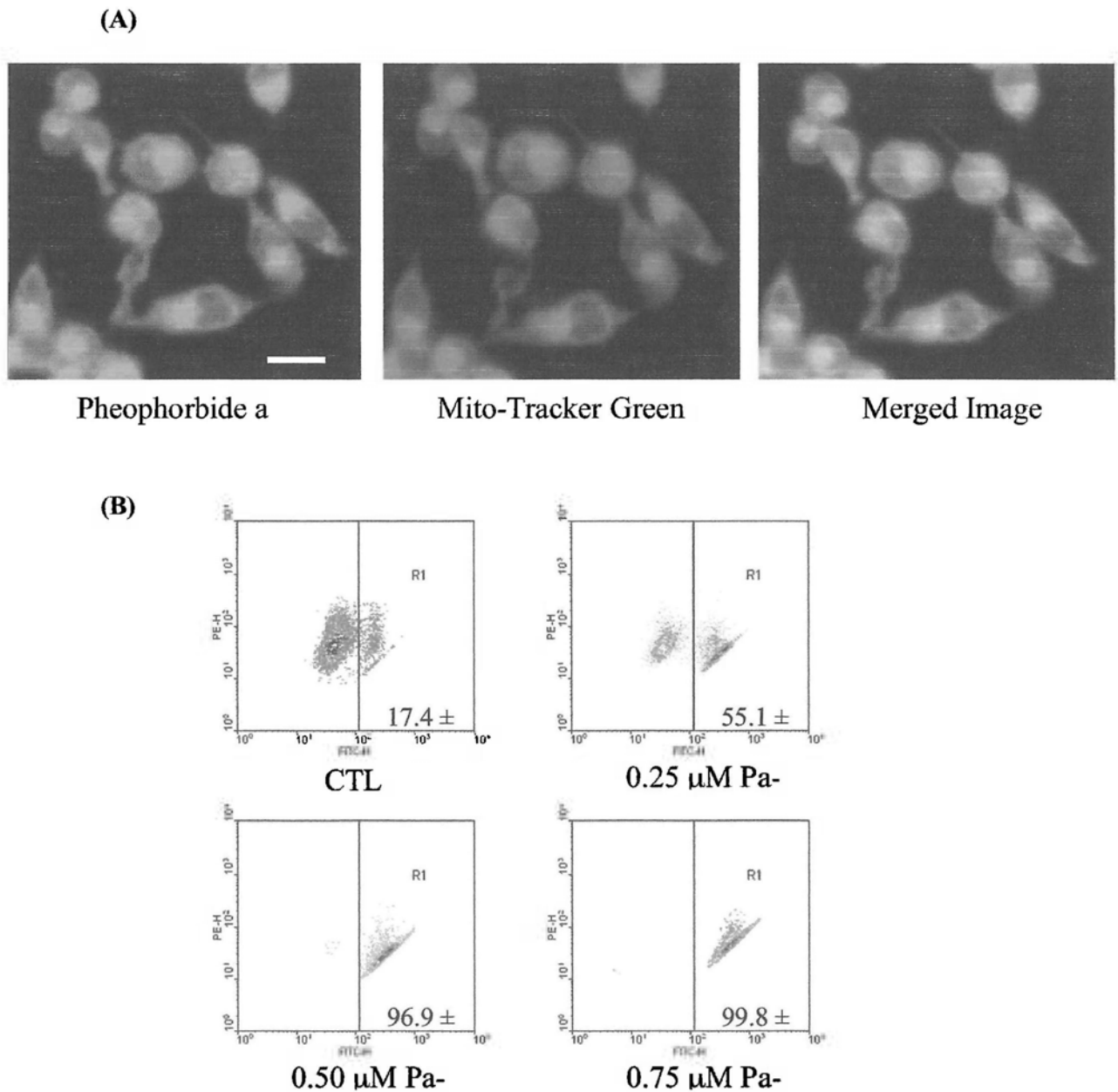
Figure 3.2 - Pa-PDT induced cell death in MDA-MB-231 cells via mitochondrial dependent machinery. (A) Subcellular localization of Pa was performed by staining cells with Pa for 2 h followed by MitoTracker Green. Fluorescence emissions were detected by a Nikon TE2000 fluorescence microscope (60x), where Pa was assigned as red, and Mitotracker Green was assigned as green in colour. Co-localization of Pa and MitoTracker was shown in yellow colour of the merged image. Images are a representative of 3 independent experiments (scale bar: 15 µm) **(B)** Pa-PDT treated cells were collected and stained with JC-1 and subjected to flow cytometric analysis for the change of mitochondrial membrane potential ($\Delta\psi$m). The numerical results are presented as mean ± S.D. of 3 independent experiments. CTL: Control.

(A)

(B)

(C)

CTL   0.25   0.5   (μM)   CTL   0.25   0.5   (μM)

p-JNK   ERK1 ERK2

p-ERK   JNK1 JNK2

β-actin   β-actin

Figure 3.3 - Pa-PDT activated MAPK pathway via ROS induction in MDA-MB-231 cells. (A) Induction of intracellular ROS generation. The MDA-MB-231 cells were treated with various concentrations of Pa with PDT. PDT cells were then stained with CM-H$_2$DCFDA dye in dark. The intensity of intracellular CM-H$_2$DCFDA fluorescence are presented as mean ± S.D. of 5 independent trials. ^{r}p value < 0.05. **(B)** Time-course study of MAPK activation. Cells were treated with 0.5 μM Pa without illumination as dark control, or 0.5 μM Pa-PDT for various time intervals. The expression of β-actin and various phosphorylated MAPK proteins were analyzed by Western blotting. Representative results are shown from 3 independent experiments with essential **similar** results. CTL: Control **(C)** Dose-course study of MAPK activation. Cells were treated with solvent control or with different Pa concentrations (0.25 μM and 0.5 μM) and whole-cell protein lysates were collected at 1 h after photo-activation, subjected to Western blot analysis. Representative results are shown from 3 independent experiments with essential similar results. CTL: Control.
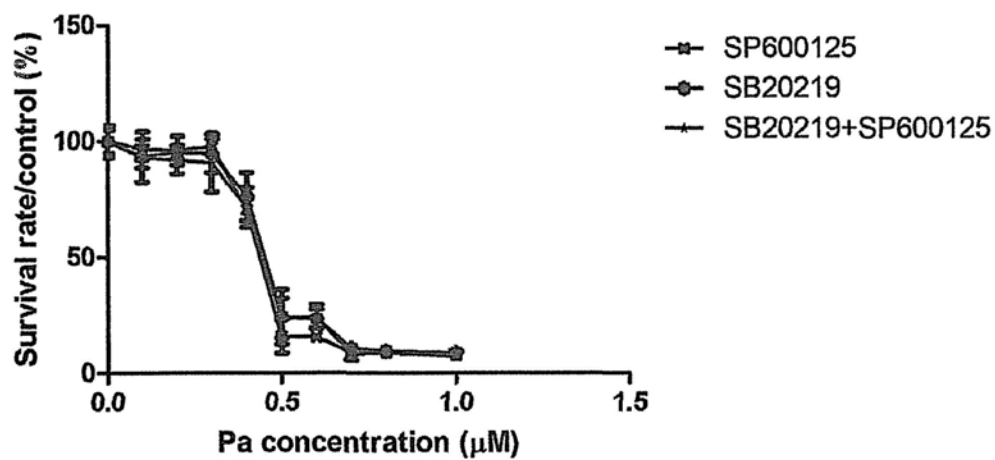
Figure 3.4 - Effect of JNK and p38 inhibitions on Pa-PDT induced cell death. Cells were incubated with Pa and inhibitor of JNK (SP600125) (1 μM) or p38 (SB20219) (1 μM) for 2 h, and then illuminated with the total energy equal to 84 J/cm^2. Cell viability was measured by MTT assay at 24 h after each treatment. The results are presented as mean ± S.D. with 3 independent experiments.
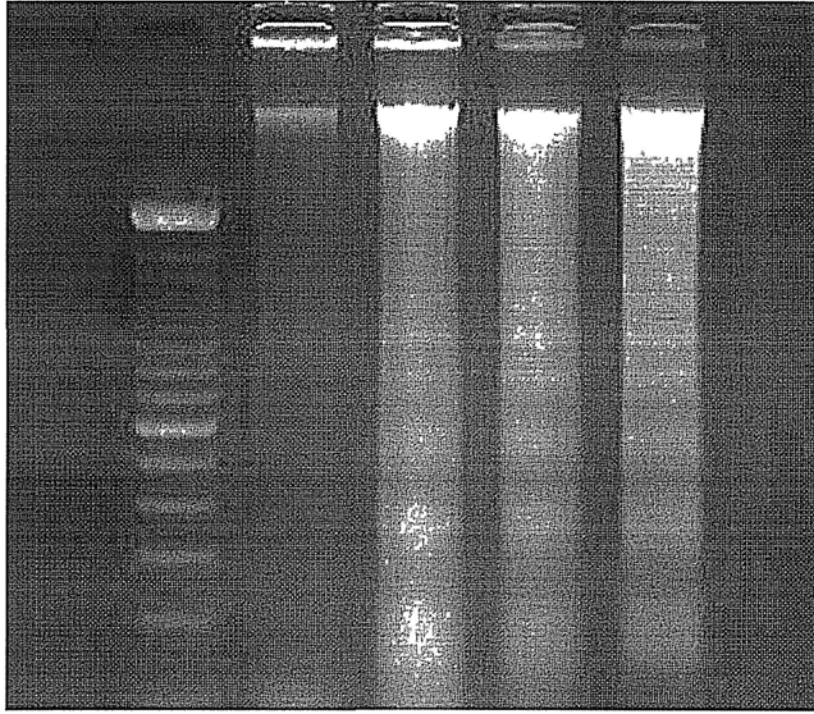
Figure 3.5 - Pa-PDT induces apoptosis via DNA fragmentation in MDA-MB-231 cells. Cells (4×10^5/well) were treated with 0.04 % ethanol (solvent control) or Pa-PDT (0.25 μM, 0.5 μM or 1.0 μM). The genomic DNA of Pa-PDT treated cells was extracted at 24 h and resolved in 1.0 % agarose gel by electrophoresis, where lane M: DNA markers (100 base pair); lane 1: solvent control; lane 2: 0.25 μM Pa-PDT; lane 3: 0.5 μM Pa-PDT, and lane 4: 1.0 μM Pa-PDT. Results shown are representatives of 5 independent experiments with essential similar results.
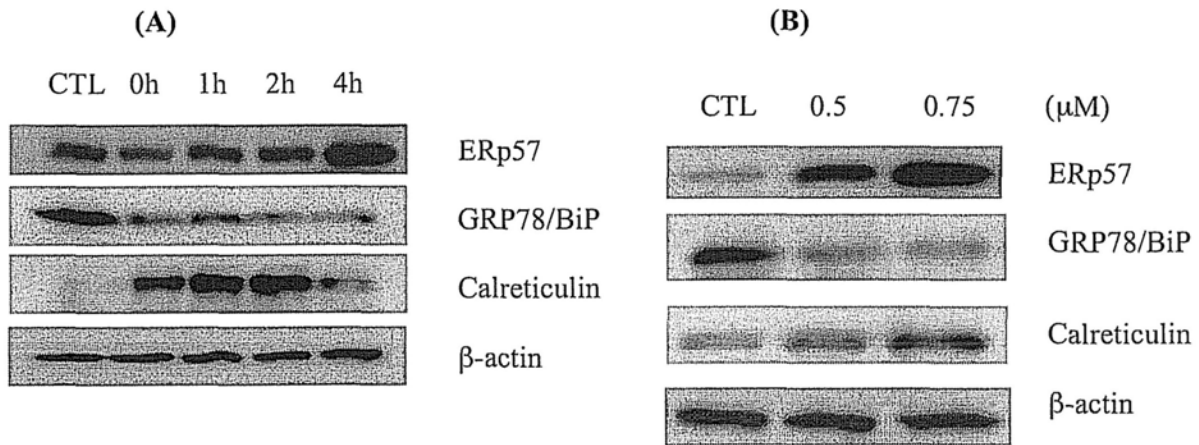
Figure 3.6 - Pa-PDT induced JNK-mediated ER stress without unfolded protein response (UPR) activation. **(A)** MDA-MB-231 cells were treated with Pa (0.5 μM) for 2 h without illumination for control, or Pa-PDT (0.5 μM) and then collected at appropriated time. A time course analysis of protein expression was monitored using Western blot. Representative results are shown from 3 independent experiments with essential similar results. **(B)** Cells were treated with solvent control or various concentrations of Pa (0.5 and 0.75 μM) for 4 h. After PDT, cells were collected for whole-cell protein lysates and analyzed by Western blot. Representative results are shown from 3 independent experiments with essential similar results. CTL: Control.

(A)

CTL   0.25   0.5   0.75   (μM)

Bcl-2

β-actin

(B)

CTL   0.5 μM Pa-PDT   0.75 μM Pa-PDT

(C)

CTL 0.25   0.5   0.75   (μM)

LC3-I
LC3-II

β-actin
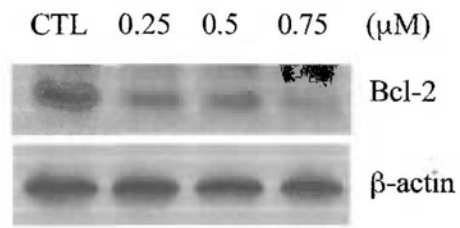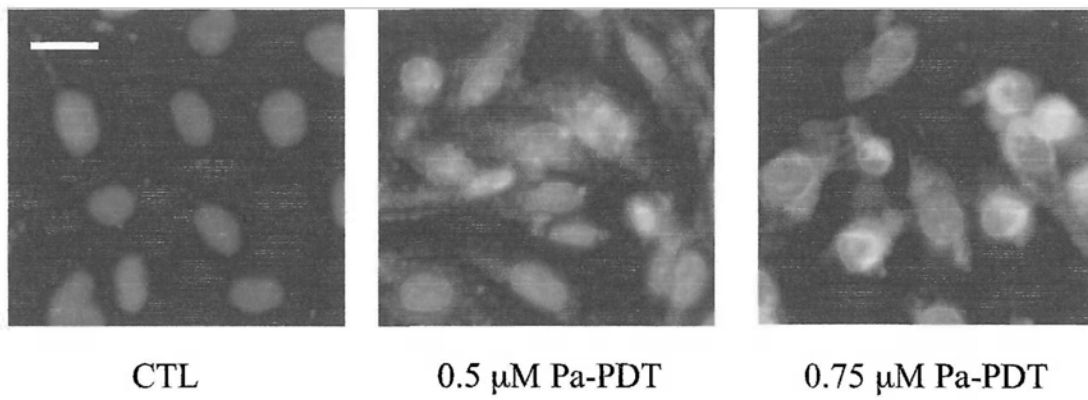
(D)

CTL   Pa-PDT   Pa-PDT with p-ERK inhibitor

(E)

Mito-Tracker Green   Acridine Orange

Merged Image   Bright-field Image   63
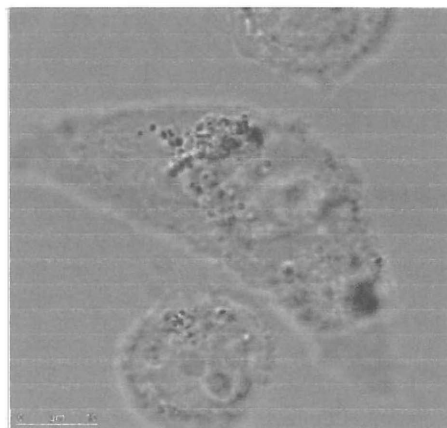
(F)
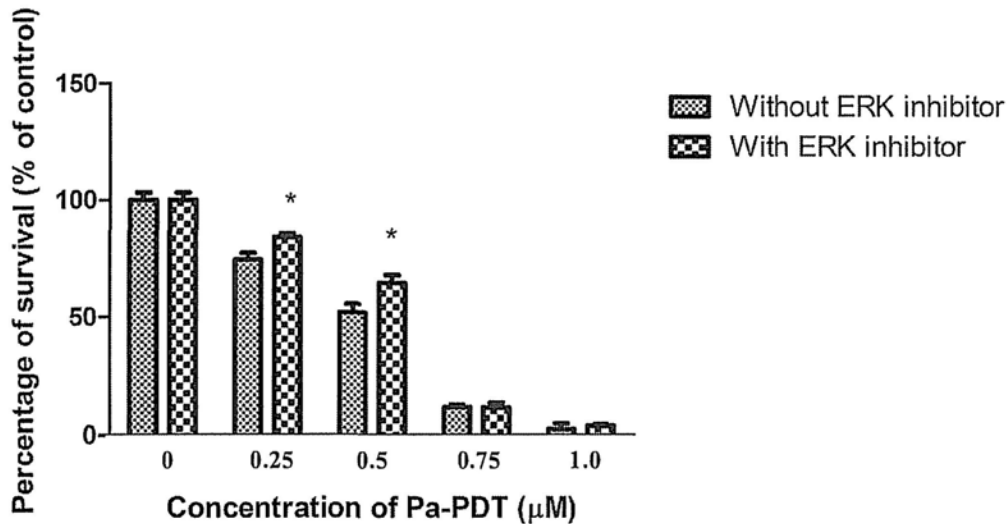
Figure 3.7 - Pa-PDT induces ERK-mediated autophagy in MDA-MB-231 cells. (A) Cells were treated with solvent control or various Pa concentrations for 2h then collected 1 h after light activation. The expression level of Bcl-2 was monitored by Western blot. Representative results are shown from 3 independent experiments with essential similar results. (B) The Pa-PDT treated cells were fixed at 1 h after PDT. Cells were stained with monoclonal LC3-B antibody then probed with FITC-conjugated secondary antibody. The nuclei were stained with 10 μM Hoechst 33342. The stained cells were examined using fluorescence microscope, where the nuclei were assigned as blue, the LC3-B was assigned as green in colour (middle panel), and the merged images of nuclei and LC3-B were shown in the right panel. Representative images are shown from 5 independent trials with essential similar results. (C) Pa-PDT treated cells were collected at 1 h after illumination. The expression of LC3-B was analyzed by Western blot. Representative results are shown from 3 independent experiments with essential similar results. (D) The cells were treate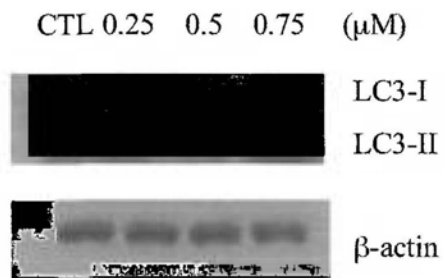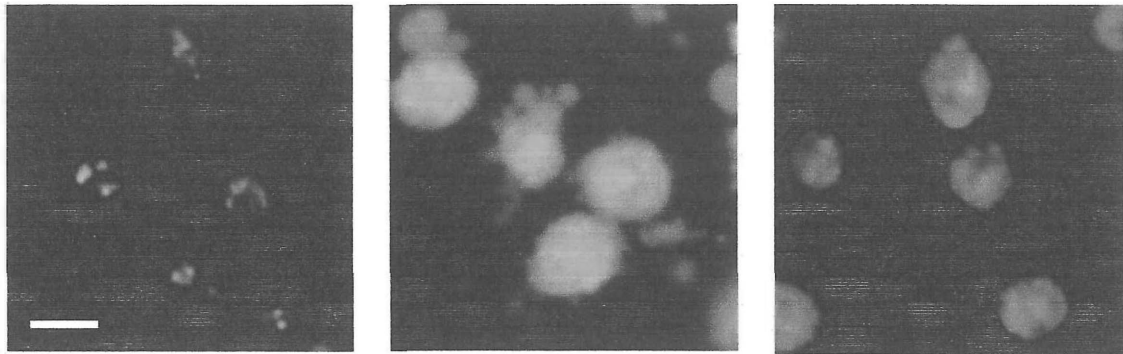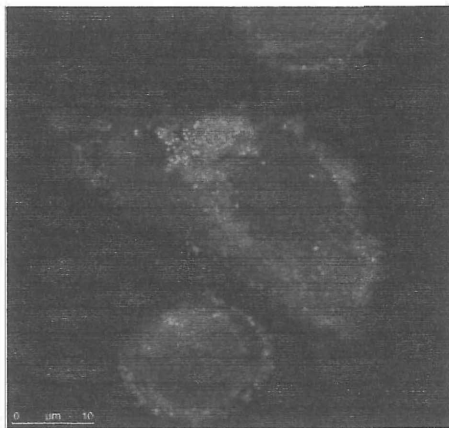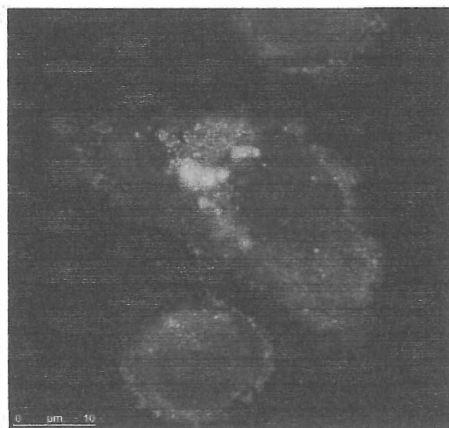d with solvent control, 0.5 μM Pa-PDT without or with 200 nM PD98059, and then stained with acridine orange and examined using fluorescence microscope. Representative images are shown from 5 independent experiments with essential similar results (scale bar: 15 μm). (E) The 0.5 μM Pa-PDT treated cells (5x10^4/well) were stained with Mitotracker Green and acridine orange, and observed under confocal microscope where the acridine orange were assigned as red (left upper panel), the Mitotracker Green was assigned as green in colour (right upper panel), and the merged and bright-field images were shown in the left and right lower panels, respectively. Representative images are shown from 3 independent trials with essential similar results (scale bar = 10 μm). (F) Cells were incubated with Pa or combination with 200 nM PD98059 for 2 h, and then received the illumination. The cell viability was measured by MTT assay at 24h and the results are presented as mean ± S.D. with 3 independent experiments (*p-value < 0.05, comparing between groups with or without PD98059). CTL: Control.

Chapter 4

Pheophorbide a based photodynamic therapy enhances the antitumour effect of tamoxifen in estrogen receptor-negative human breast cancer cells MDA-MB-231

4.1 Introduction

Breast cancer is the fifth most lethal cancer worldwide and the second most common type of cancer which is triggered by principal risk factors including aging, genetic, and lifestyle (WHO, 2006; WHO International Agency for Research on Cancer, 2003). Surgery and chemotherapy are the two most common methods to treat this cancer, however, surgery is an irreversible intervention that can cause psychological problem to female patients, and surgery requires a pattern such as chemotherapy, radiation or hormonal therapy after treatment. The recent alternative for breast cancer treatment is hormonal therapy, where tamoxifen, a selective estrogen receptor modulator (SERM), is one of the approved drugs used for this purpose (Jordan, 2006). SERM is effective only on early breast cancer cases, which are estrogen receptor positive (ER-positive). In contrast, chemotherapy is generally the first choice in the last phase of the disease, as estrogen receptor is no longer expressed (ER-negative) in the cancer cells (Jordan, 1993). Nevertheless, available chemotherapy drugs only can partially overcome the growth of breast cancer cells due to the development of multi-drug resistance (MDR) phenomenon (e.g. doxorubicin) (Robert, 1999). Therefore, patients with estrogen receptor-negative breast cancer have a poor prognosis. Taking together, photodynamic therapy (PDT) has been suggested to be a new hope for breast cancer (Dolmans et al., 2003).

In this present study, the effects of Pa-PDT combined with tamoxifen treatment were investigated. We found Pa-PDT successfully sensitized MDA-MB-231 cells to tamoxifen.

4.2 Results

4.2.1 Pa-PDT restores estrogen-receptor α expression in MDA-MB-231 cells

MDA-MB-231 cells are ER-α negative breast cancer cells. Therefore, tamoxifen reveals low efficiency in treating this cancer. After 24h of Pa-PDT treatment, using 0.2 μM to 0.5 μM of Pa, restoration of ER-α was observed in MDA-MB-231 cells. The results which were obtained by different methods including Western blot (Figure 4A), intracellular staining (Figure 4B) and immunohistochemistry (Figure 4C) are similar.

4.2.2. The effect of combination of photodynamic therapy and tamoxifen

Due to the absence of ER-α in MDA-MB-231 cells, tamoxifen has low sensitivity in treating advanced breast cancer. The combination of PDT and tamoxifen is suggested as new method to enhance the anti-tumour effect of SERMs in treating late phase breast cancer. In addition to Pa, other natural photosensitizer, riboflavin (VitB2), is used to test whether the effect is from PDT or Pa-PDT. MTT assays showed that the IC_{50} of Pa-PDT is 0.5 μM (Figure 3.1) and that of VitB2 is 50 μM (Figure 4.2) at 24 h incubation.

MTT assay of Pa-PDT or VitB2-PDT with tamoxifen were performed at IC_{10} and IC_{20} of each photosensitizer. The IC_{50} of tamoxifen shifted from 19 μM (tamoxifen alone) to lower concentrations (tamoxifen combined to PDT), depending on the loaded concentration and the type of photosensititizer. For Pa-PDT, the IC_{50} of

tamoxifen shifted from 19 µM to 18 µM and 16 µM (IC_{20} and IC_{10} respectively), for VitB2, from 19 µM to 17 µM and 15 µM (IC_{20} and IC_{10} respectively) (Figure 4.3A and B). Thus, PDT combined with tamoxifen enhanced the sensitivity of MDA-MB-231 cells to tamoxifen.

4.2.3 Pa-PDT combined with tamoxifen induces both intrinsic and extrinsic apoptosis

Apoptosis can be triggered via intrinsic (mitochondrial regulation) or extrinsic (direction signal transduction) pathways as well as both of them. The protein level of apoptosis-related proteins in Pa-PDT (0.2 µM) combined with tamoxifen (5 µM) (Pa-PDT-Tam) treated MDA-MB-231 cells at 24 h was investigated and normalized by β-actin level. As shown in Figure 4.4B, the level of procaspase-3 and bcl-2 were decreased whereas cleaved caspase-9 and p53 was increased in Pa-PDT-Tam treated cells. In addition, the level of other proteins that involved in the intrinsic pathway, including BAD, cleaved PARP (increased) were modulated in the Pa-PDT-Tam. The change ($p < 0.5$) was more significant comparing to cells treated with either Pa-PDT or tamoxifen without any combination ($p < 0.5$). Besides, the extrinsic apoptosis was also observed by the increased protein expression level of Fas and DR5, both belong to receptors of the TNF receptor (TNFR) family, in Pa-PDT-tamoxifen treated cells. In addition, truncated Bid (tBid), a pro-apoptotic protein, was also increased. tBid is the cleaved product of Bid by caspase-8, the caspase that mediates extrinsic apoptosis via TNFR induction (Figure 4.4 A).

4.3 Discussion

One of the widely used methods to cure breast cancer is hormonal therapy. This method is based on the introduction of different type of hormones, depending on the diagnosis of the patient, to control breast tumour cell growth. We can distinguish two essential hormonal therapies for clinical application: SERMs and aromatase inhibitors (Jordan, 2004). Our study has been focused on enhancing the efficient of SERMs, especially tamoxifen, in treating advanced breast cancer. Tamoxifen is a molecule that competes with estradiol to bind to estrogen-receptor (Shiau *et al.*, 1998). Its administration into the body fluid can suppress the stimulation of estradiol on breast cell growth and therefore induce breast tumour arrest or apoptosis (Mandlekar and Kong, 2001).

Breast cancer could be grouped into two main phases: early phase where estrogen receptor is expressed and advanced phase where estrogen receptor is absent. MDA-MB-231 cells are cell line that obtained from advanced breast cancer woman whom ER-α is absent. Therefore, our study is concentrated to patients that hormonal therapy is not efficient.

Pa-PDT was proved to be efficient in treating advanced breast cancer with the IC$_{50}$ equals to 0.5 μM (Bui-Xuan *et al.*, 2010). At lower concentration, e.g. inferior to 0.25 μM, the toxicity of Pa-PDT is limited (Figure 3.1). However, the produced energy is consequent to the change of cell physiology. Our hypothesis was that Pa-PDT at low concentration could activate certain gene transcriptions allowing the expression of the absent proteins. In the case of MDA-MB-231 cells, ER-α is an important receptor that its restoration can play major role in breast cancer treatment. Monitoring the expression of ER-α in Pa-PDT treated cells by Western Blot analysis showed that at 0.2 μM Pa-PDT could restore the expression of ER-α (Figure 4.1A).

The result is also confirmed by intracellular staining coupled to flow cytometric analysis and the immunohistochemistry (Figure 4.1B and C). Therefore, Pa-PDT triggers ER-α expression in MDA-MB-231 cells at the concentration ranged from 0.2 μM to 0.5 μM.

Our next question is whether Pa-PDT could enhance tamoxifen sensitivity towards MDA-MB-231 cells. IC_{10} and IC_{20} were used since at higher concentrations of Pa-PDT, the toxicity of Pa-PDT is too high and will mask tamoxifen effects. MTT assay of tamoxifen alone, tamoxifen with Pa-PDT at 0.1 μM and 0.2 μM showed that tamoxifen combined to 0.2 μM of Pa-PDT reduces the IC_{50} of tamoxifen at 24h incubation from 19 μM to 17 μM (Figure 4.3A). To confirm if the result is due to PDT method, other photosensitizer is used for similar assay. Riboflavin, also named vitamine B2 (VitB2), is another natural photosensitizer. The IC_{50} of VitB2-PDT in treating MDA-MB-231 cells is 50 μM (Figure 4.2). MTT assay was performed with tamoxifen alone, tamoxifen with VitB2-PDT at 10 μM and 20 μM showed that the IC_{50} of tamoxifen is reduced from 19 μM to 16 μM, similarly to Pa-PDT effect (Figure 4.3B). Therefore, tamoxifen in combination with PDT at low concentration could be a new method to enhance the efficiency of tamoxifen in treating late phase breast cancer.

In order to elucidate the mechanistic action of Pa-PDT combined with tamoxifen, Western Blot of apoptosis pathway related proteins were investigated. Apoptosis is the most common pathway induced by an anti-tumour agent and mediated by caspases leading to programmed cell death (Igney and Krammer, 2002). Among caspase family members, caspase-3, caspase-9, and caspase-8 have been recognized as the major caspases for apoptosis execution (Cohen, 1997). They are synthesized inside the cells under procaspase forms, which are inactive zymogens and

are divided into 2 groups: initiator caspases including procaspases-2, -8, -9 and -10, and executioner caspases including procaspases-3, -6, and -7. It can be triggered by various stimuli from outside and inside the cells. Therefore, we distinguish extrinsic and intrinsic apoptosis.

Extrinsic apoptosis pathways is commended by caspase-8 which is recruited by the death inducing signalling complex, belonged to the tumour necrosis factor receptor (TNFR) family (Nagata, 1997). TNFR gene superfamily includes TNFR-1, Fas/CD95, and the TRAIL receptors DR4 and DR5 (Ashkenazi, 2002). Figure 3.4 B showed that Pa-PDT-Tam treated cells increase the expression of both Fas and DR-5 receptors comparing to the treatment of Pa-PDT alone or tamoxifen alone. This suggests that Pa-PDT-Tam treatment could trigger extrinsic apoptosis. Nevertheless, there are two types of extrinsic apoptosis. In type I extrinsic apoptosis, only caspase 8 involved in the death execution. Once bound to the death inducing signalling complex, several procaspase-8 activates each other by autoproteolysis (Micheau and Tschopp, 2003). However, in type II extrinsic apoptosis, the signal is amplified via mitochondria-dependent apoptotic pathways. The link between the caspase signalling cascade and the mitochondria is ensured by the Bcl-2 family member Bid which is cleaved by caspase-8 in its truncated form (tBid) (Li *et al.*, 1998). tBid is translocated to the mitochondria and acts as a proapoptotic agent, together with Bax and Bak (Billen *et al.*, 2009). An increase of tBid in Pa-PDT-Tam treated cells suggested that the cell death is mediated by type II extrinsic apoptosis (Figure 4.4B).

On the other hand, mitochondria controls the integration and the propagation of death signals originating from intracellular DNA damage, oxidative stress, starvation, and those induced by chemotherapeutic drugs (Nguyen and Hussain, 2007). This mitochondria-dependent apoptosis involves procaspase-9 and regulated

71

by the Bcl-2 family (Riedl and Salvesen, 2007). The caspase 9 is cleaved by cytochrome c and active Apaf-1 into an activated form and initiates a caspase cascade involving caspase-3, caspase-7, and caspase-6 leading to cell death (Rodriguez and Lazebniz, 1999). A bcl-2 family of proteins belongs to two main groups: pro-survival members (e.g. Bcl-XL, Bcl-w, A1 and Mcl-1) and pro-apoptotic members (e.g. Bax-subfamily consists of Bax, Bak, and Bok, Bid, Bim, Bik, Bad, Bmf, Hrk, Noxa, Puma, Blk, BNIP3, and Spike) (Adams and Cory, 1998; Cory and Adams, 2002; Mund et al., 2003). In our case, an increase in active caspase-9 and a decrease in procaspase-3 were observed in the Pa-PDT-Tam treated cells (Figure 4.4A). The involvement of mitochondria machinery is also confirmed by the decrease of anti-apoptotic protein bcl-2 and the increase of pro-apoptotic protein Bad (Figure 4.4A).

Other important protein involved in mediating apoptosis is the tumour suppressor p53. It is inactivated in more than 50% of all human cancers (Hollstein et al., 1991). p53 is activated as a transcription factor resulting in growth arrest and/or apoptosis by stimulating the expression of several proteins such as p21, Bax, Puma, Noxa, Apaf-1, Fas and DR5 (Slee et al., 2004) or by repressing the expression of antiapoptotic proteins : bcl-2, Bcl-XL or survin (Kuribayashi and El-Deiry, 2007). In our study, p53 was not expressed in control MDA-MB-231 cells. However, its expression was slightly observed in Pa-PDT treated cells and tamoxifen treated cells, and significantly expressed in Pa-PDT-Tam treated cells (Figure 4.4A). Therefore, the combined treatment enhances strongly the expression of p53 which is only marginally increased in Pa-PDT or tamoxifen treatment alone. In the same way, the cleaved form of poly(ADP-ribose) polymerase (PARP) was significantly increased in Pa-PDT-Tam treatment comparing to Pa-PDT or tamoxifen treatment alone (Figure 4.4A). PARP is a protein involved mainly in DNA repair and programmed cell death. This protein can

be cleaved by many caspase-like proteases *in vitro* (Lazebnik *et al.*, 1994; Cohen, 1997) and caspase-3 *in vivo* (Nicholson *et al.*, 1995; Tewari *et al.*, 1995). PARP maintains cells viability and therefore its cleavage facilitates apoptosis process (Oliver *et al.*, 1998).

Additional to the antitumour effect through the inhibition of estrogen receptor, the antitumour activity of tamoxifen is also believed to mediate through an ER-independent mechanisms including the modulation of protein kinase C (PKC), calmodulin, transforming growth factor-β (TGF-β), and c-myc. Other pathways such as caspases, mitogen-activated protein kinase (MAPK), oxidative stress and mitochondrial related cell death induction are also involved (Mandlekar and Kong, 2001). However, Pa-PDT is believed to induce mainly by intrinsic pathway (Tang et al., 2006, 2007, 2009a,b, 2010). Our results showed that both extrinsic type II and intrinsic apoptosis were triggered in the combined treatment. The intrinsic apoptosis may be required for the amplification of the induced extrinsic apoptosis. However, the intrinsic apoptosis may also be triggered independently from the extrinsic apoptosis since a Pa-PDT (0.2 μM) may produce mitochondria potential change and ROS release (Bui-Xuan *et al.*, 2010).

PDT is not the only method which is proposed to induce ER-α expression and to enhance the sensitivity of tamoxifen towards MDA-MB-231 cells. Other drugs or molecules that were reported to induce ER-α expression including decoy oligonucleotide (Penolazzi *et al.*, 2007), valproic acid (Fortunati *et al.*, 2009), β-Sitosterol (Awad *et al.*, 2008), OSU-03012 (Weng *et al.*, 2008) and Wnt-5a (Ford *et al.*, 2009). This study demonstrated Pa-PDT as a new method in restoring ER-expression in MDA-MB-231 cells. The effect could be linked to the capacity of Pa-PDT in inducing ER-α re-expression thereby providing a potential new modality for

breast cancer treatment. However, further investigation such as using siRNA of ER-α in Pa-PDT and tamoxifen treated cells is needed to affirm the result.

4.4 Conclusion

Pa-PDT showed to be an efficient method in treating late phase of human breast cancer *in vitro* at high dose (e.g. from 0.5 μM). At lower dosage, Pa-PDT overcomes partially to prevent MDA-MB-231 cell expansion. However, in combination with tamoxifen, Pa-PDT-Tam is suggested to exert a better result in treating breast cancer by inducing both intrinsic and extrinsic apoptosis. Photodynamic therapy should be considered as a method to enhance tamoxifen sensitivity to breast cancer by enhancing the ER-α expression, especially at the late phase where tamoxifen action is limited.

(A)

MCF-7   MDA (0 μM)   MDA (0.2 μM)

ER-α

β-actin

(B)

(C)

Control   Pa = 0.25 μM
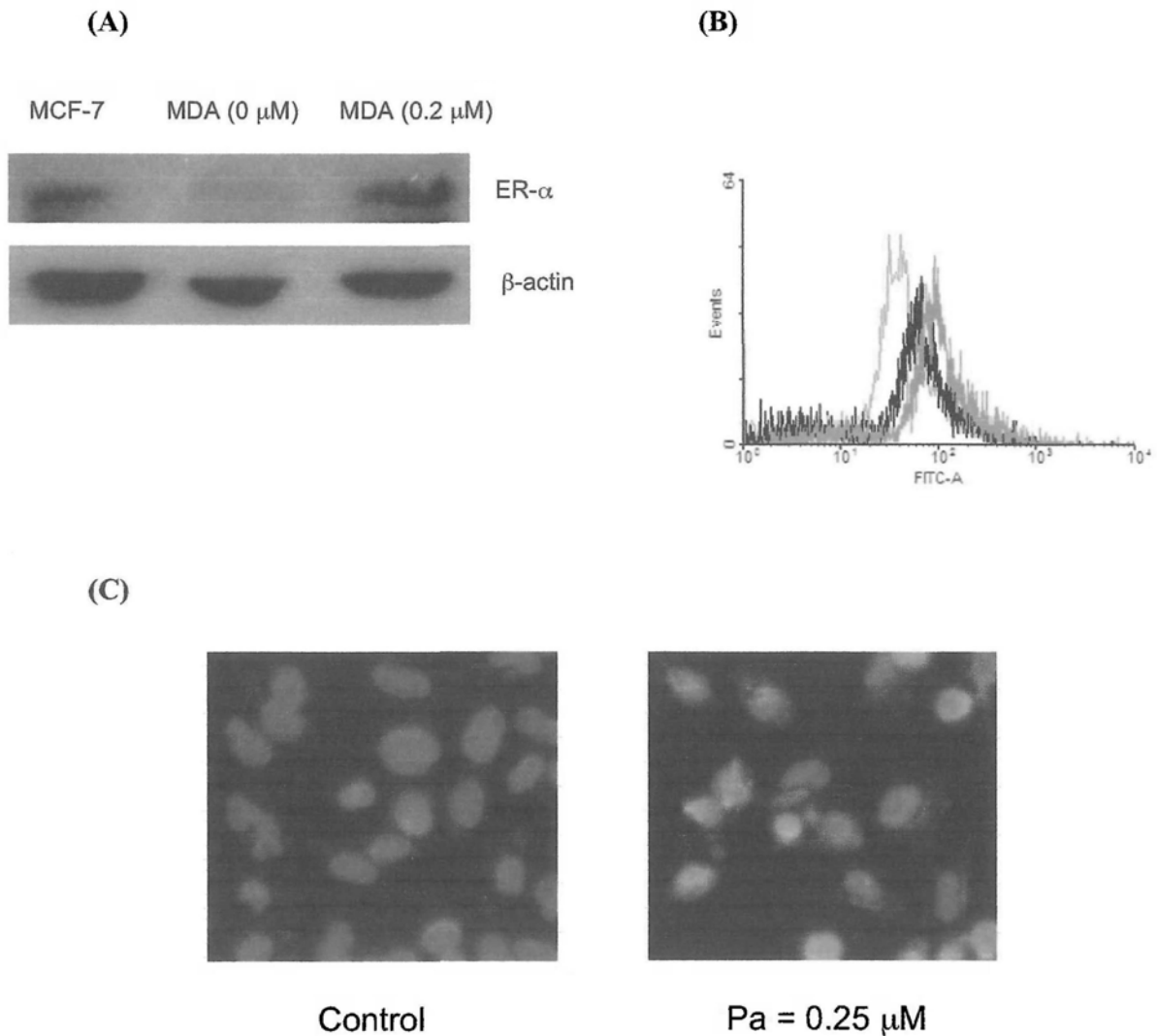
Figure 4.1 - Pa-PDT restores ER-α expression. (A) MDA-MB-231 cells were treated with vehicle control or 0.2 μM of Pa for 2 h following by 20 min of PDT. MCF-7 served as positive control. Treated cells were analysed by Western blot 24 h later to investigate the protein expression of ER-α. Representative images are shown from 3 independent trials with essential **similar** results. **(B)** MDA-MB-231 cells were treated with vesicle control or appropriate Pa concentration for 2 h, followed by 20 min of PDT. Cells were collected 24 h after treatment, fixed, permeabilized and stained with ER-α antibody for 50 min at 4°C, then with FITC secondary antibody for 25 min at 4°C. Cells were then subjected to cytometric analysis. Red: control, Black: 0.25 μM Pa, Green: 0.5 μM Pa. Representative images are shown from 3 independent trials with essential **similar** results. **(C)** The Pa-PDT treated cells were fixed at 24 h after PDT. Cells were stained with ER-α antibody then probed with FITC-conjugated secondary antibody. The nuclei were stained with 10 μM Hoechst 33342. The stained cells were analyzed using fluorescence microscope, where the nuclei were assigned as blue, the ER-α was

assigned as red in colour. Representative images are shown from 3 independent trials with essential similar results.
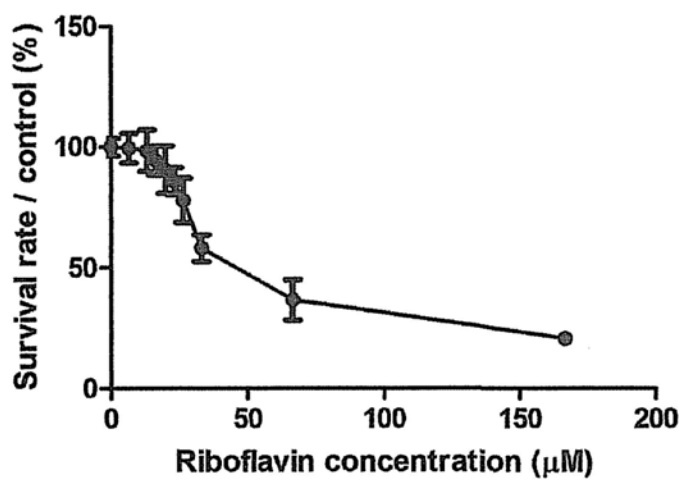
Figure 4.2 - The inhibitory effect of VitB2-PDT on MDA-MB-231 cells *in vitro*. Cells were pre-incubated with vitamin B2 for 2 h, and then illuminated. Cell activity was measured by MTT assay at 24 h after treatment. The results are reported as mean ± S.D. with 3 independent experiments.

(A)
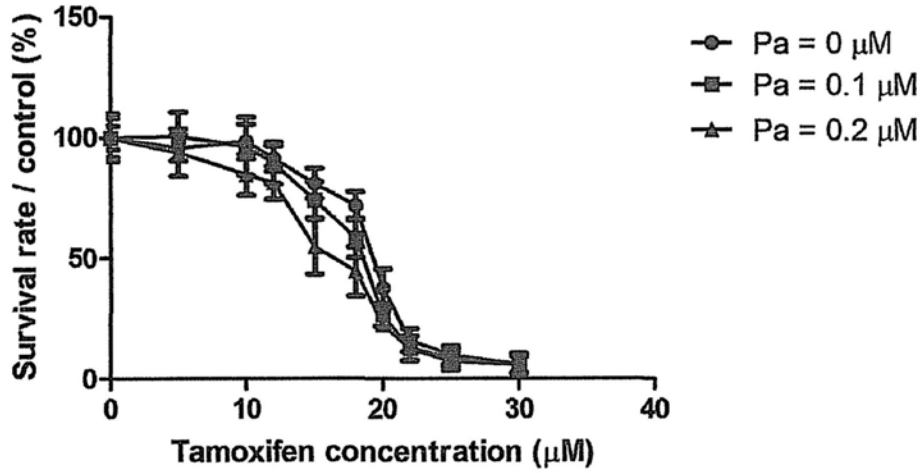
(B)
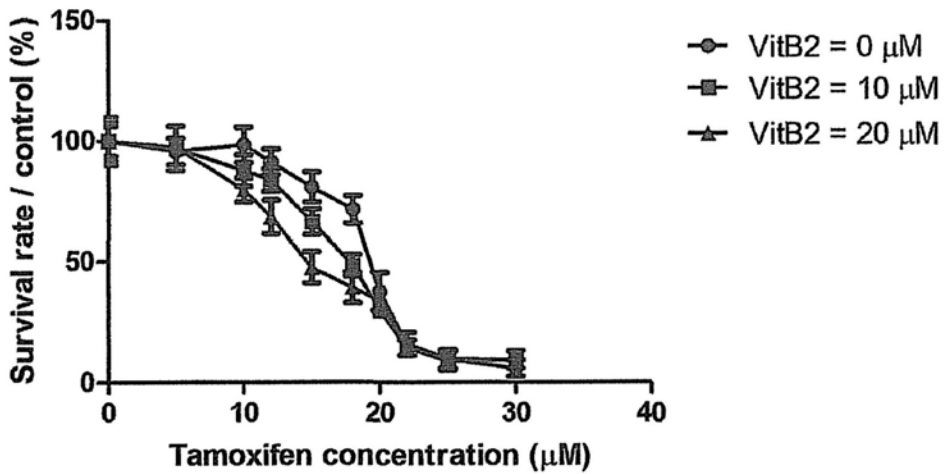
Figure 4.3 – PDT enhances the sensitivity of MDA-MB-231 cells to Tamoxifen *in vitro*. Pheophorbide a **(A)** or riboflavin **(B)** were preloaded for 2 h at IC_{10} or IC_{20} with tamoxifen followed by 20 min of photoactivation. Cells with tamoxifen alone were kept in dark. MTT assay was performed 24 h after treatment. The results are presented as mean ± S.D. with 3 independent experiments.

(A)

| Tam (5 μM) | - | - | + | + |
| Pa (0.2 μM) | - | + | + | - |

Fas

DR5

tBid

β-actin

(B)

| Tam (5 μM) | - | - | + | + |
| Pa (0.2 μM) | - | + | + | - |

bcl-2

BAD

pro-cap3

cleaved caspase 9

cleaved PARP

p53

β-actin
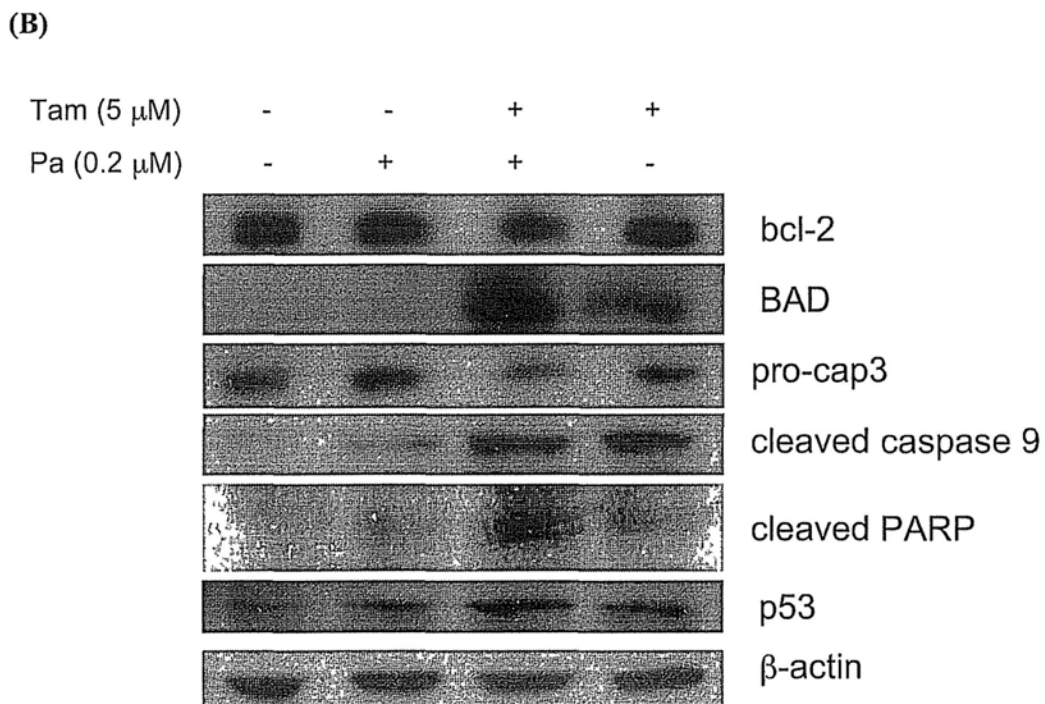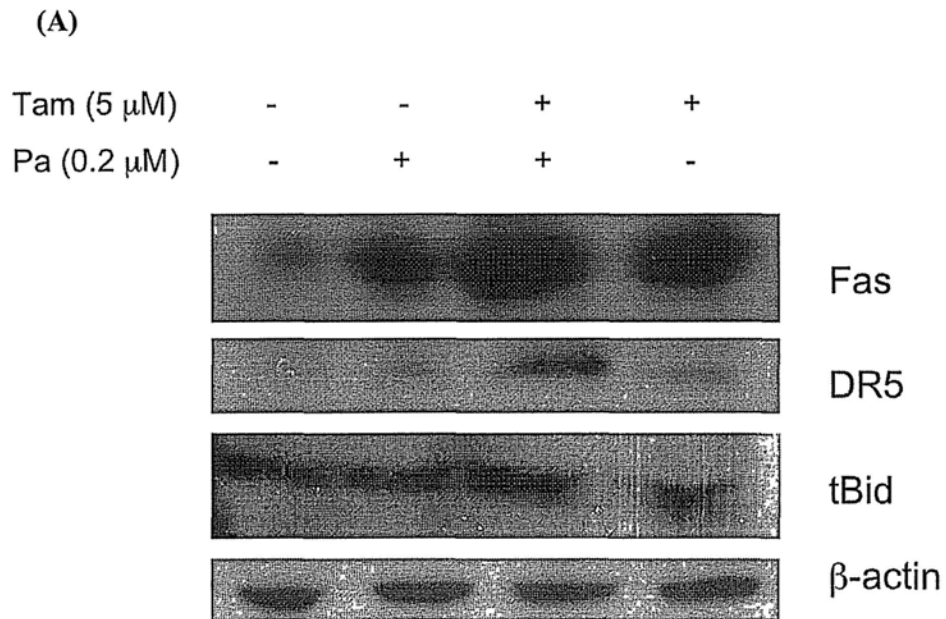
Figure 4.4 - Level of apoptosis-related proteins in Pa-PDT combined to tamoxifen treated MDA-MB-231 cells. Cells were treated with Pa-PDT (0.2 μM), or with Pa-PDT combined with tamoxifen (0 2 μM and 5 μM respectively), or tamoxifen (5 μM) or without any drug (control). The total proteins of the cells were collected 24 h after photo-activation and cell lysates were subjected to Western Blot

analysis for extrinsic apoptosis (A) or intrinsic apoptosis (B) related proteins. Representative images are shown from 3 independent trials with essential similar results.

Chapter 5

Pheophorbide a – mediated photodynamic therapy triggers HLA Class I-restricted antigen presentation in human breast adenocarcinoma

5.1 Introduction

PDT action is directly associated with necrosis and/or apoptosis of tumour cells. However, PDT has secondary effects on microvascular disruption, and suppressive or stimulatory effect on the immune system (Henderson *et al.*, 2003; Daniell and Hill, 1991; Kabingu *et al.*, 2007; Kousis *et al.*, 2007). Most of the cancer treatments such as surgery, radiotherapy or chemotherapy engender immunosuppression. Therefore, the ideal treatment should take into account the immune system of the host response against cancer. In the case of PDT, acute inflammation was observed by the expression of heat-shock proteins, invasion and infiltration of the tumour by leukocytes, and might increase the presentation of tumour-derived antigens to T cells (Krosl *et al.*, 1995). PDT induces anti-tumour immunity by enhancing maturation and activation of DCs that are able to stimulate T cells (Gollnick *et al.*, 2006) but the details of this mechanism are still unclear. Furthermore, PDT is effective as a preventive and therapeutic tumour vaccine (Gollnick and Brackett, 2010).

Proteomic method has been used to elucidate the anti-tumour effect of Pa-PDT on MDA-MB-231 cells. Besides the direct cytotoxicity, Pa-PDT triggers antigen-presentation to enhance anti-tumour immunity in breast cancer.

5.2 Results

5.2.1 Identification of Pa-PDT-Mediated Protein Expression in MDA-MB-231 Cells

Protein lysate of Pa alone (dark control) and Pa-PDT-treated MDA-MB-231 cells were analysed by two-dimensional PAGE to screen for the potential pathways mediated by Pa-PDT (Figure 5.1). The induced protein spots were detected by the PDQuest sofeware (Bio-Rad). Protein spots with significantly different expression levels were exhibited in the 0.5 μM Pa-PDT-treated sample (Figure 5.1B) comparing with the dark control (0.5 μM Pa without PDT) ($p < 0.05$) (Figure 5.1A). Proteins spots that were successfully identified by MALDI-TOF MS analysis and belonged to specific pathways are illustrated in Figure 5.1 and classified in Table 5.1.

5.2.2 Induction of Antigen-Processing Machinery in Pa-PDT treated MDA-MB-231 Cells

Antigen presentation machinery differs for two classes; class I presents intracellular antigens and class II presents extracellular antigens (Braciale *et al.*, 1987). The conventional assembly of HLA class-I molecular pathway requires endoplasmic reticulum chaperons including ERp57, however alternative HLA class-I processing and presentation could involve exogenous antigens induced by HSP70 (Grommé and Neefjes, 2002; Campoli and Ferrone, 2008). This pathway is further confirmed in Pa-PDT-treated MDA-MB-231 cells by Western blot analysis. The expression of HSP70 and ERp57 were increased in a dose-dependent manner (Figure 5.2A). Other protein expression such as HLA class-I and calreticulin (CRT), proteins

for the ERp57-mediated antigen processing machinery, were also increased in a dose-dependent manner. The increased expression of HLA class-I protein was also observed under fluorescent microscope, showing a plasma membrane localization (Figure 5.2C). Similar result was observed in Pa-PDT-treated MCF-7 cells, a tumour cell line which represents early stage of breast cancer (Figure 5.2B). Our study demonstrated that Pa-PDT treatment would activate the antigen presentation on both early and advanced stage of breast cancer cells.

5.2.3 Involvement of HSP70 in HLA Class I-Mediated Antigen Presentation during Pa-PDT

The involvement of HSP70 on antigen presentation is still controversial. The potential interaction of HSP70 with HLA class I protein was investigated. Subcellular localization of HLA class I and HSP70 was studied by immunostaining using a fluorescent microscopy. The fluorescence of HSP70 and HLA class I protein was concentrated on the plasma membrane and the two signals were well overlapped with each other (Figure 5.3A). The interaction between HSP70 and HLA class I was further confirmed by immunoprecipitation method. HSP70 was detected by Western blot in immune complexes precipitated with HLA class I specific antibody from both Pa-PDT-treated MDA-MB-231 and MCF-7 cells (Figure 5.3B). The data suggested that HSP70 was recruited by HLA class I protein during Pa-PDT treatment in breast cancer cells.

5.2.4 Induction of Phagocytic Activity of Human Macrophages by Pa-PDT-treated MDA-MB-231 Cells

PDT treatment was suggested to enhance immunogenicity of human cancer cells (Korbelik, 1996). In this study, the induction of phagocytic activity of human macrophages by Pa-PDT-treated cells was investigated. As shown in Figure 5.4, the phagocytic activity was increased by two fold with the co-incubation of Pa-PDT-treated MDA-MB-231 cells whereas the phagocytic activity was decreased to 75% in the sample of MDA-MB-231 cells treated with solvent control. The result demonstrated that Pa-PDT would also give a positive influence on the phagocytic capture and ingestion of human breast adenocarcinoma by macrophages.

5.3 Discussion

The involvement of immune system on cancer treatment after PDT has recently been investigated. Spontaneous regression of advanced tumours has been reported and the significances of PDT on immunostimulation or immunosuppression have been well described (Castano *et al.*, 2006; Korbelik, 1996; van Duijnhoven *et al.*, 2003; Canti *et al.*, 2002). PDT was suggested to induce anti-tumour immunity associated with apoptosis (Kabingu *et al.*, 2007). Therefore, it inspires an ideal cancer therapy that can give specific direct cytotoxicity to the tumour cells and at the same time trigger the immune reorganization of cancer cells. Thus, the therapeutic potential of Pa-PDT on cancer immunity was investigated in this study. Protein expression profile of Pa-PDT–treated MDA-MB-231 cells was analyzed using two-dimensional PAGE (Figure 5.1) to find out the potential induced pathways. Different proteins were

found to be upregulated and classified into different pathways including the inhibition of glycolysis, cancer marker and antigen presentation (Table 5.1).

HLA class I molecules present peptides derived from endogenous antigens. Conventional HLA class I antigen processing and presentation involve transient interactions with calnexin, calreticulin, Erp57, tapasin and TAP. Once assembled, the HLA class I complex is released from the endoplasmic reticulum and transported to the cell surface (Garbi *et al.*, 2007). Alternatively, HLA class I antigen processing and presentation could involve exogenous antigens, which are generally presented by HLA class II. This non-classical pathway is described by at least two fundamentally different mechanisms: the phagosome-to-cytosol pathway (e.g. involving the access of exogenous antigen to the conventional HLA class I loading pathway), and the post-Golgi loading of HLA class I molecules (Grommé and Neefjes, 2002), the phagosome-to-cytosol pathway. *In situ* HSP70 overexpression belongs to the phagosome-to-cytosol pathway and is known to enhance DC antigen presentation and overcomes host immune tolerance to tumour antigens. It is involved in antigen presentation and antitumour immune responses by cooperating with the antigen presenting cells (Ren *et al.*, 2004; Korbelik *et al.*, 2005). Other important protein for the formation of antigen presentation complex is ERp57, a protein disulfide isomerase, which functions together with calnexin, calreticulin, and tapasin as a molecular chaperone for the generation of a stable HLA class I-peptide complex in the endoplasmic reticulum (Garbi *et al.*, 2007; Dick, 2004; Cresswell *et al.*, 1999). Our results demonstrated that the activation of ERp57-mediated pathway occurred during Pa-PDT treatment whereas the HLA class I-restricted antigen presentation machinery was triggered and the expression of HLA class I protein was upregulated on the

84

plasma membrane of the treated MDA-MB-231 cells (Figure 5.2A and B). Our findings suggest that Pa-PDT can trigger antigen presentation in both early and advanced treated breast cancer cells to stimulate the host immune response.

HSP70 has been suggested to be involved in antigen presentation during PDT treatments. It forms stable complexes, cross-presents the tumour antigens with HLA proteins, resulting in an antigen-specific T-cell stimulation in the cancer host (Korbelik et al., 2005; Castellino et al., 2000; Bendz et al., 2007). In this study, the Pa-PDT-triggered antigen presentation was found to work together with HSP70 (Figure 5.3A and B) in both treated MCF-7 and MDA-MB-231 cells. The interaction of HSP70 and HLA class I protein was confirmed by the coimmunoprecipitation assay (Figure 5.3B). Nevertheless, there is a new approach for developing tumour vaccines by using PDT-treated cancer cell lysates, and Pa-PDT should be considered as one of the candidates (Korbelik et al., 2007). Our results supported that HSP70 was upregulated and collaborated with the HLA class I proteins to enhance the antigen presentation efficiency in the Pa-PDT–treated cells.

Furthermore, breast cancer is believed to exhibit low immunogenicity. The effect of Pa-PDT-induced immunogenicity of human breast cancer cells was also demonstrated by its effect on primary human macrophages. As shown in Figure 5.4, a significant increase of phagocytic activity was found when the macrophages were coincubated with Pa-PDT–treated MDA-MB-231 cell lysate. Interestingly, an inhibitory effect was given to the human macrophages when the MDA-MB-231 cells (dark control) were applied instead (Figure 5.4). Our finding is consistent to previous

studies, where the PDT treated cancer cells could enhance macrophage cytotoxicity (Korbelik and Krosl, 1994; Zhou *et al*., 2009).

5.5 Conclusion

Taken together, our findings therefore provide the first evidence that Pa-PDT would activate the HLA class I-restricted antigen presentation machinery in both MCF-7 and MDA-MB-231 cells and result in an enhancement of anticancer immunity in the tumour host that would enhance the efficiency of anticancer treatment with Pa-PDT. Those results are consistent with our previous finding in HepG2 cells (Tang *et al*., 2010).

Dark control   **0.5 μM Pa-PDT**
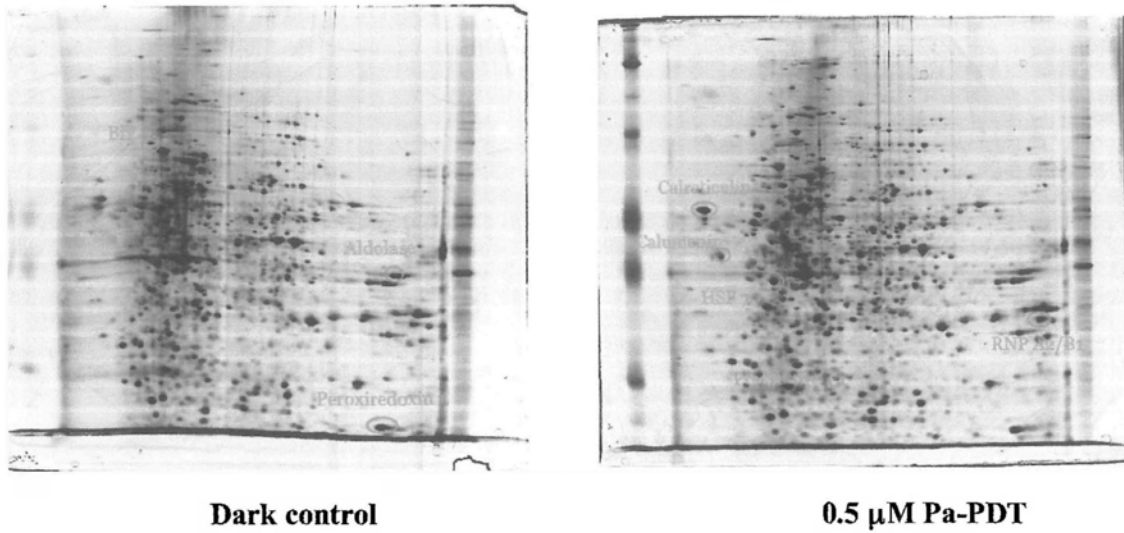
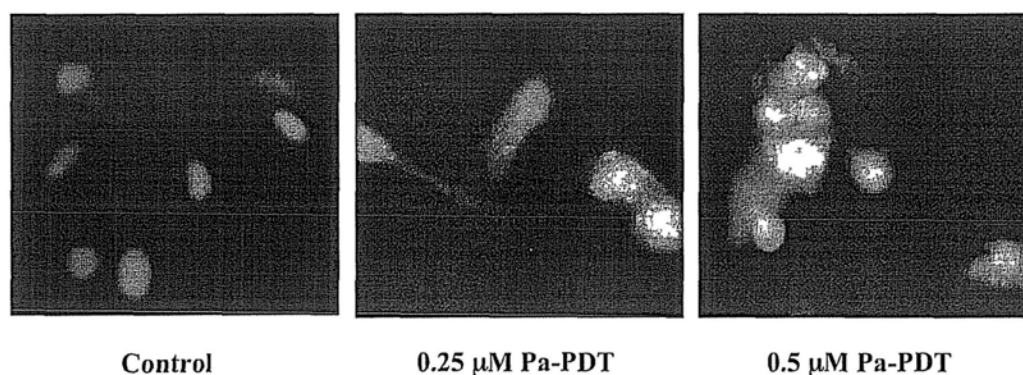**Figure 5.1 – Protein expression profile of Pa-PDT-treated MDA-MB-231 cells.** The total proteins of **(A)** 0.5 μM Pa (dark control) and **(B)** 0.5 μM Pa-PDT-treated MDA-MB-231 cells were extracted at 6 hours after illumination. The protein samples were subjected to isoelectric focusing, then separated on a 10% SDS-PAGE gel, and finally visualized by silver staining. Representative results are shown from 5 independent experiments with essential similar results.

(A)

CTL   0 5   0 75   (μM) Pa-PDT

Calreticulin

HSP70

HLA (class I)

β-actin

(B)

CTL   0 5   0 75   (μM) Pa-PDT

(C)

Control   0.25 μM Pa-PDT   0.5 μM Pa-PDT
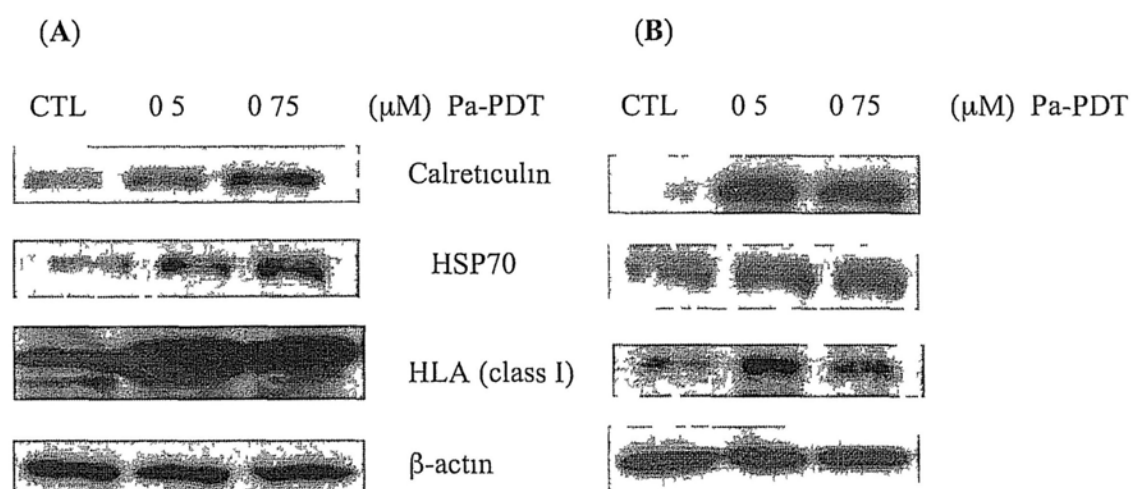
Figure 5.2 – Induction of antigen presentation by Pa-PDT treatment. Change in the expression level of proteins related to antigen presentation machinery in Pa-PDT treated **(A)** MDA-MB 231and **(B)** MCF-7 cells Cells were treated with solvent (0 04% ethanol, CTL) or Pa (0 5 and 0 75 μM) for 2 hours, then illuminated for 20 minutes Four hours after treatment, the whole-cell lysates were prepared, and the expression levels of various related proteins were analyzed using Western blot Representative results are shown from 5 independent experiments with essential similar results **(C)** The induction of HLA class I protein expression in Pa-PDT-treated MDA-MB-231 cells The Pa-PDT-treated cells were fixed at 24 hours after treatment and overnight immunostained with monoclonal anti-HLA class I antibody The stained cells were probed with FITC-conjugated secondary antibody for 2 hours before fluorescence microscope observation Fluorescence micrographs were acquired with an excitation wavelength at 400 to 440 nm and an emission wavelength at 590 to 650 nm Representative results are shown from 3 independent experiments with essential similar results CTL Control
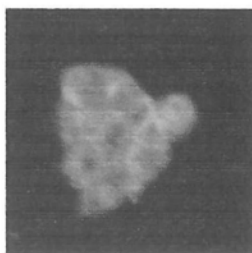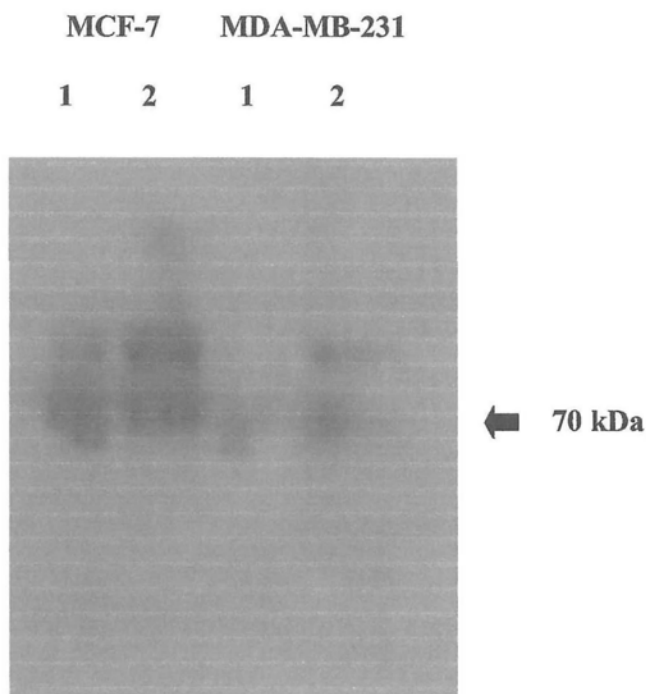
(A)

(B)
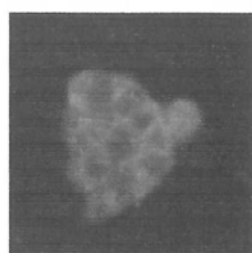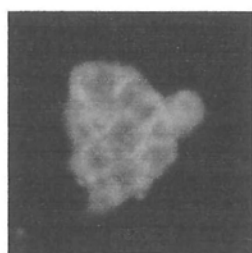
HSP 70

HLA class I

Merged Image

MCF-7   MDA-MB-231

1   2   1   2

⬅ **70 kDa**

Figure 5.3 – Association of HSP70 with HLA class I protein in Pa-PDT-treated breast cancer cells. (A) MDA-MB-231 cells were treated with 0.5 µM Pa-PDT, fixed at 24 hours after illumination, and overnight immunostained with monoclonal anti-HSP70 and anti-HLA class I antibodies. The stained cells were then further probed with secondary antibody that is either FITC - or Alexa Fluor 594–conjugated for 2 hours before observation. Fluorescence micrographs were acquired with a Nikon fluorescent microscopy, where HSP70 was assigned as green, and the HLA class I protein was assigned as red. In the merged image, colocalization of HSP70 and HLA class I protein showed yellow color. Images are a representative of 3 independent experiments with essential similar results **(B)** The samples CTL (solvent control) and 0.5 µM Pa-PDT-treated MDA-MB-231 and MCF-7 cells (Pa-PDT) were collected at 4 hours after PDT treatment and immunoprecipitated with anti–HLA class I antibodies followed by SDS-PAGE and immunoblot analysis with anti–HSP70 antibodies. Lane 1: CTL; lane 2: Pa-PDT. Representative results are shown from 3 independent experiments with essential similar results.
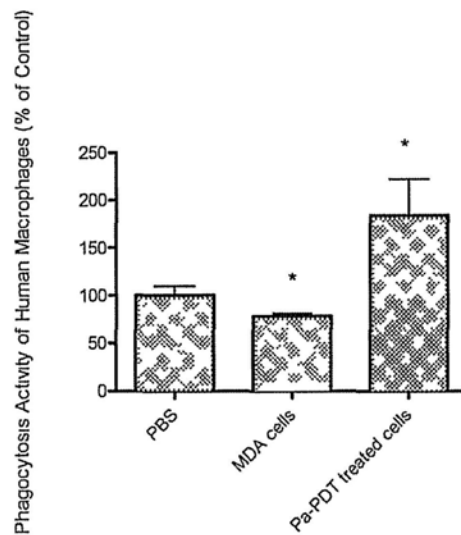
Figure 5.4 – Induction of human macrophages phagocytic activity by Pa-PDT-treated cells. The MDA-MB-231 cells were treated with Pa-PDT, collected at 2 hours, and then resuspended in PBS The human marcophages were incubated with PBS (PBS), cell lysates of MDA-MB-231 treated with 0 04% ethanol as solvent control (MDA-MB-231 cells), or cell lysate of Pa-PDT-treated MDA-MB-231 cells (Pa-PDT-treated MDA-MB-231 cells) for 1 hour, and then the phagocytosis activities of human marcophage were measured by the Vybrant Phagocytosis Assay Kit The results are presented as mean ± S D with 3 independent experiments with essential similar results ([*]p< 0 05, when compared with the PBS only control)

Protein	CI (%)	Function
Calreticulin	100	ER proteins
GRP78/BiP	100	
Calumenin	99.992	
HSP70	100	Stress related proteins
Peroxiredoxin	100	
RNP A2/B1	95.351	Cancer marker
Prohibitin	99.204	Apoptotic related
Adolase	99.993	Glycoysis

Table 5.1 – The differentially expressed main proteins mediated by Pa-PDT in MDA-MB-231 cells. The Pa-PDT-regulated proteins identified from two-dimensional gel electrophoresis and MALDI-TOF MS analysis were listed according to confidence interval (CI) and grouped by their function.

Chapter 6

Pheophorbide a: a photosensitizer with immunostimulating activities on mouse macrophage RAW 264.7 cells and human peripheral blood mononuclear cells in the absence of irradiation

6.1 Introduction

Many studies have been conducted to elucidate the action of clinically used photosensitizers in cancer eradication by PDT (Allison *et al.*, 2004; Marchal *et al.*, 2005; Kinzler *et al.*, 2007; O'Connor *et al.*, 2009). However, no study has been performed to evaluate the potential effect of those photosensitizers, in the absence of irradiation, in stimulating immunocytes for the suppression of the growth of tumour cells.

According to the bioassay guided method, our group has identified Pheophorbide a (Pa) as a potential anti-cancer agent (Chan *et al.*, 2006). Pa is the most studied chlorophyll metabolite (Hörtensteiner, 2006) with anti-tumour activity by disrupting the integrity of tumour DNA at high concentration (Chan *et al.*, 2006; Cheng *et al.*, 2001; Nakamura *et al.*, 1996; Hibasami *et al.*, 2000). Pa is also a natural photosensitizer and Pheophorbide a (Pa) based photodynamic therapy (Pa-PDT) enhances cancer suppression and reduces the effective dosages (Hajri *et al.*, 2002; Lee *et al.*, 2004; Lim *et al.*, 2004; Rapozzi *et al.*, 2009). Our group has also demonstrated that Pa is an efficient photosensitizer for cancer treatment (Tang *et al.*, 2006; 2007, 2009a,b, 2010; Bui-Xuan *et al.*, 2010). However, no study has been conducted to investigate the immunomodulatory effects of Pa. In the present work, we investigated the potential activities of Pa on a murine macrophage cell line RAW 264.7 and on human immune competent cells isolated from fresh human peripheral blood. Our data showed a stimulatory effect of Pa on both murine and human immune effector cells, which is suggested to be an outcome of the activation of MAPK pathway by Pa treatment.

6.2 Results

6.2.1 Proliferation of Pa-stimulated RAW 264.7 cells

Cell viability was measured by using MTT assay. As shown in Figure 6.1, Pa could stimulate the growth of RAW 264.7 cells at different time points from 24 to 72 h, where maximum stimulation was found at 1.0 μM. The peak cell growth is more significant comparing with the control at longer incubation time (e.g 120% at 24 h, 150% at 48 h and 165% at 72 h). Insignificant cytotoxicity was observed in Pa-treated cells at tested concentrations (0 - 5 μM).

6.2.2 Enhancement of phagocytosis and the induction of inflammatory cytokines after Pa stimulation in RAW 264.7 cells

Pa was shown to significantly activate the phagocytotic activity of RAW 264.7 cells (Figure 6.2A). Macrophages are derived from monocytes and are able to secrete a wide range of cytokines, growth factors and other inflammatory mediators. They participate in the innate immunity by phagocytosing bacteria and non-host particles. Secretions of inflammatory cytokine interleukin (IL)-6 and tumour necrosis factor (TNF)-α were triggered in Pa-treated RAW 264.7 cells (Figure 6.2B and C).

6.2.3 Screening of induced cytokines in Pa-treated human immune competent cells

Our study on murine macrophage cell line showed an induction of inflammatory cytokines in Pa-treated cells. A screening of induced cytokines in Pa-treated human immune competent cells including lymphocytes, macrophages and neutrophils was then performed. IL-6, IL-12, IL-17, IFN-γ, TNF-α and GM-CSF were induced at different concentrations (e.g. 1 μM, 5 μM and/or 10 μM of Pa) and cell type (Table 6.1).

6.2.4 Subcellular localization of Pa and ROS production in Pa-stimulated monocytes

To further investigate the underlying mechanism of Pa-mediated immune stimulation, the intracellular localization of Pa was investigated at 2 h by co-staining the Pa-treated cells with MitoTracker Green. As shown in Figure 6.3A, Pa is suggested to be localized specifically at the mitochondria in RAW 264.7 cells. In addition, JC-1 staining reveals a change of mitochondrial membrane potential in Pa-treated cells (Figure 6.3B); and the release of ROS (e.g. peroxidants), small molecules that can trigger either cell death or cell growth, was also triggered in the Pa-treated cells (Figure 6.3C). Despite the depolarization of mitochondrial membrane and an increase of ROS level, the sub-G1 population remains unchanged in Pa-treated cells and control cells according to the Figure 6.3D. Therefore, no apoptosis was observed and Pa did not exhibit any cytotoxicity at the tested concentration, consistently with the growth curve.

The cell cycle was also performed in Pa-treated human monocytes,

lymphocytes and neutrophils. Similar to murine monocytes, Pa exhibited no toxicity up to 10 μM (Figure 6.3F). In the same concentration range, ROS (e.g. peroxidants) release was observed (Figure 6.3G), accompanied with a change of mitochondrial membrane potential (Figure 6.3E)

6.2.5 Activation of mitogen activated protein kinases (MAPK) in Pa-treated immune competent cells

Generation of ROS can rapidly activate MAPK pathway, especially the phosphorylation of extracellular signal-regulated kinase (ERK) in order to induce cell proliferation. The total and phosphorylated forms of three major MAPK including c-Jun amino-terminal kinases (JNKs), ERK and p38, were monitored by Western blotting. In Figure 6.4A, the phosphorylation of ERK, JNK and p38 was activated after 2 h of Pa incubation. The phosphorylation of p38, ERK and JNK were increased in a dose-dependent manner, while the expression levels of p38, ERK1, ERK2, JNK1 and JNK2 remained unchanged (Figure 6.4B).

The expression of MAPKs in Pa-treated human immune competent cells were investigated using flow cytometric analysis of intracellular stained cells method. p-p38 activation was found to be mediated in CD4+ cells, CD14+ cells and neutrophils whereas p-JNK activation was mediated in CD4+ cells and CD14+ cells and p-ERK activation was mediated only in CD4+ cells (Figure 6.4C).

6.2.6 Activation of MAPK promotes cell growth and cytokine secretion in Pa-treated RAW 264.7 cells

Addition of MEK1/2 inhibitor at 24 h (5 μM) suppressed the growth stimulation of Pa on RAW 264.7 cells (Figure 6.5A). In addition, secretion of IL-6 and TNF-α in the Pa-treated cells were significantly inhibited by p38 inhibitor (1 μM) (Figure 6.5B and C).

6.3 Discussion

Pa is identified at first as an anti-tumour agent (Chan *et al.*, 2006; Cheng *et al.*, 2001; Nakamura *et al.*, 1996; Hibasami *et al.*, 2000). and has subsequently been shown to be a potential photosensitizer in treating colonic, leukaemia, pigmented melanoma, hepatoma, uterine and breast cancer (Hajri *et al.*, 2002; Lee *et al.*, 2004; Lim *et al.*, 2004; Rapozzi *et al.*, 2009; Tang *et al.*, 2006; 2009a, 2009b, 2010; Bui-Xuan *et al.*, 2010). Therefore, Pa and Pa-PDT are generally proposed to be a potential anti-cancer agent. However, the effect of Pa on the immune system is rarely investigated. Our present study demonstrated for the first time that Pa alone without photo-activation possesses immunostimulatory effects on mouse macrophages.

Pa was found to be specifically localized at the mitochondria, as shown in Figure 6.3A, which is the main organelle for the production of free radicals including ROS and reactive nitrogen species (RNS) (Murphy, 2009; Dröge, 2002). The mitochondria can continuously produce ROS when oxygen and oxidative substrates are available (Starkov, 2008). ROS production was observed in Pa-treated RAW 264.7 cells (Figure 6.3C) but no RNS was released (data not shown). The oxidant

character of Pa is due to its carboxyl group. At the local environment of mitochondria, Pa can change the mitochondrial membrane potential and triggers ROS production (Figure 6.3B); whereas, the generation of RNS is due to the metabolism of arginine to citrulline (Valko *et al.*, 2007) and thus RNS was not observed during Pa treatment. To maintain proper function, cells need to keep their intracellular redox environment to be constant. Overproduction of ROS may lead to cell stimulation or cell death depending on its concentration (Torres and Forman, 2003). Therefore, PI staining was performed to investigate the toxicity of Pa in treated cells. Pa-treated RAW 264.7 cells presented similar sub-G1 population number comparing with non-treated cells (Figure 6.3D), thereby showing no apoptosis. Therefore, Pa induced ROS production did not lead to cell death.

MAPK, are conserved proteins kinases involved in many cell signalling pathways of eukaryotic cells and MAPK can be activated by low dose ROS on certain types of cells (Kamata and Hirata, 1999; Roux and Blenis, 2004). Although the exact mechanism of ROS-induced MAPK activation is unclear, the regulatory roles of MAPK on cell function have been reported (Wagner and Nebreda, 2009; Yao *et al.*, 2003). Due to the induction of ROS after Pa treatment (Figure 6.3B), we investigated the MAPK activation in Pa-treated RAW 264.7 cells. Figure 6.4A reveals that MAPK signalling pathways are activated via the phosphorylation of ERK, JNK and p38 in Pa-treated RAW 264.7 cells at 2 h. This is coherent to the fact that 2 h is required for the maximal cellular up-take of Pa (data not shown).

A wide range of stimuli could induce MAPK activation, e.g. growth factors activating ERK1/2 pathway. Therefore, MAPK plays a key role for cell proliferation, whereas stress stimuli are potent to activate JNKs and p38 MAPK (Pearson *et al.*,

2001; Meloche and Pouysségur, 2007). In this study, we found that Pa stimulates RAW 264.7 cell growth at different time points from 24h to 72h (Figure 6.1). The cell growth curves are similar between the three time points with higher intensity at higher incubation time. Optimal 48h was chosen for further growth stimulating study. Co-treatment with MEK1/2 inhibitor exhibited the abolishment of cell growth induced by Pa (Figure 6.5A). The phosphorylation of ERK was also observed in the treated cells (Figure 6.4B). Our findings suggested that Pa induces RAW cell proliferation by MAPK pathway via ERK activation. Besides, the activation of stress-activated protein kinases (SAPKs) such as JNK and p38 MAPK were also found during the Pa treatment (Figure 6.4B). The role of JNK activation in macrophages is still unclear. However, the phosphorylation of p38 MAPK is believed to regulate the expression of pro-inflammatory cytokines (Kamata and Hirata, 1999; Ono and Han, 2000; Rincón and Davis, 2009). The induction of IL-6 and TNF-α release was observed in the Pa-treated cells at 24 h of treatment as shown in Figure 6.2B and 6.5C, and introduction of p38 inhibitor could suppress the IL-6 and TNF-α release (Figure 6.5B and C). Cytokine secretion has been suggested to be mediated by the activation of p38 MAPK pathway during Pa treatment. IL-6 is an inflammatory cytokine in acute phase reaction produced by activated macrophages (Heinrich *et al.*, 2003); and TNF-α is another macrophage secreted inflammatory cytokine for the induction of apoptosis and inflammation, inhibition of tumourigenesis and viral replication (Locksley *et al.*, 2001). Our observations indicated that Pa could act as a potential therapeutic agent for treating infection. Moreover, TNF-α can enhance phagocytosis of macrophages, and phagocytosis is one of the several mechanisms to internalize particles and solutes into cells (Aderem and Underhill, 1999; Ousman and David, 2001). Pa is able to enhance

the phagocytic rate in RAW 264.7 cells after 24h, as shown in Figure 6.2A, therefore, Pa-induced phagocytosis may be related to TNF-α release.

We extend our mouse model to human *ex-vivo* model. While Pa exerts immunostimulation at low concentrations (e.g. 0.5 to 2.0 μM) in murine macrophages, higher concentrations are required in human immune competent cells (e.g. 1.0 to 10.0 μM). Measurement of ROS release in the Pa-treated PBMCs showed the highest release of ROS at 10.0 μM (Figure 6.3G). The ROS release was accompanied by the change of the mitochondrial membrane potential in lymphocytes, macrophages and neutrophiles (Figure 6.3E). However, no cytotoxicity was observed at those concentrations as demonstrated by the cell cycle analysis (Figure 6.3F). The expression of three MAPKs was then investigated by different sub-types of PBMCs including CD4+ cells, CD14+ cells (e.g. lymphocytes and macrophages respectively) and neutrophils at 1.0 μM, 5.0 μM and 10.0 μM. In Pa-treated CD4+ T cells, the expression of p-ERK, p-JNK and p-p38 was up-regulated in a dose-dependant manner at 5.0 and 10.0 μM whereas only p-JNK and p-p38 are up-regulated at 1.0 and 5.0 μM in Pa-treated CD14+ macrophages and p-p38 at 1.0 μM, 5.0 μM and 10.0 μM in Pa-treated neutrophils (Figure 6.4C). This result suggests that the induction of different MAPK activities depends on Pa concentration and cell type. ROS could induce the activation of MAPKs by affecting the mitochondrial membrane potential. Since the mitochondrial membrane potential among various cell types is different, it depends on ROS concentration, in a consequence of Pa concentration, to mediate the differential activation of MAPKs in different cell types. In addition, only p-p38 was mediated in the three types of cells. It suggested that Pa is likely more effective in inducing p-p38 in human immune competent cells. As p-p38 is generally associated to cytokine

production, a cytokine prelimary screening was performed. Table 6.1 showed that IL-6, IL-12, IL-17, IFN-γ, TNF-α and GM-CSF were mediated depending on Pa concentration and the cell type. Similar to Pa-treated RAW 264.7 cells, human immune competent cells treated with Pa produce inflammatory cytokines. Therefore, the potential anti-viral property of Pa is demonstrated both in murine and human cells.

Comparing murine cells with human cells, similar results were observed. However, effective Pa concentrations were different between murine cells and human cells. This could be explained by the different drug disposition between species due to differential hepatic clearance (Walker *et al.*, 2009).

In this study, we evaluated for the first time that, at concentration lower than 10.0 μM, Pa, an anti-tumour agent and a potential photosensitizer, is capable of inducing immunostimulatory effects without cytotoxicity on both murine and human immune competent cells. The stimulation of the growth of immune cells (e.g. macrophages) can reinforce the immune defence of the host, and the production of pro-inflammatory cytokines and enhancement of phagocytic capacity could be a beneficial effect for tumour clearance after chemotherapy or photodynamic therapy. In addition to the photosensitizer characteristics of Pa, it can also be considered as an immunomodulatory agent. This novel feature offers Pa a better therapeutic potential than other photosensitizers in cancer treatment, since Pa is a good adjuvant in term of its potential in enhancing the immune system of the host against the tumour cells indirectly during Pa-PDT treatment which will exert cytotoxic effect directly on the tumour cells.
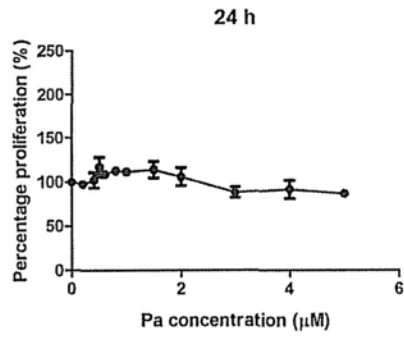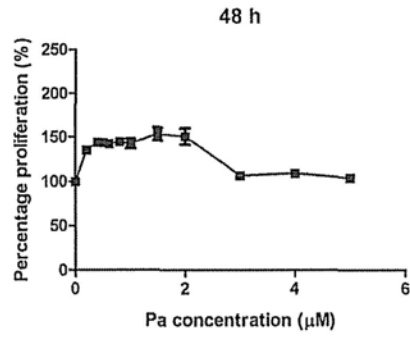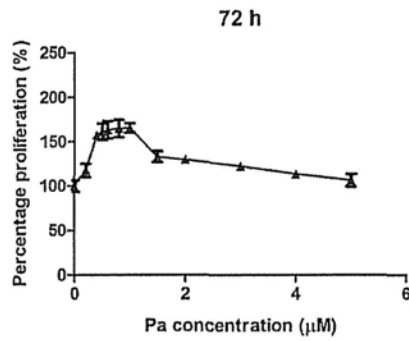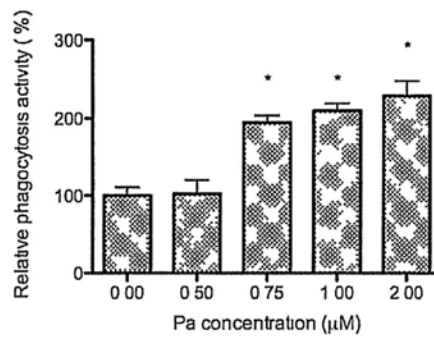
(i)   (ii)
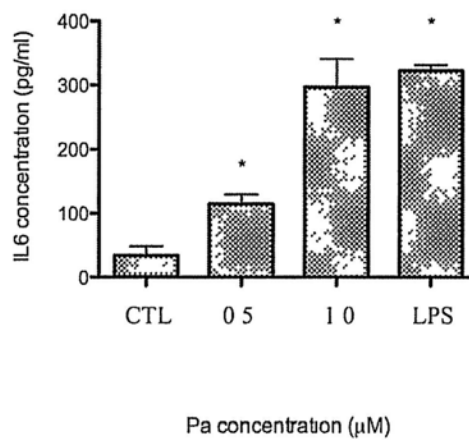

Figure 6.1 – Pa stimulates RAW 264.7 cell proliferation. RAW 264.7 cells were treated with different Pa concentration (0 - 5 µM) in dark. MTT assay was performed after (i) 24h, (ii) 48h and (iii) 72h of incubation. Results were expressed with mean ± SD of three independent experiments.

(A)

(B)

(C)
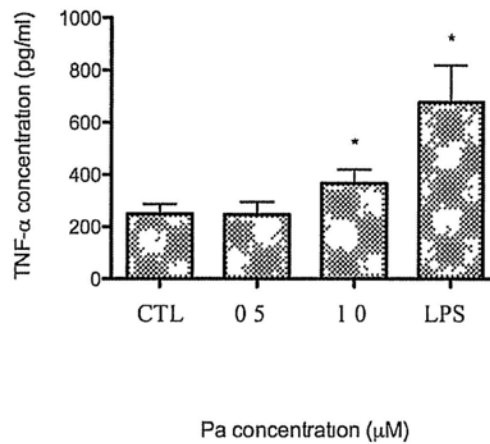
Figure 6.2 – Pa stimulates RAW 264.7 cells by inducing cytokine production and enhancing phagocytotic activity. (A) RAW 264 7 cells were treated with vehicle control or different Pa concentrations (0 5 - 2 0 μM) for 24 h in dark Murine macrophage cell line were exposed to fluorescent *E coli* particles and phagocytosis index was performed by monitoring the fluorescence **(B, C)** RAW 264 7 cells were treated with vehicle control, Pa (0 5 and 1 0 μM) or LPS (100 ng/ml) for 24 h in dark Supernatant was analyzed for (B) IL-6 and (C) TNF-α using ELISA method Results were expressed with mean ± SD of three independent experiments [1]p < 0 05, CTL control

103

(A)

Pheophorbide-a   Mito-tracker   Merged Image

(B)

(C)

(D)

CTL   0.5 μM

1.0 μM   2.0 μM

(E)

(i)

Macrophages

13 35%

50 92%

CTL   1 μM

61 35%

76 98%

5 μM   10 μM

(ii)

Lymphocytes

CTL	1 μM
22 58%	53 92%

5 μM	10 μM
79 45%	90 62%

(iii)

Neutrophils

CTL	1 μM
77 14% / 0 00%	64 98% / 0 00%

5 μM	10 μM
60 36% / 11 70%	41 72% / 26 82%

106

(F)

(i)

Macrophages

CTL

1 µM

5 µM

10 µM
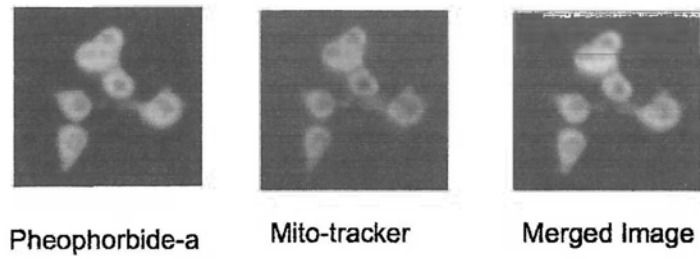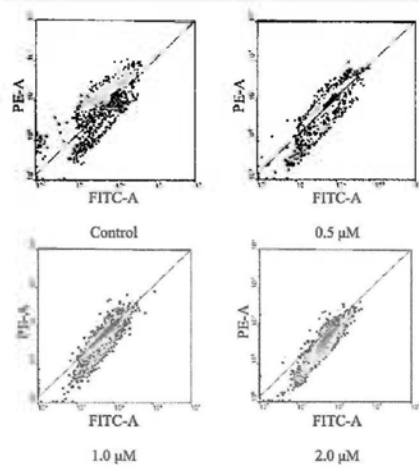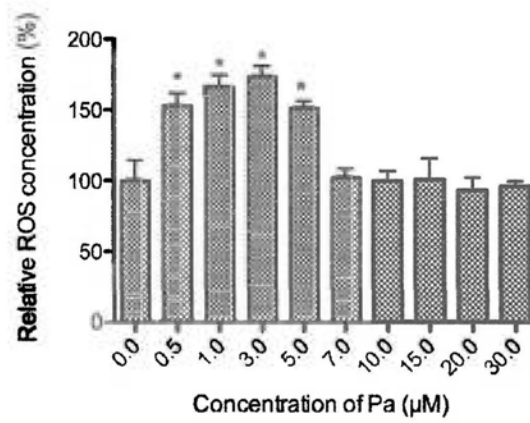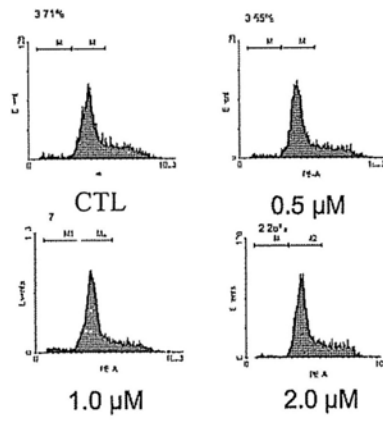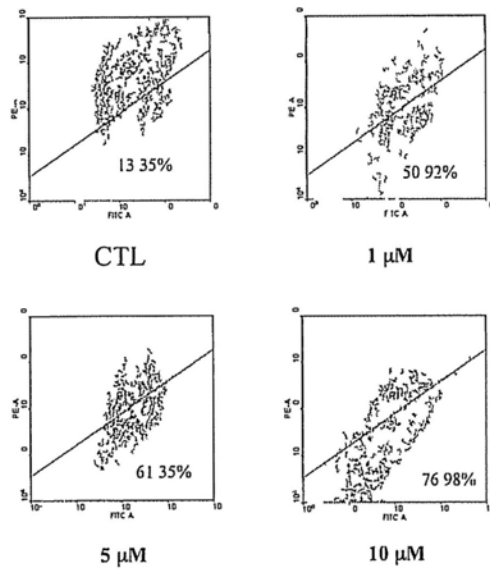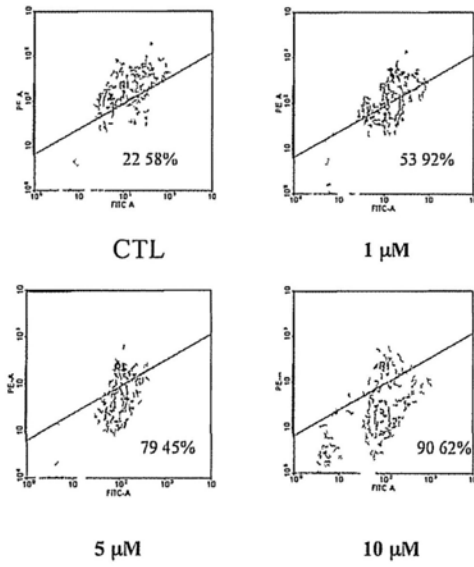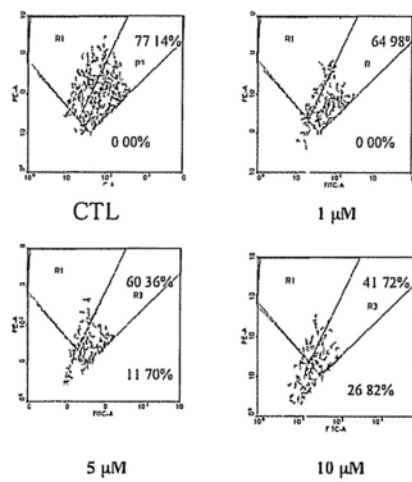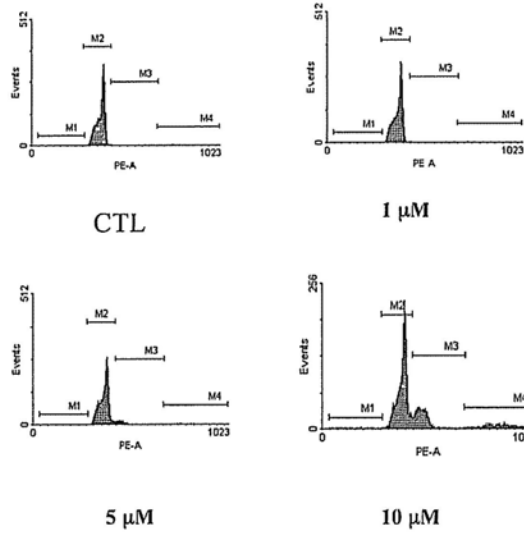
Cell cycle	Control (%)	1 µM (%)	5 µM (%)	10 µM (%)
Sub G1 (M1)	0.27	0.52	1.01	1.79
G0 G1 (M2)	96.79	96.80	90.55	66.91
S (M3)	1.33	1.34	6.35	21.72
G2/M (M4)	1.74	1.47	2.80	10.43

(ii)

Lymphocytes

CTL

1 μM

5 μM

10 μM
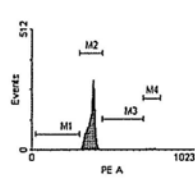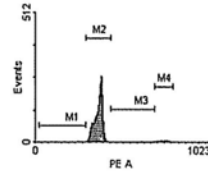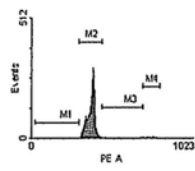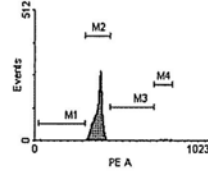
Cell cycle	Control (%)	1 μM (%)	5 μM (%)	10 μM (%)
Sub G1 (M1)	0.31	1.36	0.67	1.19
G0 G1 (M2)	96.03	93.72	94.65	95.46
S (M3)	1.07	1.38	1.67	1.04
G2/M (M4)	2.42	3.35	2.72	1.96

Neutrophils

CTL

1 μM

5 μM

10 μM
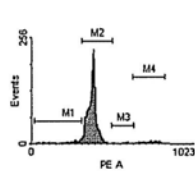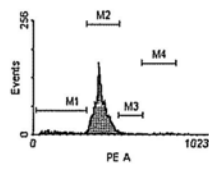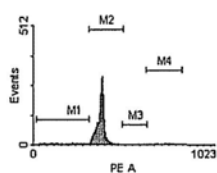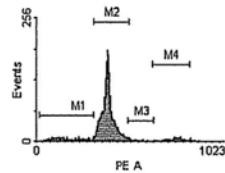
Cell cycle	Control (%)	1 μM (%)	5 μM (%)	10 μM (%)
Sub G1 (M1)	7.74	10.32	11.83	10.64
G0 G1 (M2)	87.45	83.79	80.42	83.20
S (M3)	1.25	2.94	1.54	2.67
G2/M (M4)	4.31	3.06	3.53	6.04

(G)
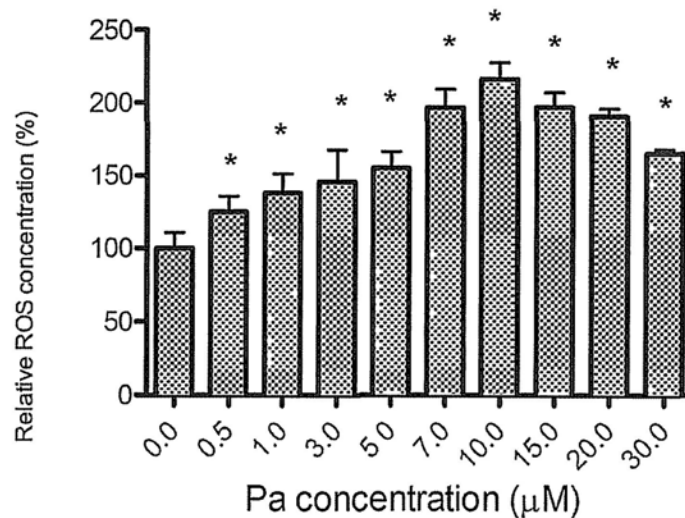
Figure 6.3 – Pa-induced ROS production of monocytes. (A) RAW 264 7 cells were co-stained with 4 µM of Pa for 2 h following by MitoTracker Green in dark. The fluorescence of either Pa or MitoTracker was detected by fluorescence microscope. Results are representative of three individual experiments with essential similar result. (B, E) RAW 264 7 cells (B) and human immune competent cells (E) were treated with vehicle control, 0 5, 1 0 and 2 0 µM of Pa for 24h in dark. Cells were then stained with JC-1 and subjected to flow cytometric analysis for the mitochondrial membrane potential change. Results are representative of three individual experiments. (C, G) RAW 264 7 cells (C) and PBMCs (G) were treated with vehicle control or different Pa concentrations (0 5 to 30 0 µM) in dark for 24 h. Cells were stained with CM-H$_2$DCFDA dye. The ROS concentration was estimated by monitoring the fluorescent signal. Results were expressed with mean plus SD from three individual experiments. (D, F) RAW 264 7 cells (D) and human macrophages (F i), lymphocytes (F ii) and neutrophils (F iii) were treated with vehicle control or different concentrations of Pa for 24 h in dark. Cells were then stained with propidium iodide (PI) and RNase A and subjected to flow cytometric analysis. Results are representative of three individual experiments. * p < 0 05. CTL medium control

(A)

	CTL	1h	2h	4h	24h	
						β-actin
						p-ERK
						ERK1/2
						p-JNK
						JNK1/2
						p-p38
						p38

(B)

	0	0 25	0 5	1 0	Pa concentration (μM)
					β-actin
					ERK 1
					ERK 2
					JNK 1
					JNK 2
					p38
					p-ERK
					p-JNK
					p-p38

111

(C)

(i) CD4+

p-ERK

p-JNK

p-p38

(ii) CD14+

p-JNK

p-p38
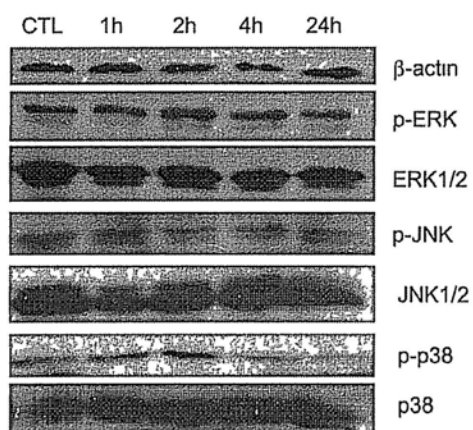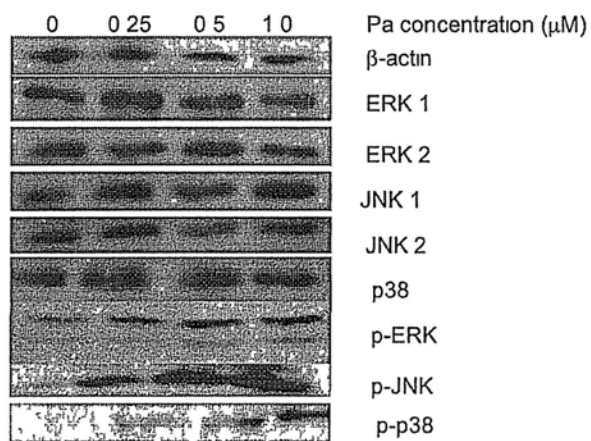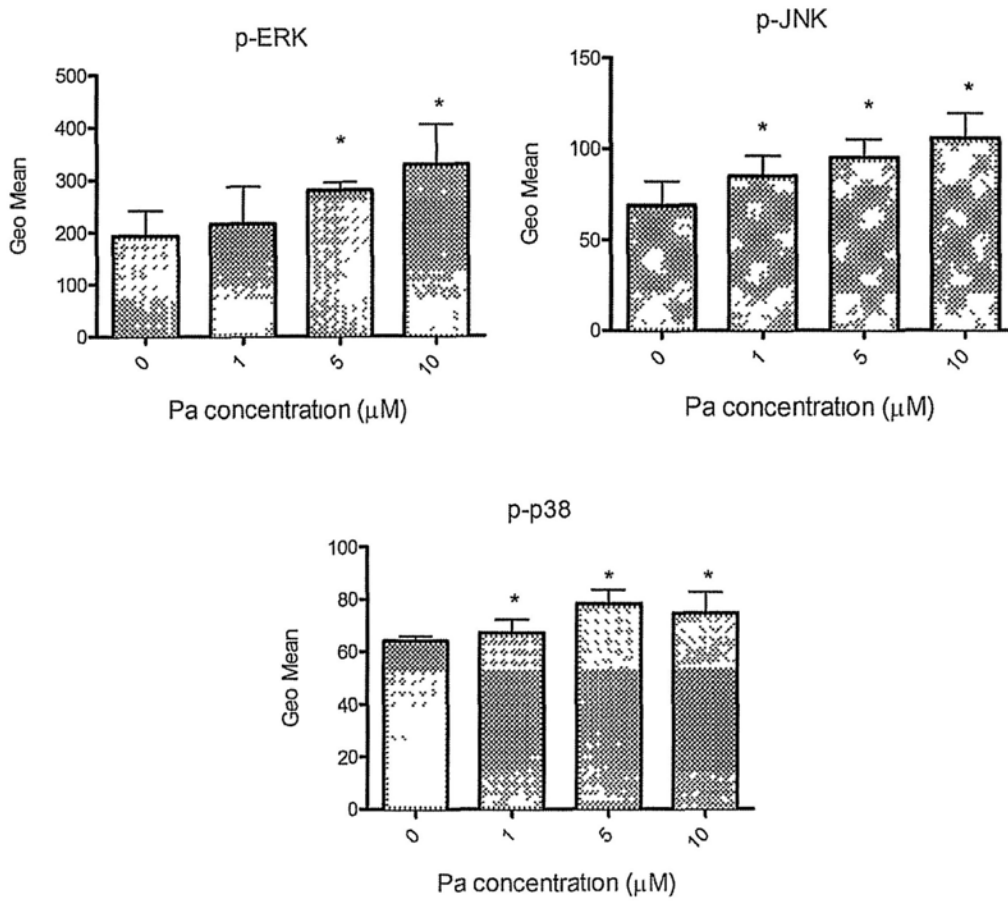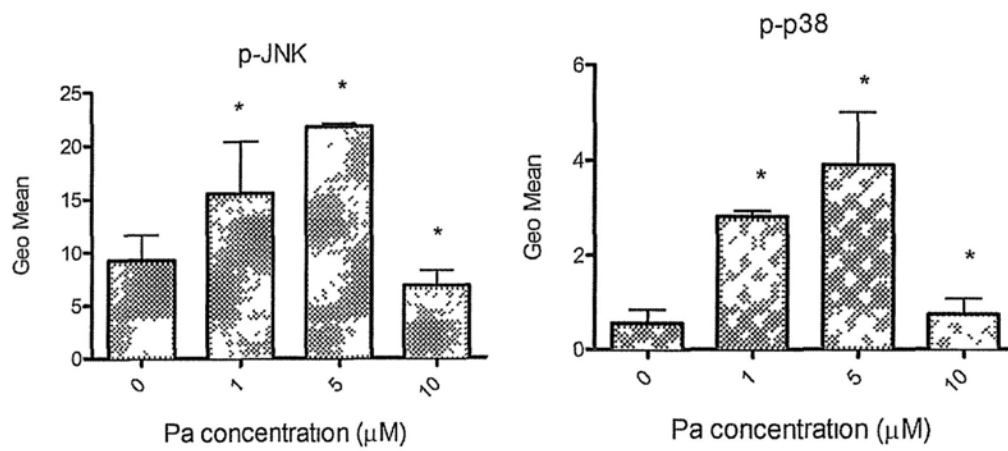
(iii) Neutrophils
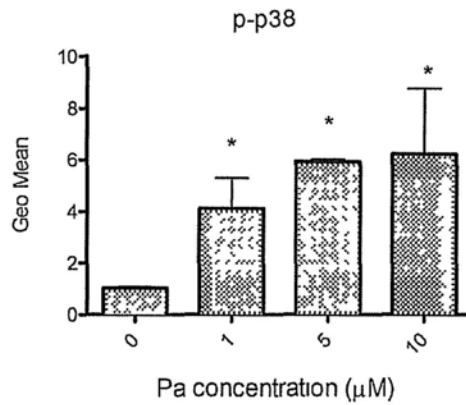
Figure 6.4 – MAPK activation in Pa-treated immunocytes. **(A)** RAW 264 7 cells were treated with vehicle control or Pa (0 5 μM) in dark for different times (1 - 24 h) and **(B)** RAW 264 7 cells were treated with vehicle control or Pa (0 25, 0 5 and 1 0 μM) in dark for 2 h Western blot was performed to evaluate the protein expression of total (phosphorylated plus unphosphorylatd forms) and phosphorylated ERK, JNK and p38 Results are representative of three independent experiments with essential similar results CTL control, p-ERK phosphorylated ERK, p-JNK phosphorylated JNK, p-p38 phosphorylated p38 **(C)** Human immune competent cells (10^6) were incubated with vesicle control or various Pa concentrations for 2 h Then, cells were collected and fixed with 4% of BD Cytofix and were permeabilized with BD Perm Buffer II Cells were further incubated with primary antibodies (e g pERK, pJNK and pp38) following with FITC conjugated goat anti-mouse IgG Stained cells were subjected to FACSCanto flow cytometric analysis Results were expressed with mean ± SD of three independent experiments *$p < 0 05$, CTL control

(A)
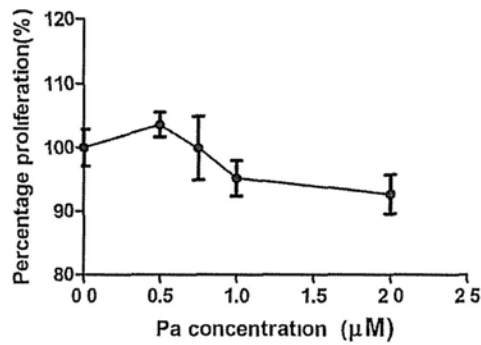
(B)
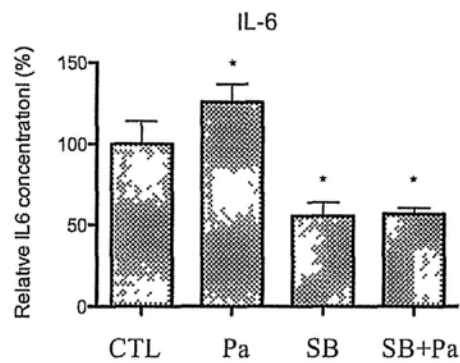
(C)
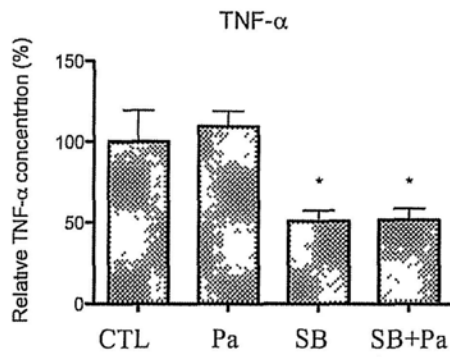
Figure 6.5 – Role of MAPK activation in Pa-treated RAW 264.7 cells. (A) RAW 264 7 cells were co-treated with different Pa concentration (0 - 2 μM) and MEK1/2 inhibitor U0126 (5 μM) in dark MTT assay was performed after 48 h of incubation Results were expressed with mean ± SD of three independent experiments **(B, C)** RAW 264 7 cells were treated with vehicle control, Pa (0 5 μM) or p38 MAPK inhibitor SB20219 (1 μM) for 24 h in dark Supernatant was analyzed for (B) IL-6 and (C) TNF-α using ELISA method Results were expressed with mean plus SD of three independent experiments CTL control, SB SB20219, ¹ p < 0 05

Cytokines	Lymphocytes	Macrophages	Neutrophils
IL-6	5 μM - 10 μM	5 μM - 10 μM	5 μM - 10 μM
IL-12	5 μM - 10 μM	5 μM - 10 μM	x
IL-17	10 μM	10 μM	x
IFN-γ	5 μM - 10μM	5 μM - 10μM	5 μM – 10 μM
TNF-α	1 μM - 5μM - 10 μM	1 μM - 5μM - 10 μM	x
GM-CSF	10 μM	10 μM	x

Table 6.1 – Screening of induced cytokines in Pa-treated human immune competent cells. Human competent cells were separated from fresh PBMCs and incubated with Pa (at 1 μM, 5 μM or 10 μM) for 24 h. Supernatants were subjected to cytokine quantification using Bio-Plex cytokine assay kit. Data showed concentration of Pa that is up-regulated comparing to control cells in a dose dependent manner.

Chapter 7

General Discussion

Pheophorbide a is a metabolite of chlorophyll a. It is contained in all green leaves and could be purified at significant yield from *Scutellaria barbata*, and *Psychotria acuminata*, as well as silkworm excreta (Chan *et al.*, 2006; Glinski *et al.*, 1995; Lim *et al.*, 2002). Pa has been described as an anti-tumour agent (Nakamura *et al.*, 1996). Later, Pa was reported to be efficient with lower dose as a natural photosentizer for photodynamic therapy (PDT) (Tang *et al.*, 2006). Recently, PDT has been approved for clinical treatment in several developed countries for the treatment on actinic keratosis, macular degeneration, Barrett's esophagus, obstructing esophageal carcinoma, early and obstructing tracheobronchial carcinoma, palliative treatment of head and neck cancer, and basal and squamous cell skin cancers (Klein *et al.*, 2008; Biel, 2006).

Several studies about Pa-PDT action on cancer cells were published by different groups, mainly by ours, including leukaemia, pigmented melanoma, colonic cancer, hepatoma and uterine carcinosarcoma (Lee *et al.*, 2004; Lim *et al.*, 2004; Hajri *et al.*, 2002; Li *et al.*, 2007; Tang *et al.*, 2006; Tang *et al.*, 2007; Tang *et al.*, 2009a; Tang *et al.*, 2009b; Tang *et al.*, 2010; Bui-Xuan *et al.*, 2010). However, until now no study investigates the action of Pa-PDT on human breast adenocarcinoma. This study proposes for the first time to elucidate the potential therapeutic property of Pa-PDT on human breast cancer via different aspects: mechanistic study for direct

toxicity, combination with tamoxifen for treating advanced breast cancer and the enhancement of cancer immunity. The immunostimulation of photosentizer in the absence of radiation is another important and new aspect of PDT that was also investigated in this study.

7.1 Direct cytotoxicity of Pa-PDT toward MDA-MB-231 cells

Pa-PDT is effective in treating advanced human breast cancer with an IC_{50} equals to 0.5 μM at 24 h incubation via apoptosis induction as the main mechanism. This result is consistent with previous reports on liver and uterine cancer (Tang *et al.*, 2006; Tang *et al.*, 2007; Tang *et al.*, 2009a; Tang *et al.*, 2009b; Tang *et al.*, 2010). Particularly, Pa-PDT reveals different additional pathways leading to cancer cell death including endoplasmic reticulum stress and ERK-mediated autophagy (Bui-Xuan *et al.*, 2010). Other clinical photosensitizers inhibit cell growth via several possible pathways including apoptosis, cell cycle arrest, necrosis, autophagy and endoplasmic reticulum stress (Table 7.1). However, they do not induce all of these mechanisms. Therefore, Pa-PDT is the most efficient breast cancer treatment method.

Photosensitizer	Substance	Cell cycle arrest	Apoptosis	Necrosis	Autophagy	ER stress
Pheophorbide a		yes (Tang *et al.*, 2007)	yes (Bui-Xuan *et al.*, 2010)	yes (not shown)	yes (Bui-Xuan *et al.*, 2010)	yes (Bui-Xuan *et al.*, 2010)
Photofrin	HpD	Yes (Tong *et al.*, 2002)	Yes (Engbrecht *et al.*, 1999)	Yes (Murakami *et al.*, 2009)	n/a	Yes (Hsieh *et al.*, 2010)
Photogem	HpD	n/a	n/a	Yes (Ribeiro *et al.*, 2010)	n/a	n/a
Levulan	ALA	No (Allman *et al.*, 2000)	Yes (Noodt *et al.*, 1996)	Yes (Noodt *et al.*, 1996)	Yes (Ji *et al.*, 2010)	n/a
Visudyne	Verteporfin	n/a	Yes (Matsubara *et al.*, 2007)	Yes (Opitz *et al.*, 2007)	n/a	n/a
Foscan	Temoporfin	Yes (Sasnauskiene *et al.*, 2009)	Yes (Marchal *et al.*, 2005)	Yes (Marchal *et al.*, 2005)	Yes (Sasnauskiene *et al.*, 2009)	n/a
Photolon	Talaporfin	n/a	n/a	n/a	n/a	n/a
Antrin	Lutexaphyrin	n/a	n/a	n/a	n/a	n/a
Photosens	Phthalocyanine	n/a	Yes (Plaetzer *et al.*, 2002)	Yes (de Castro Pazos *et al.*, 2003)	n/a	n/a

Table 7.1 – Induced pathways by Photodynamic Therapy (n/a, not available)

7.2 Pa-PDT sensitises tamoxifen to MDA-MB-231 cells

Tamoxifen is a common drug employed in hormonal therapy for breast cancer treatment. However, besides several side effects, tamoxifen is limited to treat only early stage of breast cancer but with low efficient in treating advanced stage. In order to increase tamoxifen sensitivity to late phase breast tumour, the combination of tamoxifen with other drugs or agents is generally suggested (Penolazzi *et al.*, 2007; Fortunati *et al.*, 2009; Awad *et al.*, 2008; Weng *et al.*, 2008; Ford *et al.*, 2009). According to a similar approach, Pa-PDT combined with tamoxifen has been tested in MDA-MB-231 cells in this study. Interestingly, Pa-PDT sensitises tamoxifen to estrogen receptor-negative breast cancer cell model. This result is supported by VitB2-PDT suggesting that combination effect could be the general effect of PDT and not specifically to Pa-PDT. This synergetic effect is due to the high induction of apoptosis (Figure 4.4).

Pa-PDT is also demonstrated to restore ER-α expression which is absent in MDA-MB-231 cells. This could be a reason how Pa-PDT exerts synergetic effect with tamoxifen.

7.3 PDT and tumour immunity

Tumour immunity is one of the other interested aspects of PDT in oncology research instead of tumour toxicity. Both pre-clinical and clinical studies have shown that PDT treatment of tumours can enhance the systemic anti-tumour immunity (Gollnick and Brackett, 2010). Intensive researches were conducted to investigate the potential of PDT as an immunotherapy. Even though PDT generates direct cytotoxicity via production of reactive oxygen, PDT was shown to induce acute inflammation resulting in an increased induction of pro-inflammatory cytokines

including IL-1β, TNF-α and IL-6 (Korbelik, 2006), adhesion molecules E-selectin and Inter-Cellular Adhesion Molecule 1 (ICAM-1) (Gollnick et al., 2003) and rapid leukocyte infiltration into the treated tumour site (Krosl et al., 1995). Moreover, animal study using murine model showed an induction of anti-tumour immunity in PDT treated tumours (Kousis et al., 2007). Similarly, systemic immune reactivity was observed in clinical setting (Kabingu et al., 2009). Those properties contribute significantly to the long-term tumour growth control by PDT (Henderson and Gollnick, 2003). Although in vitro and in vivo studies support that PDT can enhance the anti-tumour immunity, the mechanisms remains unclear.

PDT-treated tumour cells has been believed to generate effective preventative anti-tumour vaccines in vitro (Gollnick et al., 2002) which are more effective than tumour cells treated with UV or ionizing irradiation or cells subjected to freeze–thaw cycles. The mechanism was distributed to the role of TLR ligands and heat shock protein 70 (HSP70) (Gollnick and Brackett, 2010). Our study demonstrated that HSP70 is induced by PDT, which is consistent with findings of Gomer et al. (Gomer et al., 1996). Generally, the level of the expression of HSP70 was associated with the stimulation of DC maturation (Kuppner et al., 2001). Our findings showed that Pa-PDT could induce HSP70 expression and the antigen presentation. However, several studies demonstrated that DC activation could be HSP70 independent (Jalili et al., 2004). Therefore, it is important to recognize that cell surface receptors other than innate immune response receptor members of the Toll-like receptor/NOD-like receptor/RIG-I-like Receptor (TLR/NLR/RLR) families (Karin et al., 2006; Savill et al., 2002) may also act as danger receptors. Some studies suggest other critical pathways to the efficacy of PDT-generated vaccines such as Korbelik and Sun's work,

where PDT-treated cells exihibited HSP70 on their surface and were opsonized by complement C3 (Korbelik and Sun, 2006).

Although numerous pre-clinical studies have demonstrated that PDT can result in an increase in anti-tumour immunity (Castano *et al.*, 2006), until recently, only few studies have examined the ability of PDT to enhance anti-tumour immunity in a clinical setting (Garg *et al.*, 2010). Therefore, it will take long time before PDT to be clinically approved as an immunotherapy.

7.4 Immunostimulation of Pa in the absence of photoactivation

Photodynamic therapy is a treatment method that requires long time incubation of photosensitizer before activation, usually 90h to 110h (Foscan product information). Studying the effect of photosensitizer in the blood stream without illumination reveals that it is necessary to investigate its potential toxicity or benefit. Since photosensitizers are often overwhelmed by their anti-tumour activities, which lead to little studies focusing on their potential effects on the immune system. Therefore, our present study attempts to elucidate the potential effects of Pa on the immune effector cells at optimized concentration of Pa-PDT in anti-tumour treatment. Our study showed that Pa without photoactivation could stimulate murine cell growth mediated by ERK activation. Also, the release of IL-6 and TNF-α was observed and controlled by p38 MAPK. Similarly, Pa induces cytokine secretion and MAPK activation in human competent cells. All together, Pa is demonstrated to be a good immunostimulating agent, besides its anti-tumour property and its photosensitizer

characteristic. This study provides a biochemical basis for the immunomodulatory effects of Pa on immunocytes.

7.5 Pa-PDT: anti-tumour and adjuvant treatment

The National Cancer Institute of the USA defines adjuvant as an "additional cancer treatment given after the primary treatment to lower the risk that the cancer will come back. Adjuvant therapy may include chemotherapy, radiation therapy, hormone therapy, targeted therapy, or biological therapy". In our study, Pa is demonstrated to be an anti-tumour agent and a promising photosensitizer for photodynamic therapy. Besides direct cytotoxicity, Pa-PDT is demonstrated to enhance tumour immunity. In combination with hormonal therapy, Pa-PDT could sensitise ER-α negative breast cancer to tamoxifen. Furthermore, Pa alone without illumination stimulates immunocytes. Taking together, Pa-PDT is a good anti-tumour device and a potential adjuvant in cancer treatment for immunotherapy as well as hormonal therapy.

7.6 Clinical perspectives

Until present, no clinical studies were conducted using neither Pa nor Pa-PDT for cancer treatment. However, BZL101, an aqueous solution of Ban Zhi Lian (BZL) extract, is under clinical trial in the USA for breast cancer treatment (Perez *et al.*, 2010). Since Pa is one of the active components of BZL, Pa and Pa-PDT could be considered for clinical study in future.

References

Adams JM, Cory S. 1998. The Bcl-2 protein family: arbiters of cell survival. Science. 281:1322-1326.

Aderem A, Underhill DM. 1999. Mechanisms of phagocytosis in macrophages. Annu. Rev. Immunol. 17:593-623.

Allison RR, Downie GH, Cuenca R, Hu XH, Childs CJH, Sibata CH. 2004. Photosensitizers in clinical PDT. Photodiagnosis and Photodynamic Therapy. 1:27-42.

Allman R, Cowburn P, Mason M. 2000. Effect of photodynamic therapy in combination with ionizing radiation on human squamous cell carcinoma cell lines of the head and neck. Br J Cancer. 83:655-661.

Aouri S, Brahim S, De Waard M, Bréard J. 2009. Efficient induction of apoptosis by doxorubicin coupled to cell-penetrating peptides compared to unconjugated doxorubicin in the human breast cancer cell line MDA-MB-231. Cancer Lett. 285: 28-38.

Ashkenazi A. 2002. Targeting death and decoy receptors of the tumour-necrosis factor superfamily. Nat Rev Can. 2:420-430.

Awad AB, Barta SL, Fink CS, Bradford PG. 2008. β-Sitosterol enhances tamoxifen effectiveness on breast cancer cells by affecting ceramide metabolism. Mol Nutr Food Res. 52:419-426.

Bendz H, Ruhland SC, Pandya MJ, Hainzl O, Riegelsberger S, Braüchle C, Mayer MP, Buchner J, Issels RD, Noessner E. 2007. Human heat shock protein 70 enhances tumor antigen presentation through complex formation and intracellular antigen delivery without innate immune signaling. J Biol Chem. 282:31688-31702.

Biel M. 2006. Advances in photodynamic therapy for the treatment of head and neck cancers. Lasers Surg Med. 38: 349-355.

Billen LP, Shamas-Din A, Andrews DW. 2009. Bid: a Bax-like BH3 protein. Oncogene. 27:S93-S104.

Braciale TJ, Morrison LA, Sweetser MT, Sambrook J, Gething MJ, Braciale VL. 1987. Antigen presentation pathways to class I and class II MHC-restricted T lymphocytes. Immunol Rev. 98:95-114.

Brauch H, Mürdter TE, Eichelbaum M, Schwab M. 2009. Pharmacogenomics of tamoxifen therapy. Clin Chem. 55:1770-1782.

Bui-Xuan NH, Tang PM, Wong CK, Fung KP. 2010. Photo-activated pheophorbide-a, an active component of Scutellaria barbata, enhances apoptosis via the suppression of ERK-mediated autophagy in the estrogen receptor-negative human breast adenocarcinoma cells MDA-MB-231. J Ethnopharmacol. 131:95-103.

Buytaert E, Dewaele M, Agostinis P. 2007. Molecular effectors of multiple celldeath pathways initiated by photodynamic therapy. Biochim Biophys Acta. 1776:86-107.

Camphausen KA, Cola LR. 2008. Principles of Radiation Therapy. Cancer Management: A Multidisciplinary Approach. Chapter 2. p1-5.

Campoli M, Ferrone S. 2008. HLA antigen changes in malignant cells: epigenetic mechanisms and biologic significance. Oncogene. 27:5869-5885.

Canti G, De Simone A, and Korbelik M. 2002. Photodynamic therapy and the immune system in experimental oncology. Photochem Photobiol Sci. 1:79–80.

Castano AP, Mroz P, Hamblin MR. 2006. Photodynamic therapy and antitumour immunity. Nat Rev Cancer. 6:535–545.

Castellino F, Boucher PE, Eichelberg K, Mayhew M, Rothman JE, Houghton AN, Germain RN. 2000. Receptor-mediated uptake of antigen/heat shock protein complexes results

in major histocompatibility complex class I antigen presentation via two distinct processing pathways. J Exp Med. 191:1957-1964.

Cha YY, Lee EO, Lee HJ, Park YD, Ko SG, Kim DH, Kim HM, Kang IC, Kim SH. 2004. Methylene chloride fraction of Scutellaria barbata induces apoptosis in human U937 leukemia cells via the mitochondrial signaling pathway. Clinica Chimica Acta. 348:41-48.

Chan JY, Tang PM, Hon PM, Au SW, Tsui SK, Waye MM, Kong SK, Mak TC, Fung KP. 2006. Pheophorbide a, a major antitumor component purified from Scutellaria barbata, induces apoptosis in human hepatocellular carcinoma cells. Planta Medica. 72:28-33.

Cheng HH, Wang HK, Ito J, Bastow KF, Tachibana Y, Nakanishi Y, Xu Z, Luo TY, Lee KH. 2001. Cytotoxic pheophorbide-related compound from Clerodendrum calamitosum and C. cyrtophyllum. J Nat Prod. 64:915-919.

Cohen GM. 1997. Caspases: the executioners of apoptosis. Biochem J. 326:1-18.

Corcelle E, Djerbi N, Mari M, Nebout M, Fiorini C, Fénichel P, Hofman P, Poujeol P, Mograbi B. 2007. Control of the autophagy maturation step by the MAPK ERK and p38: lessons from environmental carcinogens. Autophagy. 3:57-59.

Cory S, Adams JM. 2002. The Bcl2 family: regulators of the cellular life-or-death switch. Nat Rev Cancer. 2:647-656.

Cresswell P, Arunachalam B, Bangia N, Dick T, Diedrich G, Hughes E, Maric M. 1999. Thiol oxidation and reduction in MHC-restricted antigen processing and presentation. Immunol Res. 19:191-200.

Dai ZJ, Wang XJ, Li ZF, Ji ZZ, Ren HT, Tang W, Liu XX, Kang HF, Guan HT, Song LQ. 2008. Scutellaria barbate extract induces apoptosis of hapatoma H22 cells via the mitochondrial pathway involving caspase-3. World J Gastroenterol. 14:7321-7328.

Daniell MD, Hill JS. 1991. A history of photodynamic therapy. Aust N Z J Surg. 61:340-348.

de Castro Pazos M, Pacheco-Soares C, Soares da Silva N, DaMatta RA, Pacheco MT. 2003. Ultrastructural effects of two phthalocyanines in CHO-K1 and HeLa cells after laser irradiation. Biocell. 27:301-309.

Dharmananda S. 2004. Oldenlandia and Scutellaria, Antitoxin and Anticancer Herbs. Institute for Traditional Medicine, Portland, OR.

Di X, Shiu RP, Newsham IF, Gewirtz DA. 2009. Apoptosis, autophagy, accelerated senescence and reactive oxygen in the response of human breast tumor cells to Adriamycin. Biochem Pharmacol. 77:1139-1150.

Dick TP. 2004. Assembly of MHC class I peptide complexes from the perspective of disulfide bond formation. Cell Mol Life Sci. 61:547-556.

Dolmans DE, Fukumura D, Jain RK. Photodynamic therapy for cancer. 2003. Nat Rev Cancer. 3:380-387.

Dougherty TJ, Henderson BW, Schwartz S, Winkelman JW, Lipson RL. 1992. Historical perspective. In: Henderson BW, Dougherty TJ, editors. Photodynamic therapy. New York: MarcelDekker. 1-15.

Dröge W. 2002. Free Radicals in the Physiological Control of Cell Function. Physiol Rev. 82:47-95.

Duncan JA, Reeves JR, Cooke TG. 1998. BRCA1 and BRCA2 proteins: roles in health and disease. Mol Path. 51:237-247.

Engbrecht BW, Menon C, Kachur AV, Hahn SM, Fraker DL. 1999. Photofrin-mediated photodynamic therapy induces vascular occlusion and apoptosis in a human sarcoma xenograft model. Cancer Res. 59:4334-4342.

Fong S, Shoemaker M, Cadaoas J, Lo A, Liao W, Tagliaferri M, Cohen I, Shtivelman E. 2008. Molecular mechanisms underlying selective cytotoxic activity of BZL101, an extract of Scutellaria barbata, towards breast cancer cells. Cancer Biol Ther. 7:577-586.

Ford CE, Ekström EJ, Andersson T. 2009. Wnt-5a signaling restores tamoxifen sensitivity in estrogen receptor-negative breast cancer cells. Proc Natl Acad Sci U S A. 106:3919-3924.

Fortunati N, Bertino S, Costantino L, De Bortoli M, Compagnone A, Bandino A, Catalano MG, Boccuzzi G. 2010. Valproic acid restores ER alpha and antiestrogen sensitivity to ER alpha-negative breast cancer cells. Mol Cell Endocrinol. 314:17-22.

Galindev O, Badraa N, Dalantai M, Sengee GI, Dorjnamjin D, Shim YK. 2008. Synthesis of pyrazol substituted methyl pheophorbide-a derivatives and their preliminary in vitro cell viabilities. Photochem Photobiol Sci. 7:1273-1281.

Garbi N, Hämmerling G, Tanaka S. 2007. Interaction of ERp57 and tapasin in the generation of MHC class I-peptide complexes. Curr Opin Immunol. 19:99-105.

Garg AD, Nowis D, Golab J, Agostinis P. 2010. Photodynamic therapy: illuminating the road from cell death towards anti-tumour immunity. Apoptosis. In Press.

Gewirtz DA. 1999. A Critical Evaluation of the Mechanisms of Action Proposed for the Antitumour Effects of the Anthracycline Antibiotics Adriamycin and Daunorubicin. Biochem Pharmacol. 57:727-741.

Gibson L, Lawrence D, Dawson C, Bliss J. 2009. Aromatase inhibitors for treatment of advanced breast cancer in postmenopausal women. Cochrane Database Syst Rev. (4):CD003370.

Glinski JA, David E, Warren TC, Hansen G, Leonard SF, Pitner P, Pay S, Arvigo R, Balick MJ, Panti E, Grob PM. 1995. Inactivation of cell surface receptors by pheophorbide a,

a green pigment isolated from Psychotria acuminata. Photochem Photobiol. 62:144-150.

Goel S, Sharma R, Hamilton A, Beith J. 2009. LHRH agonists for adjuvant therapy of early breast cancer in premenopausal women. Cochrane Database Syst Rev. 4:CD004562.

Goh D, Lee YH, Ong ES. 2005. Inhibitory effects of a chemically standardized extract from Scutellaria barbata in human colon cancer cell lines, LoVo. J Agric Food Chem. 53:8197-8204.

Gollnick SO, Brackett CM. 2010. Enhancement of anti-tumor immunity by photodynamic therapy. Immunol Res. 46:216-226.

Gollnick SO, Evans SS, Baumann H, Owczarczak B, Maier P, Vaughan L, Wang WC, Unger E, Henderson BW. 2003. Role of cytokines in photodynamic therapy-induced local and systemic inflammation. Br J Cancer. 88:1772-1779.

Gollnick SO, Owczarczak B, Maier P. 2006. Photodynamic therapy and anti-tumor immunity. Lasers Surg Med. 38:509-515.

Gollnick SO, Vaughan LA, Henderson BW. 2002. Generation of effective anti-tumor vaccines using photodynamic therapy. Cancer Res. 62:1604-8.

Gomer CJ, Ryter SW, Ferrairo A, Ryffel N, Woodard A, Fisher AMR. 1996. Photodynamic therapymediated oxidative stress can induce expression of heat shock proteins. Cancer Res. 56:2355-2360.

Grommé M, Neefjes J. 2002. Antigen degradation or presentation by MHC class I molecules via classical and non-classical pathways. Mol Immunol. 39:181-202.

Hajri A, Coffy S, Vallat F, Evrard S, Marescaux J, Aprahamian M. 1999. Human pancreatic carcinoma cells are sensitive to photodynamic therapy in vitro and in vivo. Br J Surg. 86:899-906.

Hajri A, Wack S, Meyer C, Smith MK, Leberquier C, Kedinger M, Aprahamian M. 2002. In vitro and in vivo efficacy of photofrin and pheophorbide a, a bacteriochlorin, in photodynamic therapy of colonic cancer cells. Photochem Photobiol. 75:140-148.

Heinrich PC, Behrmann I, Haan S, Hermanns HM, Müller-Newen G, Schaper F. 2003. Principles of interleukin (IL)-6-type cytokine signalling and its regulation. Biochem J. 374:1-20.

Henderson BW, Gollnick SO. 2003. Mechanistic principles of photodynamic therapy. In: Vo-Dinh, T., editor. Biomedical photonics handbook. Boca Raton: CRC Press.

Hibasami H, Kyohkon M, Ohwaki S, Katsuzaki H, Imai K, Nakagawa M, Ishi Y, Komiya T. 2000. Pheophorbide a, a moiety of chlorophyll a, induces apoptosis in human lymphoid leukemia molt 4B cells. Int J Mol Med. 6:277-279.

Hippert MM, O'Toole PS, Thorburn A. 2006. Autophagy in cancer: good, bad, or both? Cancer Res. 66:9349-9351.

Hsieh YJ, Yu JS, Lyu PC. 2010. Characterization of photodynamic therapy responses elicited in A431 cells containing intracellular organelle-localized Photofrin. J Cell Biochem. In Press.

Hollstein M, Sidransky D, Vogelstein B, Harris CC. 1991. p53 mutations in human cancers. Science. 253:49-53.

Hörtensteiner S. 2006 Chlorophyll degradation during senescence. Annu Rev Plant Biol. 57:55-77.

Hoye AT, Davoren JE, Wipf P, Fink MP, Kagan VE. 2008. Targeting mitochondria. Acc Chem Res. 41:87-97.

Hu S, Wong CK, Lam CW. 2010. Activation of eosinophils by IL-12 family cytokine IL-27: Implications of the pleiotropic roles of IL-27 in allergic responses. Immunobiol. In Press.

Igney FH, Krammer PH. 2002. Death and anti-death: Tumour resistance to apoptosis. Nat Rev Can. 2:277-288.

Inanami O, Yoshito A, Takahashi K, Hiraoka W, Kuwabara M. 1999. Effects of BAPTA-AM and forskolin on apoptosis and cytochrome c release in photosensitized Chinese hamster V79 cells. Photochem Photobiol. 70:650-655.

Iriuchishima T, Saito A, Aizawa S, Taira K, Yamamoto T, Ryu J. 2008. The minimum influences for the murine normal joint tissue by novel bactericidal treatment and photodynamic therapy using na-pheophorbide a for septic arthritis. Photomed Laser Surg. 26:153-158.

Jalili A, Makowski M, Switaj T, Nowis D, Wilczynski GM, Wilczek E, Chorazy-Massalska M, Radzikowska A, Maslinski W, Bialy L, Sienko J, Sieron A, Adamek M, Basak G, Mróz P, Krasnodebski IW, Jakóbisiak M, Golab J. 2004. Effective photoimmunotherapy of murine colon carcinoma induced by the combination of photodynamic therapy and dendritic cells. Clin Cancer Res. 10:4498-4508.

Ji HT, Chien LT, Lin YH, Chien HF, Chen CT. 2010. 5-ALA mediated photodynamic therapy induces autophagic cell death via AMP-activated protein kinase. Mol Cancer. 9:91.

Jiangsu New Medical College. 1977. Dictionary of Chinese Materia Medical. Science and Technology Press of Shanghai.

Jordan VC. 1993. A current view of tamoxifen for the treatment and prevention of breast cancer. Fourteenth Gaddum Memorial Lecture. Br J Pharmacol. 110:507-517.

Jordan VC. 2004. Selective estrogen receptor modulation: Concept and consequences in cancer. Cancer Cell. 5:207-213.

Jordan VC. 2006. Tamoxifen (ICI46,474) as a targeted therapy to treat and prevent breast cancer. Br J Pharmacol. 147:S269-S276.

Juarranz A, Jaén P, Sanz-Rodríguez F, Cuevas J, González S. 2008. Photodynamic therapy of cancer. Basic principles and applications. Clin Transl Oncol. 10:148-154.

Kabingu E, Oseroff AR, Wilding GE, Gollnick SO. 2009. Enhanced systemic immune reactivity to a Basal cell carcinoma associated antigen following photodynamic therapy. Clin Cancer Res. 15:4460-4466.

Kabingu E, Vaughan L, Owczarczak B, Ramsey KD, Gollnick SO. 2007. CD8+ T cell–mediated control of distant tumours following local photodynamic therapy is independent of CD4+ T cells and dependent on natural killer cells. Br J Cancer. 96:1839–1848.

Kamata H, Hirata H. 1999. Redox Regulation of Cellular Signalling. Cell Signal. 11:1-14.

Kanzawa T, Kondo Y, Ito H, Kondo S, Germano I. 2003. Induction of autophagic cell death in malignant glioma cells by arsenic trioxide. Cancer Res. 63:2103-2108.

Karin M, Lawrence T, Nizet V. 2006. Innate immunity gone awry: linking microbial infections to chronic inflammation and cancer. Cell. 124:823–835.

Klein A, Babilas P, Karrer S, Landthaler M, Szeimies RM. 2008. Photodynamic therapy in dermatology--an update 2008. J Dtsch Dermatol Ges. 6:839-846.

Knop K, Mingotaud AF, El-Akra N, Violleau F, Souchard JP. 2009. Monomeric pheophorbide(a)-containing poly(ethyleneglycol-b-epsilon-caprolactone) micelles for photodynamic therapy. Photochem Photobiol Sci. 8:396-404.

Kondo Y, Kondo S. 2006. Autophagy and cancer therapy. Autophagy. 2:85-90.

Korbelik M. 1996. Induction of tumor immunity by photodynamic therapy. J Clin Laser Med Surg. 14:329–334.

Korbelik M. 2006. PDT-associated host response and its role in the therapy outcome. Lasers Surg Med. 38:500-508.

Korbelik M, Krosl G. 1994. Enhanced macrophage cytotoxicity against tumor cells treated with photodynamic therapy. Photochem Photobiol. 60:497-502.

Korbelik M, Stott B, Sun J. 2007. Photodynamic therapy–generated vaccines: relevance of tumour cell death expression. Br J Cancer. 97:1381-1387.

Korbelik M, Sun J. 2006. Photodynamic therapy-generated vaccine for cancer therapy. Cancer Immunol Immunother. 55:900-909.

Kousis PC, Henderson BW, Maier PG, and Gollnick SO. 2007. Photodynamic therapy enhancement of antitumor immunity is regulated by neutrophils. Cancer Res. 67:10501–10510.

Kim R, Emi M, Tanabe K, Murakami S. 2006. Role of the unfolded protein response in cell death. Apoptosis. 11:5-13.

Kim EK, Kwon KB, Han MJ, Song MY, Lee JH, Ko YS, Shin BC, Yu J, Lee YR, Ryu DG, Park JW, Park BH. 2007. Induction of G1 arrest and apoptosis by Scutellaria barbata in the human promyelocytic leukemia HL-60 cell line. Int J Mol Med. 20:123-128.

Kim KW, Jin UH, Kim DI, Lee TK, Kim MS, Oh MJ, Kim MS, Kwon DY, Lee YC, Kim CH. 2008. Antiproliferative effect of Scutellaria barbata D. Don. on cultered human uterine leiomyoma cells by down-regulation of the expression of Bcl-2 protein. Phytother Res. 22:583-590.

Kinzler I, Haseroth E, Hauser C, Rück A. 2007. Role of mitochondria in cell death induced by Photofrin-PDT and ursodeoxycholicacid by means of SLIM. Photochem Photobiol Sci. 6:1332-1340.

Kishino K, Hashimoto K, Amano O, Kochi M, Liu WK, Sakagami H. 2008. Tumor-specific cytotoxicity and type of cell death induced by sodium 5,6-benzylidene-L-ascorbate. Anticancer Res. 28:2577-2584.

Korbelik M, Sun J, and Cecic I. 2005. Photodynamic therapy–induced cell surface expression and release of heat shock proteins: relevance for tumor response. Cancer Res. 65:1018-1026.

Kousis PC, Henderson BW, Maier PG, Gollnick SO. 2007. Photodynamic therapy enhancement of antitumor immunity is regulated by neutrophils. Cancer Res. 67:10501-10510.

Krosl G, Korbelik M, and Dougherty GJ. 1995. Induction of immune cell infiltration into murine SCCVII tumour by photofrin-based photodynamic therapy. Br J Cancer. 71:549-555.

Kuppner MC, Gastpar R, Gelwer S, Nössner E, Ochmann O, Scharner A, Issels RD. 2001. The role of heat shock protein (hsp70) in dendritic cell maturation: hsp70 induces the maturation of immature dendritic cells but reduces DC differentiation from monocyte precursors. Eur J Immunol. 31:1602-1609.

Kuribayashi K, El-Deiry WS. 2007. Programmed Cell Death in Cancer Progression and Therapy. Chapter 10: Regulation of programmed cell death by the p53 pathway. Adv Exp Med Biol. 615:201-221.

Lazebnik YA, Kaufmann, Desnoyers S, Poirier GG, Earnshaw WC. 1994. Cleavage of poly(ADP-ribose) polymerase by a proteinase with properties like ICE. Nature. 371:346-347.

Lee AS. 2007. GRP78 induction in cancer: therapeutic and prognostic implications. Cancer Res. 67:3496-3499.

Lee WY, Lim DS, Ko SH, Park YJ, Ryu KS, Ahn MY, Kim YR, Lee DW, Cho CW. 2004. Photoactivation of pheophorbide a induces a mitochondrial-mediated apoptosis in Jurkat leukaemia cells. J Photochem Photobiol B. 75:119-126.

Li H, Zhu H, Xu C, Yuan J. 1998. Cleavage of BID by caspase 8 mediates the mitochondrial damage in the Fas pathway of apoptosis. Cell. 94:491-501.

Li WT, Tsao HW, Chen YY, Cheng SW, Hsu YC. 2007. A study on the photodynamic properties of chlorophyll derivatives using human hepatocellular carcinoma cells. Photochem Photobiol Sci. 6:341-1348.

Lim DS, Ko SH, Kim SJ, Park YJ, Park JH, Lee WY. 2002. Photoinactivation of vesicular stomatitis virus by a photodynamic agent, chlorophyll derivatives from silkworm excreta. J Photochem Photobiol B. 67:149-156.

Lim DS, Ko SH, Lee WY. 2004. Silkworm-phephorbide alpha mediated photodynamic therapy against B16F10 pigmented melanoma. J Photochem Photobiol B. 74:1-6.

Locksley RM, Killeen N, Lenardo MJ. 2001. The TNF and TNF Receptor Superfamilies: Integrating Mammalian Biology. Cell. 104:487-501.

Macdonald IJ, Dougherty TJ. 2001. Basic principles of photodynamic therapy. J Porphyr Phthalocya. 5:105-129.

Mandlekar S, Kong ANT. 2001. Mechanisms of tamoxifen-induced apoptosis. Apoptosis. 6:469-477.

Matsubara A, Nakazawa T, Noda K, She H, Connolly E, Young TA, Ogura Y, Gragoudas ES, Miller JW. 2007. Photodynamic therapy induces caspase-dependent apoptosis in rat CNV model. Invest Ophthalmol Vis Sci. 48:4741-4747.

Marchal S, Fadloun A, Maugain E, D'Hallewin MA, Guillemin F, Bezdetnaya L. 2005. Necrotic and apoptotic features of cell death in response to Foscan photosensitization of HT29 monolayer and multicell spheroids. Biochem Pharmacol. 69:1167-1176.

McCaughan JS Jr. 1999. Photodynamic therapy: a review. Drugs Aging. 15:49-68.

McKnight JA. 2003. Principles of chemotherapy. Clinical Techniques in Small Animal Practice. 18:67-72.

Meloche S, Pouysségur J. 2007. The ERK1/2 mitogen-activated protein kinase pathway as a master regulator of the G1- to S-phase transition. Oncogen. 26:3227-3239.

Michalak M, Groenendyk J, Szabo E, Gold LI, Opas M. 2009. Calreticulin, a multi-process calcium-buffering chaperone of the endoplasmic reticulum. Biochem J. 417:651-666.

Micheau O, Tschopp J. 2003. Induction of TNF Receptor I-mediated apoptosis via two sequential signaling complexes. Cell. 114:181-190.

Minotti G, Menna P, Salvatorelli E, Cairo G, Gianni L. 2004. Anthracyclines: molecular advances and pharmacologic developments in antitumor activity and cardiotoxicity. Pharmacol Rev. 56:185-229.

Motyl T, Gajkowska B, Zarzyńska J, Gajewska M, Lamparska-Przybysz M. 2006. Apoptosis and autophagy in mammary gland remodeling and breast cancer chemotherapy. J Physiol Pharmacol. 57 (Suppl 7):17-32.

Mund T, Gewies A, Schoenfeld N, Bauer MKA, Grimm S. 2003. Spike, a novel BH3-only protein, regulates apoptosis at the endoplasmic reticulum. FASEB J. 17:696-698.

Murakami H, Kohno E, Kohmura Y, Oawa H, Ito H, Sugihara K, Horiuchi K, Hirano T, Kanayama N. 2009. Antitumor effect of photodynamic therapy in mice using direct application of Photofrin dissolved in lidocaine jelly. Photodermatol Photoimmunol Photomed. 25:259-263.

Murphy MP. How mitochondria produce reactive oxygen species. Biochem J. 417:1-13.

Nagata S. 1997. Apoptosis by death factor. Cell. 88:355-365.

Nakamura Y, Murakami A, Koshimizu K, Ohigashi H. 1996. Inhibitory effect of pheophorbide a, a chlorophyll-related compound, on skin tumor promotion in ICR mouse. Cancer Lett. 108:247-255.

Ni M, Lee AS. 2007. ER chaperones in mammalian development and human diseases. FEBS Lett. 581:3641-3651.

Nicholson DW, Ali A, Thornberry NA, Vaillancourt JP, Ding CK, Gallant M, Gareau Y, Griffin PR, Labelle M, Lazebnik YA, Munday NA, Raju SM, Smulson ME, Yamin TT, Yu VL, Miller DK. 1995. Identification and inhibition of the ICE/CED-3 protease necessary for mammalian apoptosis. Nature. 376:37-43.

Nguyen DM, Hussain M. 2007. The role of the mitochondria in mediating cytotocixity of anti-cancer therapies. J Bioenerg Biomembr. 39:13-21.

Noodt BB, Berg K, Stokke T, Peng Q, Nesland JM. 1996. Apoptosis and necrosis induced with light and 5-aminolaevulinic acid-derived protoporphyrin IX. Br J Cancer. 74:22-29.

O'Connor AE, Gallagher WM, Byrne AT. 2009. Porphyrin and nonporphyrin photosensitizers in oncology: preclinical and clinical advances in photodynamic therapy. Photochem Photobiol. 85:1053-1074.

Oliver FJ, de la Rubia G, Rolli V, Ruiz-Ruiz MC, de Murcia G, de Murcia JM. 1998. Importance of Poly(ADP-ribose) polymerase and its cleavage in apoptosis lesson from an uncleavable mutant. J Biol Chem. 273:33533-33539.

Opitz I, Krueger T, Pan Y, Altermatt HJ, Wagnières G, Ris HB. 2006. Preclinical comparison of mTHPC and verteporfin for intracavitary photodynamic therapy of malignant pleural mesothelioma. Eur Surg Res. 38:333-339.

Ousman SS, David S. 2001. MIP-1α, MCP-1. GM-CSF, and TNF-α Control the Immune Cell Response That Mediates Rapid Phagocytosis of Myelin from the Adult Mouse Spinal Cord. J Neurosci. 21:4649-4656.

Pearson G, Robinson F, Beers Gibson T, Xu BE, Karandikar M, Berman K, Cobb MH. 2001. Mitogen-activated protein (MAP) kinase pathways: regulation and physiological functions. Endocr Rev. 22:153-183.

Penolazzi L, Zennaro M, Lambertini E, Tavanti E, Torreggiani, Gambari R, Piva R. 2007. Induction of estrogen receptor α expression with decoy oligonucleotide targeted to NFATc1 binding sites in osteoblasts. Mol Pharmacol. 71:1457-1462.

Perez AT, Arun B, Tripathy D, Tagliaferri MA, Shaw HS, Kimmick GG, Cohen I, Shtivelman E, Caygill KA, Grady D, Schactman M, Shapiro CL. 2010. A phase 1B dose escalation trial of Scutellaria barbata (BZL101) for patients with metastatic breast cancer. Breast Cancer Res Treat. 120:111-118.

Plaetzer K, Kiesslich T, Krammer B, Hammerl P. 2002. Characterization of the cell death modes and the associated changes in cellular energy supply in response to AlPcS4-PDT. Photochem Photobiol Sci. 1:172-177.

Potelle B, Junot H, Poisson N. 2008. La thérapie photodynamique: indications et impact économique à l'hôpital. Poster. Congrès de la Société Française de Pharmacie Clinique.

Pruzinská A, Anders I, Aubry S, Schenk N, Tapernoux-Lüthi E, Müller T, Kräutler B, Hörtensteiner S. 2007. In vivo participation of red chlorophyll catabolite reductase in chlorophyll breakdown. Plant Cell. 19:369-387.

Raab O. 1900. Uber die wirkung fluorescirener stoffen. Infosaria Z Biol. 39, 524.

Radestock A, Elsner P, Gitter B, Hipler UC. 2007. Induction of apoptosis in HaCaT cells by photodynamic therapy with chlorin e6 or pheophorbide a. Skin Pharmacol Physiol. 20:3-9.

Rapozzi V, Miculan M, Xodo Le. 2009. Evidence that photoactivated pheophorbide a causes in human cancer cells a photodynamic effect involving lipid peroxidation. Cancer Biol Ther. 8:1318-1327.

Rebbeck TR, Lynch HT, Neuhausen SL, Narod SA, Van't Veer L, Garber JE, Evans G, Isaacs C, Daly MB, Matloff E, Olopade OI, Weber BL. 2002. Prevention and

Observation of Surgical End Points Study Group. Prophylactic oophorectomy in carriers of BRCA1 or BRCA2 mutations. N Engl J Med. 346:1616-1622.

Ren W, Strube R, Zhang X, Chen SY, and Huang XF. 2004. Potent tumorspecific immunity induced by an in vivo heat shock protein-suicide gene-based tumor vaccine. Cancer Res. 64:6645-6651.

Ribeiro AP, Pavarina AC, Trindade FZ, Inada NM, Bagnato VS, de Souza Costa CA. 2010. Photodynamic therapy associating Photogem and blue LED on L929 and MDPC-23 cell culture. Cell Bio Int. 34:343-351.

Riedl SJ, Salvesen GS. 2007. The apoptosome: signalling platform of cell death. Nat Rev Mol Cell Biol. 8:405-413.

Robert J. 1999. Multidrug resistance in oncology: diagnostic and therapeutic approaches. Eur J Clin Invest. 29:536-545.

Robey RW, Steadman K, Polgar O, Morisaki K, BlayneyM, Mistry P, Bates SE. 2004. Pheophorbide a is a specific probe for ABCG2 function and inhibition. Cancer Res. 64:1242-1246.

Rodriguez J, Lazebnik Y. 1999. Caspase-9 and APAF-1 form an active holoenzyme. Genes Dev. 13:3179-3184.

Rodriguez L, de Bruijn HS, Di Venosa G, Mamone L, Robinson DJ, Juarranz A, Batlle A, Casas A. 2009. Porphyrin synthesis from aminolevulinic acid esters inendothelial cells and its role in photodynamic therapy. J Photochem Photobiol B. 96:249-254.

Roux PP, Blenis J. 2004ERK and p38 MAPK-Activated Protein Kinases: a Family of Protein Kinases with Diverse Biological Functions. Microbiol Mol Biol Rev. 68:320-344.

Rugo H, Shtivelman E, Perez A, Vogel C, Franco S, Tan Chiu E, Melisko M, Tagliaferri M, Cohen I, Shoemaker M, Tran Z, Tripathy D. 2007. Phase I trial and antitumor effects

of BZL101 for patients with advanced breast cancer. Breast Cancer Res Treat. 105:17-28.

Savill J, Dransfield I, Gregory C, Haslett C. 2002. A blast from the past: clearance of apoptotic cells regulates immune responses. Nat Rev Immunol. 2:965-975.

Sasnauskiene A, Kadziauskas J, Vezelyte N, Jonusiene V, Kirveliene V. 2009. Apoptosis, autophagy and cell cycle arrest following photodamage to mitochondrial interior. Apoptosis. 14:276-286.

Shiau AK, Barstad D, Loria PM, Cheng L, Kushner PJ, Agard DA, Greene GL. 1998. The structural basis of estrogen receptor/coactivator recognition and the antagonism of this interaction by tamoxifen. Cell. 95:927-937.

Slee EA, O'Connor DJ, Lu X. 2004. To die or not to die: how does p53 decide? Oncogene. 23:2809-2818.

Srivastava RK, Sollott SJ, Khan L, Hansford R, Lakatta EG, Longo DL. 1999. Bcl-2 and Bcl-X(L) block thapsigargin-induced nitric oxide generation, c-Jun NH(2)-terminal kinase activity, and apoptosis. Mol Cell Biol. 19:5659-5674.

Starkov AA. 2008. The role of mitochondria in reactive oxygen species metabolism and signalling. Ann N Y Acad Sci. 1147:37-52.

Stein RA, Chang CY, Kazmin DA, Way J, Schroeder T, Wergin M, Dewhirst MW, McDonnell DP. 2008. Estrogen-related receptor alpha is critical for the growth of estrogen receptor-negative breast cancer. Cancer Res. 68:8805-8812.

Suh SJ, Yoon JW, Lee TK, Jin UH, Kim SL, Kim MS, Kwon DY, Lee YC, Kim CH. 2007. Chemoprevention of Scutellaria bardata on human cancer cells and tumorigenesis in skin cancer. Phytother Res. 21:135-141.

Takamiya KI, Tsuchiya T, Ohta H. 2000. Degradation pathway(s) of chlorophyll: what has gene cloning revealed? Trends Plant Sci. 5:426-431.

Takimoto CH, Calvo E. 2008. Principles of Oncologic Pharmacotherapy. Cancer Management: A Multidisciplinary Approach. Chapter 3. p1-4.

Tang PM, Bui-Xuan NH, Wong CK, Fong WP, Fung KP. 2010. Pheophorbide a-Mediated Photodynamic Therapy Triggers HLA Class 1-Restricted Antigen Presentation in Human Hepatocellular Carcinoma. Transl Oncol. 3:114-122.

Tang PM, Chan JY, Au SW, Kong SK, Tsui SK, Waye MM, Mak TC, Fong WP, Fong WP, Fung KP. 2006. Pheophorbide a, an active compound isolated from Scutellaria barbata, possesses photodynamic activities by inducing apoptosis in human hepatocellular carcinoma. Cancer Biol Ther. 5:1111-1116.

Tang PMK, Chan JYM, Zhang DM, Au SWN, Fong WP, Kong SK, Tsui SKW, Waye MMY, Mak TCW, Fung KP. 2007. Pheophorbide a, an active component in scutellaria barbata, reverses P-glycoprotein-mediated multidrug resistance on a human hepatoma cell line R-HepG2. Cancer Biol Ther. 6:504-509.

Tang PM, Liu XZ, Zhang DM, Fong WP, Fung KP. 2009a. Pheophorbide a based photodynamic therapy induces apoptosis via mitochondrial-mediated pathway in human uterine carcinosarcoma. Cancer Biol Ther. 8:533-539.

Tang PMK, Zhang DM, Bui-Xuan NH, Tsui SKW, Waye MMY, Kong SK, Fong WP, Fung KP. 2009b. Photodynamic therapy inhibits p-glycoprotein mediated multidrug resistance via JNK activation in human hepatocellular carcinoma using the photosensitizer phephorbide a. Mol Cancer. 8.

Tappeiner HV, Jesoniek A. 1903. Therapeutische versuchi mit fluoreszeirender stoff. Muchen Med Wehnschr. 1, 2042-2044.

Tewari M, Quan LT, O'Rourke K, Desnoyers S, Zheng Z, Beidler DR, Poirier GG, Salvesen GS, Dixit VM. 1995. Yama/CPP32β, a mammalian homolog of CED-3, is a

CrmA-inhibitable protease that cleaves the death substrate poly(ADP-ribose) polymerase. Cell. 81:801-809.

Tong Z, Singh G, Rainbow AJ. 2002. Sustained activation of the extracellular signal-regulated kinase pathway protects cells from photofrin-mediated photodynamic therapy. Cancer Res. 62:5528-5535.

Torres M, Forman HJ. 2003. Redox signalling and the MAP kinase pathways. BioFactors. 17:287-296.

Urano F, Wang X, Bertolotti A, Zhang Y, Chung P, Harding HP, Ron D. 2000. Coupling of stress in the ER to activation of JNK protein kinases by transmembrane protein kinase IRE1. Science. 287:664-666.

U.S Department of heath and human services. 2009. What you need to know about breast cancer. NIH Publication No.09-1556.

Valko M, Leibfritz D, Moncol J, Cronin MTD, Mazur M, Telser J. 2007. Free radicals and antioxidants in normal physiological functions and human disease. Int J Biochem Cell Biol. 39:44-84.

van Duijnhoven FH, Aalbers RI, Rovers JP, Terpstra OT, and Kuppen PJ. 2003. The immunological consequences of photodynamic treatment of cancer, a literature review. Immunobiol. 207:105-113.

Veronesi U, Cascinelli N, Mariani L, Greco M, Saccozzi R, Luini A, Aguilar M, Marubini E. 2002. Twenty-year follow-up of a randomized study comparing breast-conserving surgery with radical mastectomy for early breast cancer. N Engl J Med. 347:1227-1232.

Vrouenraets MB, Visser GWM, Snow GB, van Dongen GAMS. 2003. Basic principles, applications in oncology and improved selectivity of photodynamic therapy. Anticancer Res. 23:505-522.

Wagner EF, Nebreda AR. 2009. Signal integration by JNK and p38 MAPK pathways in cancer development. Nat Rev Cancer. 9:537-549.

Walker DK, Davis J, Houle C, Gardner IB, Webster R. 2009. Species differences in the multiple-dose pharmacokinetics of the non-nucleoside reverse transcriptase inhibitor (NNRTI) UK-453,061 in animals and man: implications for safety considerations. Xenobiotica. 39:534-543.

Weng SC, Kashida Y, Kulp SK, Wang D, Brueggemeir RW, Shapiro CL, Chen CS. 2008. Sensitizing estrogen receptor-negative breast cancer cells to tamoxifen with OSU-03012, a novel celecoxib-derived phosphoinositide-dependent protein kinase-1/Akt signaling inhibitor. Mol Cancer Ther. 7:800-808.

Widakowich C, de Castro G Jr, de Azambuja E, Dinh P, Awada A. 2007. Review: side effects of approved molecular targeted therapies in solid cancers. Oncologist. 12:1443-1455.

Wong BY, Nguyen DL, Lin T, Wong HH, Cavalcante A, Greenberg NM, Hausted RP, Zheng J. 2009. Chinese Medicinal herb Scutellaria barbata modulates apoptosis and cell survival in murine and human prostate cancer cells and tumor development in TRAMP mice. Eur J Cancer Prev. 18:331-341.

World Health Organization. 2006. Fact sheet No. 297.

World Health Organization. 2008. Traditional medicine. Fact sheet No. 134.

World Health Organization International Agency for Research on Cancer. *World Cancer Report*. 2003.

Wu Y, Chen DF. 2009. Anti-complementary effect of polysaccharide B3-PS1 in Herba Scutellariae Barbatae (Scutellaria barbata). Immunopharmacol Immunotoxicol. 31:696-701.

Wu WS, Wu JR, Hu CT. 2008. Signal cross talks for sustained MAPK activation and cell migration: the potential role of reactive oxygen species. Cancer Metastasis Rev. 27:303-314.

Xu D, Perez RE, Rezaiekhaligh MH, Bourdi M, Truog WE. 2009. Knockdown of ERp57 Increases BiP/GRP78 Induction and Protects against Hyperoxia and Tunicamycin-induced Apoptosis. Am J Physiol Lung Cell Mol Physiol. 297:L44-51.

Yao Y, Li W, Wu J, Germann UA, Su MS, Kuida K, Boucher DM. 2003. Extracellular signal-regulated kinase 2 is necessary for mesoderm differentiation. Proc Natl Acad Sci USA. 100:12759-12764.

Yin X, Zhou J, Jie C, Xing D, Zhang Y. 2004. Anticancer activity and mechanism of Scutellaria barbata extract on human lung cancer cell line A549. Life Sci 75:2233-2244.

Yorimitsu T, Klionsky DJ. 2007. Endoplasmic reticulum stress: a new pathway to induce autophagy. Autophagy. 3:160-162.

Yu J, Lei J, Yu H, Cai X, Zou G. 2004. Chemical composition and antimicrobial activity of the essential oil of Scutellaria barbata. Phytochem. 65:881-884.

Yu J, Liu H, Lei J, Tan W, Hu X, Zou G. 2007. Antitumor activity of chloroform fraction of Scutellaria barbata and its active constituents. Phytother Res. 21:817-822.

Zane C, Capezzera R, Sala R, Venturini M, Calzavara-Pinton P. 2007. Clinical and echographic analysis of photodynamic therapy using methylaminolevulinate as sensitizer in the treatment of photodamaged facial skin. Lasers Surg Med. 39:203-209.

Zhou F, Xing D, Chen WR. 2009. Regulation of HSP70 on activating macrophages using PDT-induced apoptotic cells. Int J Cancer. 125:1380-1389.

Zuluaga MF, Lange N. 2008. Combination of photodynamic therapy with anti-cancer agents. Curr Med Chem. 15:1655-1673.